66-652

LOAN COPY

Local Library

183

ANTENNA LABORATORY

Technical Report No. 54

# THE COUPLING AND MUTUAL IMPEDANCE BETWEEN BALANCED WIRE-ARM CONICAL LOG-SPIRAL ANTENNAS

by

John D. Dyson

Contract AF33(657)-8460
Project No. 6278, Task No. 40572

June 1962

Sponsored by:
AERONAUTICAL SYSTEMS DIVISION
WRIGHT-PATTERSON AIR FORCE BASE, OHIO

ELECTRICAL ENGINEERING RESEARCH LABORATORY
ENGINEERING EXPERIMENT STATION
UNIVERSITY OF ILLINOIS
URBANA, ILLINOIS

Antenna Laboratory

Technical Report No. 54

# THE COUPLING AND MUTUAL IMPEDANCE BETWEEN BALANCED WIRE-ARM CONICAL LOG-SPIRAL ANTENNAS

by

John D. Dyson

Contract AF33(657)8460
Project N6278, Task No. 40572

June 1962

Sponsored by:

Aeronautical Systems Division

ELECTRICAL ENGINEERING RESEARCH LABORATORY
ENGINEERING EXPERIMENT STATION
UNIVERSITY OF ILLINOIS
URBANA, ILLINOIS

# PREFACE

This work was presented in a somewhat abbreviated form as a paper at the IRE International Convention, March 1962. "The Coupling and Mutual Impedance Between Conical Log-Spiral Antennas in Simple Arrays", Proc. of the 1962 IRE International Convention, Vol. I.

# ABSTRACT

The radiation characteristics of the conical logarithmic spiral antenna make it attractive as an element for circularly polarized arrays. The design of such arrays requires a knowledge of the radiation coupling and mutual impedance between these log-spiral elements as a function of rotation as well as element spacing, and for some array configurations a knowledge of the location of the phase center of the elements.

A general consideration of the conical log-spiral antenna as a locally periodic, slow wave structure is outlined, and in so doing a quasi-empirical formula for the location of the antenna phase center is developed.

This investigation of the mutual impedance between the log-spiral antennas has shown it to be very low. Information on the mutual impedance and on the coefficient of coupling between antennas is supplied for two different geometrical array configurations and for various antenna parameters. Pattern modification due to the presence of parasitic elements has been investigated. For element to element spacing of at least one half wavelength, this consists primarily of an increase in beamwidth. Radiation patterns for several arrays are shown.

# ACKNOWLEDGEMENT

The author would like to acknowledge many helpful discussions with members of the University of Illinois Antenna Laboratory, in particular Professors G. A. Deschamps and P. E. Mayes, and Mr. O. L. McClelland.

In addition, he is pleased to acknowledge the assistance of the members of the laboratory in the measurements. Mr. R. E. Griswold made the extensive coupling and mutual impedance measurements.

# CONTENTS

Page

1. Introduction 1

2. Theoretical Considerations 4

    2.1 Coupled Antennas 4
    2.2 The Phase Center 8

3. Experimental Considerations 19

4. Measurements 25

    4.1 Coefficient of Coupling 25

        4.1.1 Parallel Arrays 25
        4.1.2 Conical Arrays 29

    4.2 Mutual Impedance 34

        4.2.1 Parallel Arrays 34
        4.2.2 Conical Arrays 45

    4.3 Radiation Patterns 45

        4.3.1 Parasitic Arrays 45
        4.3.2 Driven Arrays 62

5. Conclusions 75

References 76

Appendix A 78

## ILLUSTRATIONS

| Figure Number | | Page |
|---|---|---|
| 1 | Possible Arrays of the Conical Log-Spiral Antenna | 2 |
| 2 | Equivalent Network for Coupled Antennas | 5 |
| 3 | Truncated Portion of Conical Log-Spiral Antenna | 9 |
| 4 | Brillouin Diagram for Bifilar Helix | 11 |
| 5 | Measured Phase Centers for Several Wire Arm Conical Log-Spiral Antennas | 16 |
| 6 | Approximate Circumference in Wavelengths at the Phase Center of Balanced Wire Arm Conical Log-Spiral Antennas ($N = 2$, $m = 1$) | 17 |
| 7 | A Conical Antenna with Associated Coordinate System | 20 |
| 8 | Photograph of Conical Log-Spiral Antennas | 21 |
| 9 | Phase Center Location in Wavelengths from the Vertex of 15° Conical Wire-arm Antenna Versus Spiral Angle | 23 |
| 10 | Phase Center Location in Wavelengths from the Vertex of a 15° Conical Wire-Arm Antenna as a Function of Frequency, $\alpha = 73^{\circ}$ | 23 |
| 11 | Experimental Set Up for Measuring the Complex Coefficient of Coupling and Mutual Impedance | 24 |
| 12 | Magnitude of Coupling Coefficient Measured Between Parallel Antennas as a Function of Spacing Between Antennas in a Parallel Array | 26 |
| 13 | Coupling as a Function of Rotation in a Parallel Array | 27 |
| 14 | Coupling between Contrawound Antennas Directed at Each Other to Indicate Dipole Coupling Effect | 28 |
| 15 | Coupling between the $n^{th}$ and $n+2$ Element in a Parallel Array | 30 |
| 16 | Coupling between Contrawound Antennas as a Function of Spacing in a Parallel Array | 31 |
| 17 | Coupling between Contrawound Antennas in a Parallel Array as a Function of Relative Rotation | 32 |

Figure Number Page

18 Magnitude of Coupling Coefficient Measured between Antennas in a Conical Array as a Function of the Array Angle 33

19 Coupling as a Function of Rotation in a Conical Array 35

20 Coupling Between the $n^{th}$ and n+2 Element in a Conical Array 36

21 Coupling Between Contrawound Antennas in a Conical Array as a Function of the Array Angle 37

22 Coupling Between Contrawound Antennas in a Conical Array as a Function of Relative Rotation 38

23 Mutual Impedance as a Function of Spacing in a Parallel Array, $\alpha = 60^{o}$ 39

24 Mutual Impedance as a Function of Spacing in a Parallel Array, $\alpha = 73^{o}$ 40

25 Mutual Impedance as a Function of Spacing in a Parallel Array, $\alpha = 83^{o}$ 41

26 Mutual Impedance as a Function of Rotation in a Parallel Array, $\alpha = 60^{o}$ 42

27 Mutual Impedance as a Function of Rotation in a Parallel Array, $\alpha = 73^{o}$ 43

28 Mutual Impedance as a Function of Rotation in a Parallel Array, $\alpha = 83^{o}$ 44

29 Mutual Impedance Vs Array Angle in a Conical Array, $\alpha = 60^{o}$ 47

30 Mutual Impedance Vs Array Angle in a Conical Array, $\alpha = 73^{o}$ 48

31 Mutual Impedance Vs Array Angle in a Conical Array, $\alpha = 83^{o}$ 49

32 Mutual Impedance Vs Relative Rotation in a Conical Array, $\alpha = 60^{o}$ 50

33 Mutual Impedance Vs Relative Rotation in a Conical Array, $\alpha = 73^{o}$ 51

34 Mutual Impedance Vs Relative Rotation in a Conical Array, $\alpha = 83^{o}$ 52

Figure Number Page

35 Electric Field Patterns of Conical Log-Spiral Antenna With and Without a Parasitic Antenna Present in a Parallel Array, $\alpha = 60^\circ$ 53

36 Electric Field Patterns of Conical Log-Spiral Antenna With and Without a Parasitic Antenna Present in a Parallel Array, $\alpha = 73^\circ$ 54

37 Electric Field Patterns of Conical Antenna With and Without a Parasitic Antenna Present in a Parallel Array, $\alpha = 83^\circ$ 55

38 Electric Field Patterns of Conical Antenna With and Without a Parasitic Antenna Present in a Conical Array, $\alpha = 60^\circ$ 56

39 Electric Field Patterns of Conical Antenna With and Without a Parasitic Antenna Present in a Conical Array, $\alpha = 73^\circ$ 57

40 Electric Field Patterns of Conical Antenna With and Without a Parasitic Antenna Present in a Conical Array, $\alpha = 83^\circ$ 58

41 Three Element Parallel Parasitic Array, Variable Spacing. $\phi_2 = \phi_3 = \phi_1$, $\alpha = 73^\circ$ (linear array in $\phi = 0$ plane) 59

42 Three Element Conical Parasitic Array, Variable Array Antle. $\phi_1 = \phi_2 = \phi_3$, $\alpha = 73^\circ$ 60

43 Radiation Patterns of Two Element Conical Parasitic Array as a Function of Rotation of Parasitic Element, $\alpha = 73^\circ$, $\psi = 18^\circ$ 61

44 Half Power Beamwidth of the Element Function $\cos^n \theta$ 63

45 Calculated Array Pattern for Two Element Parallel In-phase Array, $S = \lambda/2$, $\alpha = 73^\circ$ 64

46 Radiation Patterns of Two Element Parallel Array, Variable Spacing. $\phi_2 = \phi_3$, $\alpha = 73^\circ$ (linear array in $\phi = 0$ plane) 65

47 Radiation Patterns of Two Element Parallel Array, Variable Orientation of One Element. $S = \lambda/2$, $\alpha = 73^\circ$ (linear array in $\phi = 0$ plane) 66

Figure Number Page

48 Radiation Patterns of Three Element Parallel Array, Variable Spacing, $\phi_1 = \phi_2 = \phi_3$, $\alpha = 73^\circ$ (linear array in $\phi = 0$ plane) 67

49 Geometry of Two Element Conical Array 68

50 Radiation Pattern for Two Element Conical In-phase Array, $S = \lambda/2$ ($\psi = 34^\circ$), $\alpha = 73^\circ$ 69

51 Radiation Patterns for Two Element Conical Array, Variable Array Angle. $\phi_1 = \phi_2$, $\alpha = 73^\circ$ (linear array in $\phi = 0$ plane) 71

52 Radiation Patterns for Two Element Conical Array, Variable Orientation of One Element, $S = \lambda/2$, $\alpha = 73^\circ$ (linear array in $\phi = 0$ plane) 72

53 Radiation Patterns for Three Element Conical Array, Variable Array Angle. $\phi_1 = \phi_2 = \phi_3$, $\alpha = 73^\circ$ (linear array in $\phi = 0$ plane) 73

54 Half-power Beamwidth of Two Element Parallel and Conical Arrays 74

# 1. INTRODUCTION

There are many applications which require a circularly polarized field with narrower beamwidths and higher gains than can be secured with the individual planar and conical logarithmic spiral antennas which have been developed to date[1]. Many of these applications have been filled by constructing arrays of helical antennas. For wide-band applications, it would appear that a considerable advantage could be obtained from the extremely wide bandwidth of the conical log-spiral antenna as an array element. Thus, although the array factor of conventional arrays would be a limiting factor, the element factor could be made essentially independent of frequency over a considerable band of frequencies. In addition to bandwidth, the conical log-spiral antenna is unique in that the radiated fields are essentially circularly polarized over considerable angles off the axis of the antenna.

There are various geometrical configurations that can be used when arraying the conical antennas.[2] Four of these are shown in Figure 1. The parallel array and the collinear array would have a frequency dependent array pattern; however, the conical array and coaxial arrays could theoretically be designed to be independent of frequency. The geometry of the conical array is that used by DuHamel and Berry when arraying log-periodic elements.[3] This geometry limits the array to a few log-spiral elements; therefore, to obtain very narrow beamwidths from an array the conventional parallel configuration may offer the only solution. In addition to the use of arrays as primary radiators, consideration has recently been given to using an array of two contrawould conical log-spiral antennas as the feed for large parabolic tracking antennas.[4-6]

The design of arrays of conical antennas requires a knowledge of the radiation coupling between antennas to determine the effect on the element pattern, and the mutual impedance between antennas to compute the element terminal impedance. Since a simple rotation of these antennas about their axes allows phasing of the array, a knowledge of the radiation coupling and mutual impedance as a function of rotation, as well as a function of element spacing, is desirable. The determination of the element to element separation requires a knowledge of the location of the element phase center. The purpose

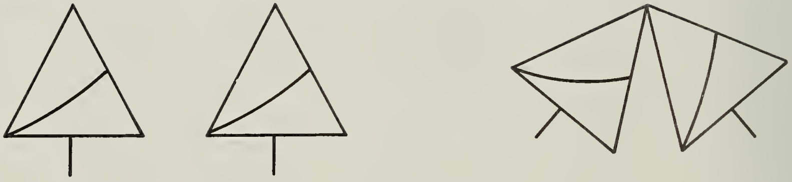

PARALLEL ARRAY

CONICAL ARRAY

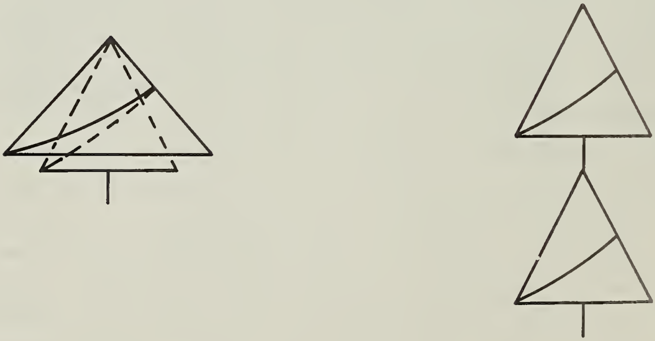

COAXIAL ARRAY

COLLINEAR ARRAY

Figure 1. Possible Arrays of the Conical Log-Spiral Antenna

of this paper is to supply this information for parallel and conical linear arrays over a restricted, although representative, range of antenna parameters. Experimental information is also supplied on the radiation patterns, half-power beamwidth, and axial ratio of typical two and three element parallel and conical arrays.

# 2. THEORETICAL CONSIDERATIONS

## 2.1 Coupled Antennas

Consider a two element array in which currents $I_1$ and $I_2$ flow as a result of voltages $V_1$ and $V_2$ applied across the feed terminals of the two elements. As far as these terminal voltages and currents are concerned, the two antennas may be represented by the general four-terminal network in Figure 2a.

In this network, $Z_{11}$ is the mesh impedance of mesh 1 (less the generator impedance) and is the impedance of antenna 1 with antenna 2 present and open circuited (not equal to the self-impedance of antenna 1 when isolated). Thus, we have

$$\begin{aligned} V_1 &= Z_{11} I_1 + Z_{12} I_2 \\ V_2 &= Z_{21} I_1 + Z_{22} I_2 \end{aligned} \tag{1}$$

where $Z_{12}$ is the mutual impedance between the antennas. In the usual case where the medium is reciprocal, $Z_{12} = Z_{21}$. If $V_2 = 0$, the input presented to the generator at reference plane $A_1$ by antenna 1 with antenna 2 present is

$$\frac{V_1}{I_1} = Z_{11} - \frac{Z_{12} Z_{21}}{Z_{22}} \tag{2}$$

Rearranging; we can express this ratio as

$$\frac{V_1}{I_1} = Z_{11} (1 - k^2) \tag{3}$$

where

$$k = \frac{Z_{12}}{\sqrt{Z_{11} Z_{22}}} \tag{4}$$

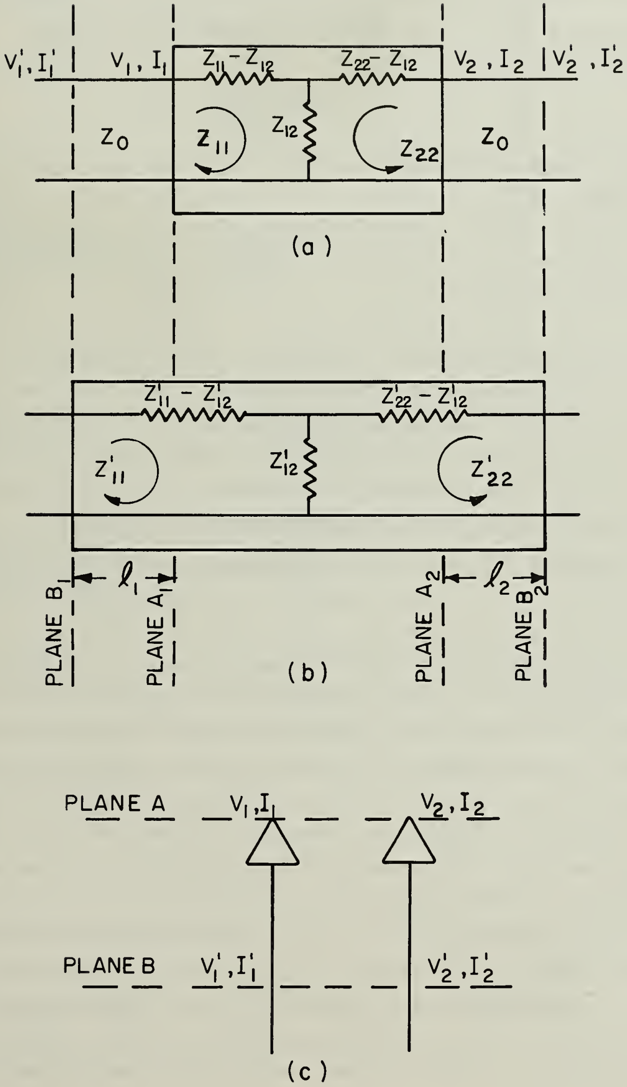

Figure 2. Equivalent Network for Coupled Antennas

The complex number k is defined to be the coefficient of coupling between antennas one and two[7,8]. For identical antennas $Z_{11} = Z_{22}$ and

$$Z_{12} = k\, Z_{11} \tag{5}$$

If antenna 1 is driven and antenna 2 open circuited, $I_2 = 0$, and it can be shown that

$$k = \frac{V_2}{V_1} \tag{6}$$

Thus the measurement procedure is reduced to the determination of one impedance and the complex ratio of two voltages[9]. This method has advantages of accuracy and ease of measurement over the short circuit-open circuit method or the symmetric-antisymmetric method when measuring low values of mutual impedance. These advantages have been pointed out by Stratoti and Wilkinson who measured the coupling between short helices.[10]

The impedance of the antenna and its mutual impedance with the other antenna, referred to the feed terminals, are the basic quantities of interest. However for the conical log-spiral, which radiates a broad lobe off the apex of the cone, it is not practical to attempt to measure the magnitude and phase of the voltage across the feed terminals which are situated at this apex. Thus it is necessary to measure the coupling and mutual impedance at some length of a transmission line and, taking into account line loss, transform these quantities down this line to the antenna terminals. Consider the equivalent network in Figure 2(b). Although it is not convenient to establish and measure the open circuit voltage at reference plane $A_2$ (apex terminals of antenna 2), it is still desirable to use the impedance-voltage-ratio method, hence we force $I_2'$, the current at the desired reference plane $B_2$ to be zero. For $I_2' = 0$, and $Z_{11} = Z_{22}$, the terminal impedance $Z_{11}$ and the mutual impedance $Z_{12}$ can be expressed in terms of the measurable quantities $Z'_{11}$, $Z'_{22}$ and $Z'_{12}$ at reference planes $B_1$ and $B_2$, and the characteristic impedance and length of the transmission lines involved, by the following equations:

$$Z_{11} = \frac{\left[jZ_o \tan \beta\ell_2\right]\left[Z_o \frac{Z'_{11} - \frac{Z'^{\,2}_{12}}{Z'_{22}} - jZ_o \tan \beta\ell_1}{Z_o - j\left(Z'_{11} - \frac{Z'^{\,2}_{12}}{Z'_{22}}\right)\tan \beta\ell_1}\right] + \left[jZ_o \text{ Cot } \beta\ell_2\right]\left[Z_o \frac{Z'_{11} - jZ_o \tan \beta\ell_1}{Z_o - jZ'_{11} \tan \beta\ell_1}\right]}{\left[jZ_o(\tan \beta\ell_2 + \text{Cot } \beta\ell_2)\right] + \left[Z_o \frac{Z'_{11} - jZ_o \tan \beta\ell_1}{Z_o - jZ'_{11} \tan \beta\ell_1}\right] - \left[Z_o \frac{Z'_{11} - \frac{Z'^{\,2}_{12}}{Z'_{22}} - jZ_o \tan \beta\ell_1}{Z_o - j(Z'_{11} - \frac{Z'^{\,2}_{12}}{Z'_{22}})\tan \beta\ell_1}\right]} \tag{7}$$

and

$$Z_{12}^{\,2} = Z_{11}^{\,2} - jZ_{11}Z_o \text{ Cot } \beta\ell_2 - Z_{11}Z_o \frac{Z'_{11} - jZ_o \tan \beta\ell_1}{Z_o - jZ'_{11} \tan \beta\ell_1}$$

$$+ \left[Z_o \frac{Z'_{11} - jZ_o \tan \beta\ell_1}{Z_o - jZ_{11} \tan \beta\ell_1}\right]\left[jZ_o \text{ Cot } \beta\ell_2\right] \tag{8}$$

If $\ell_1 = \ell_2$ and $Z_{11}' = Z_{22}'$ only one impedance measurement is required. These equations are developed in the appendix. Since in practice the antennas will be fed by a transmission line of arbitrary length, ralations transforming the terminal impedances $Z_{11}$ and $Z_{22}$ away from the antenna terminals are also given in the appendix.

The coupled energy measured at the antenna terminals may be only a partial indication of the interaction of antennas operated in an array. This is true in particular for traveling wave antennas. Recently Rupp[11] has proposed that this measured characteristic be referred to as the "terminal coupling factor" to differentiate it from a "pattern modification factor". He aptly points out that since traveling wave antennas may couple to each other in a directional manner, a pair of such antennas may be considered to be a radiating directional coupler. Under certain conditions it would thus be possible for more coupled energy to be radiated than transmitted to the terminals. For these reasons a study was made of the modification of the radiation pattern due to the presence of parasitic elements. This study will be the basis for a subsequent report, however representative radiation patterns indicating the general magnitude of pattern distortion are included in the present paper.

## 2.2 The Phase Center

In the parallel array the effective spacing of the antennas is simply the separation between the axes of the cones. In the conical array the effective separation is the spacing in wavelengths between the phase centers of the antennas. Thus a knowledge of the relative position of the phase center is required to calculate conical array patterns. In this section we shall outline a general application of the "backward-wave concept" to the conical log-spiral antenna and in so doing develop a quasi-empirical formula for the location of the phase center of the radiated field.

Mayes, Deschamps, and Patton[12] introduced the basic idea that the logarithmic periodic antenna could be considered to be a locally periodic structure whose period varies slowly, increasing linearly with the distance to the point of excitation. It was pointed out that for normal operation there is a radiation region with a phase of excitation such that the structure will radiate toward the feedpoint. Among such structures the backward wave zig-zag antenna is the counterpart of the log-periodic zig-zag, and the backward wave bifilar helix the periodic counterpart of the conical log-spiral antenna. To apply this concept to the conical log-spiral antenna, it is instructive to consider some of the techniques which have been useful in the study of helices.

Consider the truncated portion of the wire version of the conical log-spiral antenna shown in Figure 3. This structure is of the same basic geometry as the helix, and a local period of the structure can be defined in terms of a helix with parameters equivalent to the corresponding log-spiral parameters averaged over that period. The study of periodic structures such as the helix has been facilitated for a number of years by the use of Brillouin or "$k$-$\beta$" diagrams to display the frequency variation of the propagation constant along the structure. Recently this approach has been applied to radiating structures[13,14].

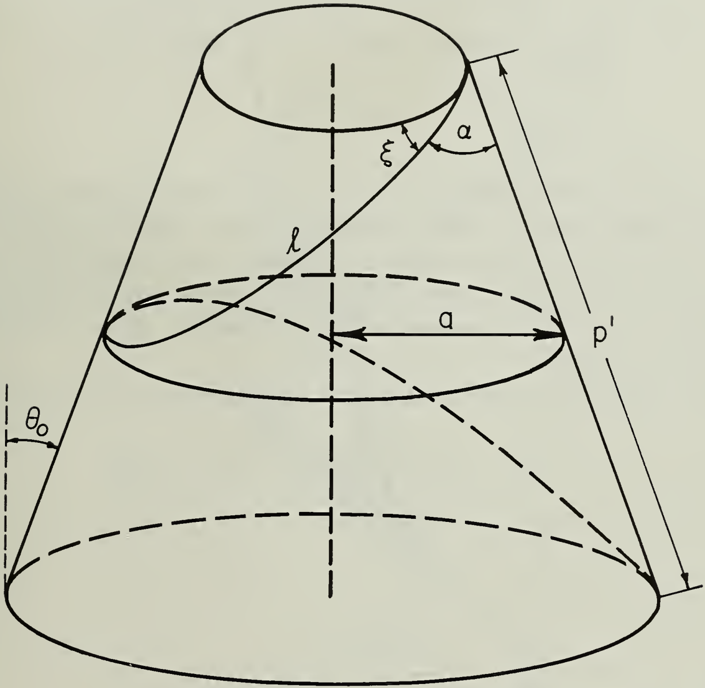

$$\ell = \frac{\rho_2 - \rho_1}{\cos\alpha} = \frac{p'}{\cos\alpha} \qquad \frac{C}{\lambda_0} = \frac{2\pi a}{\lambda_0} = ka$$

Figure 3. Truncated Portion of Conical Log-Spiral Antenna

The solution of the determinantal equation for the real phase constants on the helix, as a function of ka, requires that the fields go to zero amplitude as the distance extends to infinity. As a result we require

$$|\beta_n a| > ka \tag{9}$$

where $\beta_n$ is the phase constant of the nth space harmonic on the structure, k is the phase constant of wave propagation in free space and "a" is the radius of the helix. Thus there are regions in the k-β diagram where the roots of the transcendental equation are real, corresponding to slow waves. Similarly this condition produces so-called "forbidden regions" in which solutions are complex.

The boundaries of these regions can be expressed by the inequalities[15]

$$|m| + \frac{ka}{\cot \xi} \leq \frac{|\beta_n| a}{\cot \xi} \leq |m| - \frac{ka}{\cot \xi} \tag{10}$$

and

$$\frac{ka}{\cot \xi} \leq \frac{N}{2}$$

where for multi-wire helices in the higher modes

$$m = -1 + nN \tag{11}$$

$\xi$ is the pitch angle, N is the number of wires or arms, and n is an integer. For a two wire symmetrical helix with the arms excited with a 180° phase reversal, the k-β diagram takes the form of Figure 4.

The parameters normally plotted for the helix are the pitch normalized to the wavelength in free space and to the wavelength of the surface wave. On the conical spiral the pitch distance on the surface is p', and

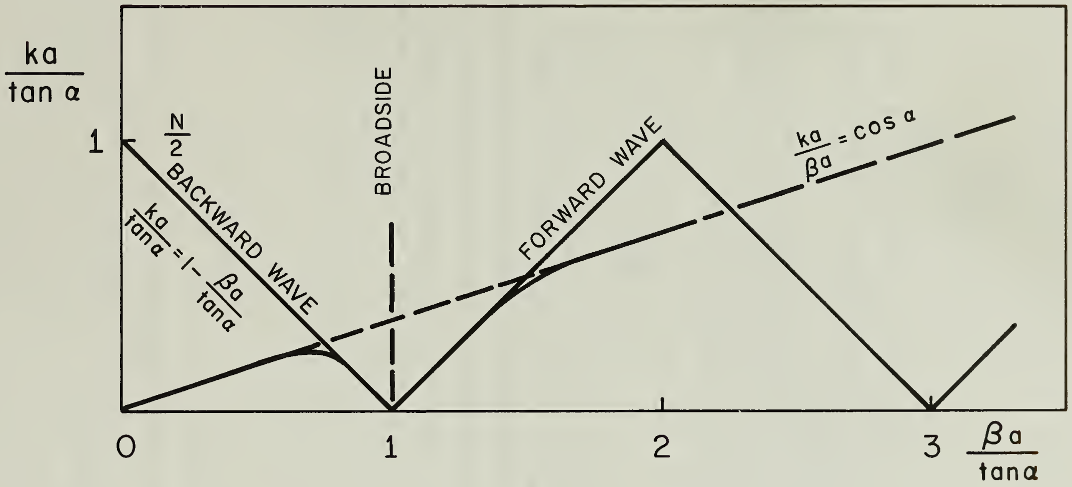

Figure 4. Brillouin Diagram for Bifilar Helix

$$\frac{p'}{\lambda_o} \simeq \frac{ka}{\cot \xi} = \frac{ka}{\tan \alpha}$$

$$\frac{p'}{\lambda_s} \simeq \frac{\beta a}{\tan \alpha} \tag{12}$$

where a is the average radius of the period with pitch p', $\lambda_o$ the wavelength in free space and $\lambda_s$ the wavelength of the surface wave. These are the parameters used in Figure 4.

Sensiper[15] has shown that a good approximation to the locus of phase constants on the helix for ka in the range of interest here, is a straight line drawn through the origin with slope

$$\frac{ka}{\beta a} = \sin \xi \tag{13}$$

and the boundaries of the m = 1 forbidden region. Such an approximation assumes propagation of energy with the speed of light along the arms. Although the determination of the propagation constant along the surface of the cylindrical helix applies to the infinite structure, it has been shown that the solution is useful for interpretation of the characteristics of the finite monofilar endfire helix[16,17] and the finite backward wave bifilar helix[18] with thin wire arms.

On the conical spiral the ratio of the velocity of the slow wave to that in free space is given by

$$\frac{ka}{\beta a} = \frac{p'}{\ell} = \cos \alpha \tag{14}$$

The radius "a" of the cylindrical helix is a constant, therefore as the frequency of operation is increased the parameter ka increases. Under the above approximation, as ka is increased the propagation constant of the wave propagating along the surface of the structure away from the point of excitation increases and as it approaches that of the 1st backward space wave there will be strong coupling between these waves. When coupling begins the propagation constant will depart from the straight line approximation. The slope of this curve at any point on the curve, is the ratio of the group velocity of the surface wave, $v_s$, to that in free space and hence when

$$\frac{d(ka)}{d(\beta a)} = \frac{v_s}{v_o} = 0 \tag{15}$$

propagation in the surface wave stops. This point corresponds to one end point of a stop band. For ka above this point the propagation constant is complex[19]. In the open structure this implies a transfer of energy to the backward space wave, and experimental evidence indicates that the effective phase center of the antenna is located in this region in normal backward wave radiation. As ka is increased further it is possible to force the beam to scan through the visible region of the spectrum.

In the above discussion we have considered operating conditions with a change in ka. On a periodic structure such as the helix, with constant radius and pitch angle, a change in ka implies a change in the frequency of operation. On the conical log-spiral antenna the spiral angle $\alpha$ is constant but the radius "a" is a linearly varying function of the distance from the apex along the conical surface. Thus a change of ka can result from either a change in position on the cone or from a change in frequency. Further, on the structure of infinite length any particular value of ka can be found for any frequency of operation. Thus, to consider the behavior of the structure one of these two variables must be held fixed. Again, we will consider only those waves predicted by the straight line approximation above, since there is experimental evidence indicating that only the lowest order mode, consistent with the excitation and winding of the arms, contributes significantly to the radiation pattern of the two arm balanced conical antenna when operated such that there is negligible "end effect"[20].

If we assume operation at a fixed frequency, a wave propagating along the arms away from the apex implies an increasing ka. Hence at some point on the structure, the propagation constant of the surface wave associated with the flow of energy along the arms increases until there is coupling of energy to the backward space wave and rapid radiation. Experimental evidence indicates that the position of the phase center, expressed in wavelengths to the apex, remains essentially fixed.[*] Therefore since $a/\lambda_o$ at the phase center remains constant, ka remains constant for all frequencies of operation, excluding those frequencies where normal operation is distorted by the finite truncations of the antenna, i.e. end-effect. The operating point of the frequency independent antenna does not scan along the line $ka = \beta a \cos \alpha$ with a change in frequency; instead the parameters ka and $\beta a$ scale with frequency.

In Figure 4 if we calculate an expression for the intersection of the asymptote

$$ka = \beta a \cos \alpha \tag{16}$$

and the edge of the m = 1 forbidden region, we obtain the expression

$$ka = \frac{\sin \alpha}{1 + \cos \alpha} \tag{17}$$

which is the circumference such that the antenna is phased to radiate backward along the surface of the cone. However, a study of the symmetry of the conical antenna indicates that all radiation from that along the surface of the cone out to that at an angle of $\theta_o$ from the surface will radiate in the backward direction. Thus it can be shown that the average circumference, of the period such that the following relationship is satisfied is the approximate region on the conical log-spiral structure that is phased for backward radiation.

$$\frac{\sin \alpha}{1 + \cos \alpha} \leq ka \leq \frac{\sin \alpha}{1 + \cos \alpha \cos \theta_o} \tag{18}$$

If the efficiency of excitation of the first backward space wave is high enough, it can be postulated in the light of the above discussion that the radiating region is confined to approximately that circumference which satisfies Equation (18). However, Sensiper has shown that the approximation due to the use of the asymptote and the region boundaries results in a ka that is slightly high since the coupling between these waves forces the curve down. Thus, this intersection point can be considered as only an upper bound for the start of the backward wave radiating region.

---

[*] For example see Figure 10.

The measured phase centers of several antennas with narrow constant width arms and with cone and spiral angles varying from $15^{\circ} \leq 2\,\theta_o \leq 30^{\circ}$ and $60^{\circ} \leq \alpha \leq 83^{\circ}$ are plotted in Figure 5. These phase centers occur at a ka below the intersection point and their location on the k-β diagram may be approximated by a straight line.

The orientation of this line is interesting. The distance between the intersections of the asymptote for that particular antenna and this line, and the edge of the m = 1 forbidden region is directly related to the beamwidth of the antenna. As this distance decreases more of the active region is moved into the visible region of the spectrum and more energy is radiated at an angle from the surface. Wire antennas wound with an $\alpha$ of $60^{\circ}$ have a wide beamwidth (on the order of 110 to $120^{\circ}$) while those with $\alpha = 83^{\circ}$ have patterns with beamwidths on the order of 70 degrees. The line also implies that at a spiral angle $\alpha$ of $45^{\circ}$ the antenna at the phase center (and hence we could expect the major portion of the active region) is phased to radiate at an angle from the axis of the antenna. In agreement with this, it has been determined that thin wire antennas wound with an $\alpha$ of $45^{\circ}$ have multiple sidelobes and a major portion of the radiation directed in an endfire direction.

The data plotted in Figure 5 is for wire antennas. From pattern information, and a previous study of the near fields on the planar antenna, we might expect the slope of the approximate locus of the phase centers for antennas with wider exponentially expanding arms, to become more negative and thus more nearly parallel to the region boundary, with a minimum change for large $\alpha$.

If we calculate an expression for the intersection of the phase center line and the asymptote, taking into account the cone angle $\theta_o$ we get the approximate expression

$$ka \simeq \frac{1.2 \sin \alpha}{1.4 + \cos \alpha \cos \theta_o} \tag{19}$$

Equations (17) and (19) have been plotted in Figure 6. Families of curves,

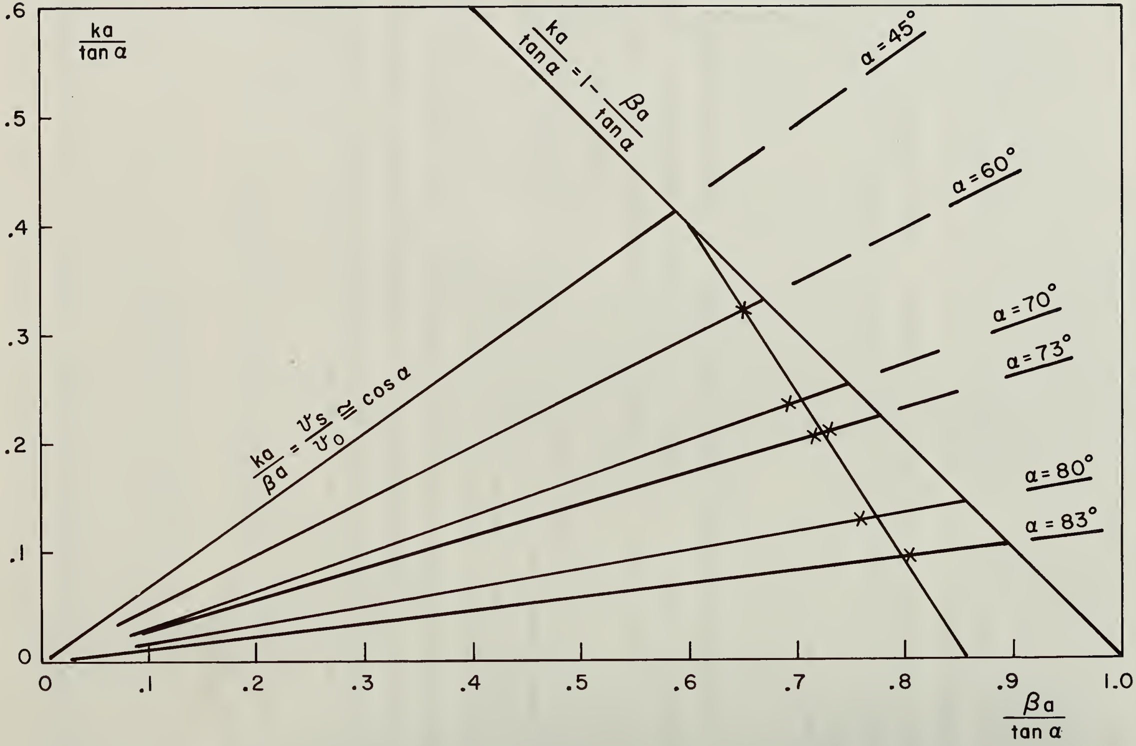

Figure 5. Measured Phase Centers for Several Wire Arm Conical Log-Spiral Antennas

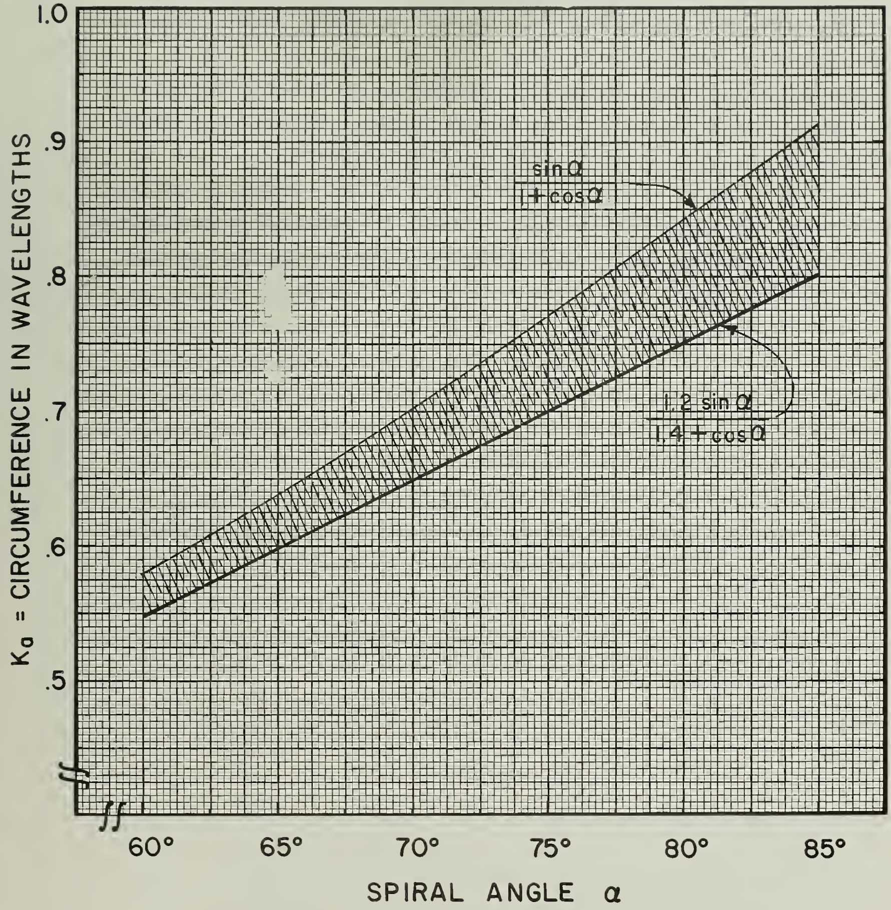

Figure 6. Approximate Circumference in Wavelengths at the Phase Center of Balanced Wire Arm Conical Log-Spiral Antennas (N=2, m=1)

one for each value of $\theta_o$ could be plotted, but for antennas that are good unidirectional radiators the cone angle varies as $10^o \leq 2\theta_o \leq 45^o$ and therefore $.996 \leq \cos\theta_o \leq .924$. Thus $\cos\theta_o \simeq 1$, and it is felt that the single curves are sufficient.

For normal frequency independent operation, the circumference at the phase center should lie within this bounded region. Present information indicates that it will lie on or near the lower boundary.

A recent study of the near fields on the conical log-spiral antenna by McClelland indicates good agreement between the measured characteristics of the near fields and those predicted in terms of the applications of the above concepts.[21]

## 3. EXPERIMENTAL CONSIDERATIONS

The conical log-spiral antenna with controlling parameters and an associated coordinate system is shown in Figure 7. For the present investigation a series of antennas with parameters $2\theta_o = 15^o$, D = 17.5 cm, d = 4.5 cm, h = 47.3 cm and $\alpha$ = 60, 73, and $83^o$ were used. The antennas were constructed from 1/4 inch copper tubing supported by 1/2 × 1 inch wood struts as shown in Figure 8. The feed cable RG-141/U was carried through one of the arms to the apex of the cone.

All measurements were made at a frequency of 610 mc which, for these antennas was near the low end of the range of frequencies where the antennas could be expected to operate in a frequency independent manner. Thus the active region was at the lower portion of the antenna and, in the case of parallel antennas, the coupling could be expected to be the tightest.

The approximate half-power beamwidth of the radiation patterns of these antennas is shown in Table I.

TABLE I

HALF-POWER BEAMWIDTH OF RADIATION PATTERN OF CONICAL ANTENNA

$2\theta_o = 15^o$, 1/4 copper arms, D = 17.5 cm, d = 4.5 cm, f = 610 mc

| | $\varphi = 0$ | | $\varphi = 90$ | |
|---|---|---|---|---|
| $\alpha$ | $E_\theta$ | $E_\varphi$ | $E_\theta$ | $E_\varphi$ |
| $60^o$ | 118 | 116 | 117 | 137 |
| $73^o$ | 77 | 83.5 | 78 | 85 |
| $83^o$ | 64.5 | 65 | 63.5 | 70 |

These values of the half-power beamwidth are only approximate since there is some variation in beamwidth with the angle $\varphi$. For the individual antenna, $\varphi = 0$ is arbitrarily taken to be the plane of the feed gap between the ends of the antenna arms at the truncated apex of the cone. Thus initially the two arms lie perpendicular to the $\varphi = 0$ plane.

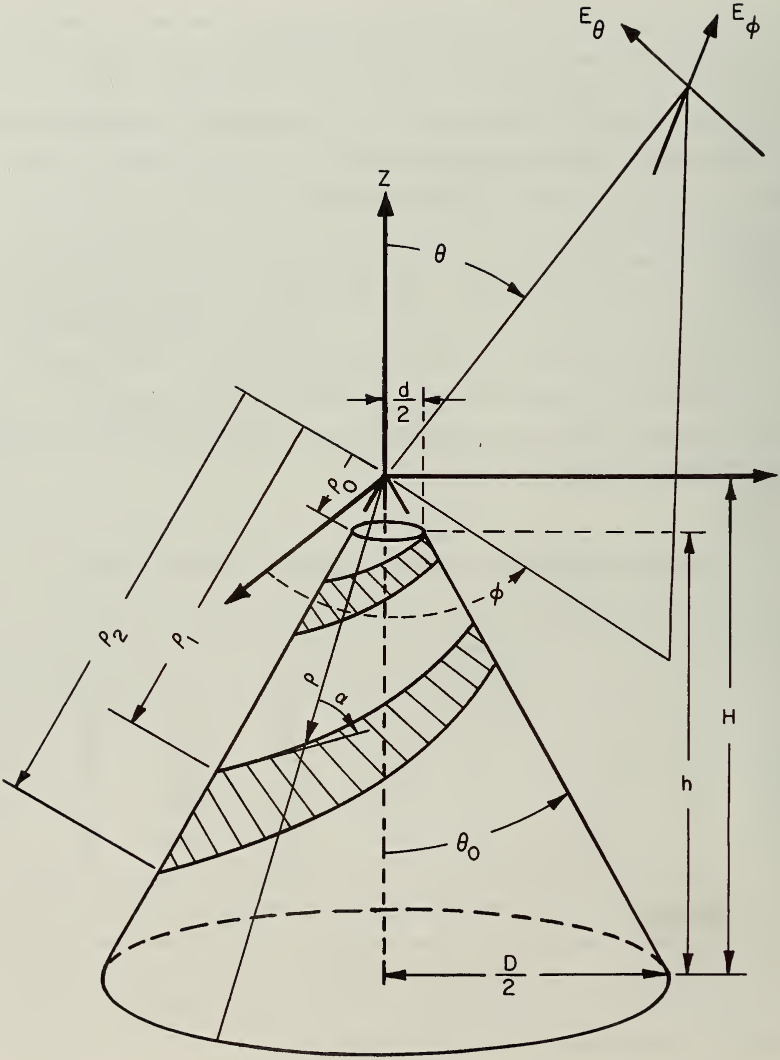

Figure 7. A Conical Antenna with Associated Coordinate System

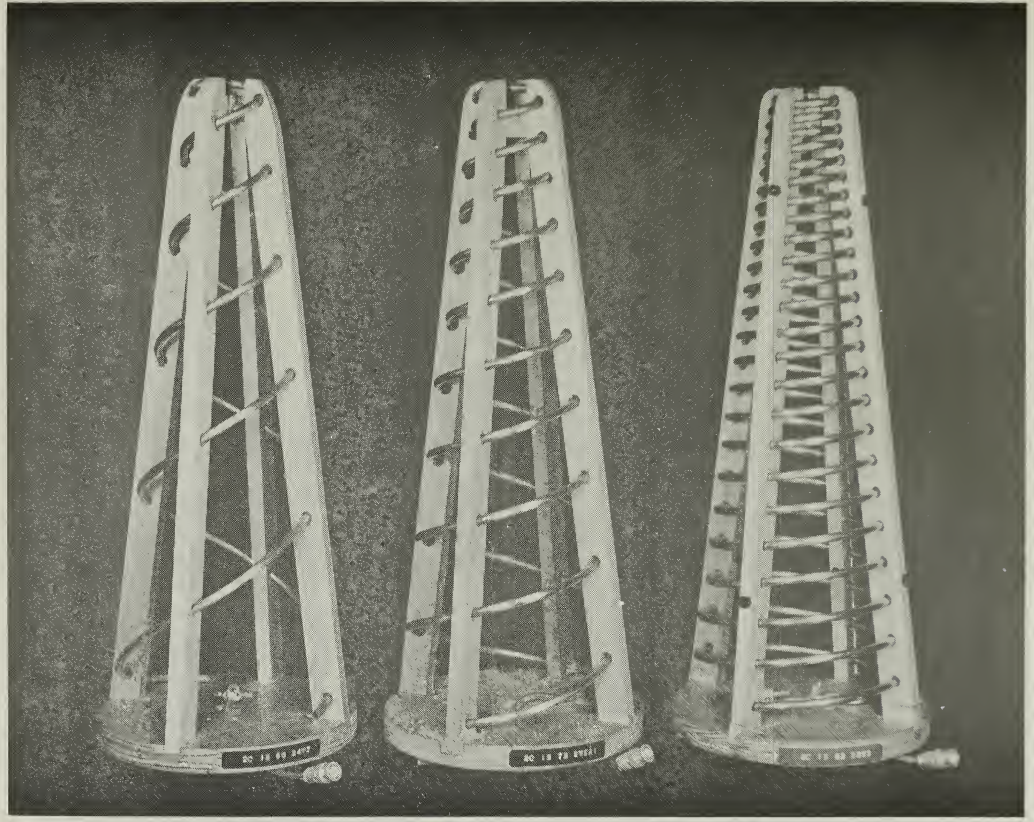

Figure 8. Photograph of Conical Log-Spiral Antennas

The apparent phase centers of the individual antennas referred to in Figure 5 were determined by mounting the antenna in question on a vertical rotating mast with the axis of the antenna perpendicular to the mast and measuring the phase of the received signal from a distant transmitting antenna. The center of rotation of the antenna was adjusted for a minimum phase variation over a $120^{\circ}$ sector in the direction of the radiated beam. Over most of this sector an apparent phase center on the axis of the antenna was well defined. For the three antennas in Figure 8, the distance from the phase center to the true apex of the cone is shown in Figure 9 for the range of parameters of interest. This distance in wavelengths is also plotted as a function of frequency, for one value of the spiral angle $\alpha$, in Figure 10. The distance to the phase center in wavelengths remains essentially constant with a change in frequency of operation.

The position of the phase center was initially measured for two orthogonally oriented incident waves ($E_{\theta}$ and $E_{\varphi}$). For these antennas, the apparent phase center differed by considerably less than 1/10 wavelength for the two polarizations. Moreover, since the phase center for a circularly polarized incident wave was measured to be the average of the two positions for orthogonal linearly polarized waves, measurements were confined to this condition.

A schematic diagram of the experimental set up used to measure the coefficient of coupling and mutual impedance is shown in Figure 11. The voltage probes at plane B were loosely coupled to the transmission line and carefully balanced. The measurement of the input impedance, $Z'_{11}$, and the coefficient of coupling, $k'$, (equal to the complex ratio of $V'_2/V'_1$) at reference plane B was by means of established methods.

For a fixed arbitrary length of lossless transmission line Equation (8) will provide the terminal impedance $Z_{12}$. However for a systematic study of this impedance these equations involve a great deal of computation. If the transmission line can be any desired length, it is convenient to make it a multiple of $\lambda/2$. For $\ell_1 = \ell_2 = n\lambda/2$ it can easily be shown that $Z_{11} = Z'_{11}$ and $Z_{12} = Z'_{12}$.

For the present study, the feed lines were constructed to be a multiple of a half-wavelength for all measurements except one. As a check on the transformation equations, $Z'_{12}$ was measured at the end of an arbitrary length of line and transformed to the apex terminals. These results were checked against measurements made with $\ell = n\lambda/2$.

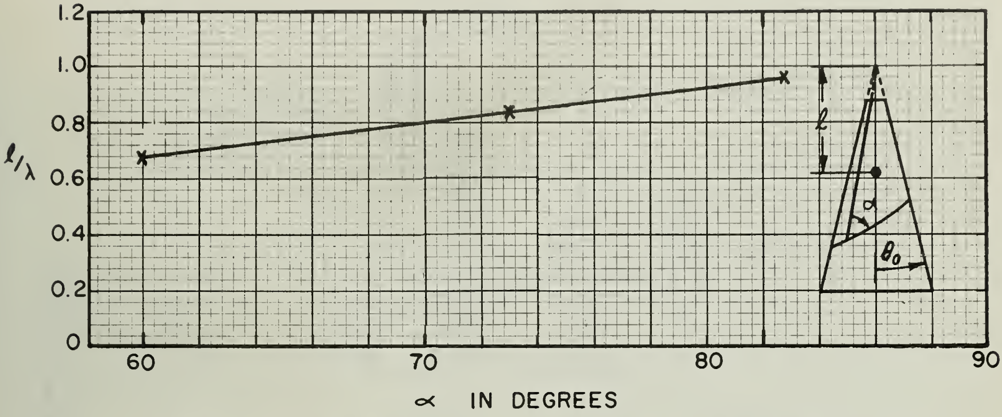

Figure 9. Phase Center Location in Wavelengths from the Vertex of 15° Conical Wire-arm Antenna Versus Spiral Angle

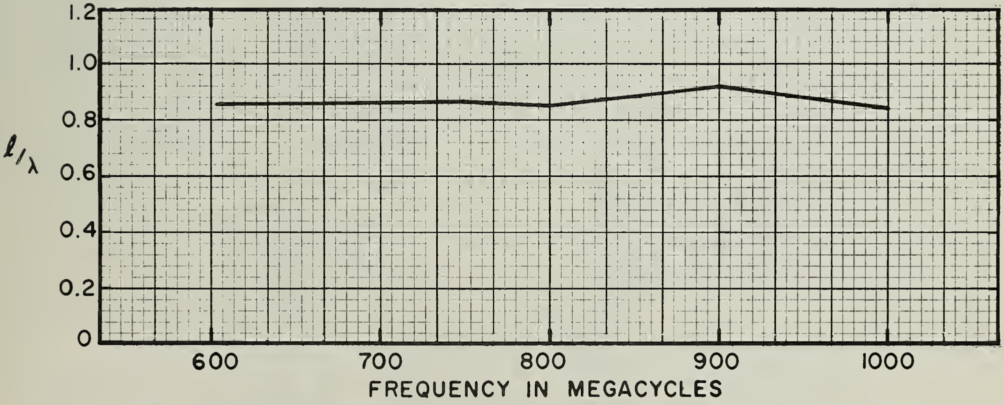

Figure 10. Phase Center Location in Wavelengths from the Vertex of a 15° Conical Wire-arm Antenna as a Function of Frequency, $\alpha = 73^{\circ}$

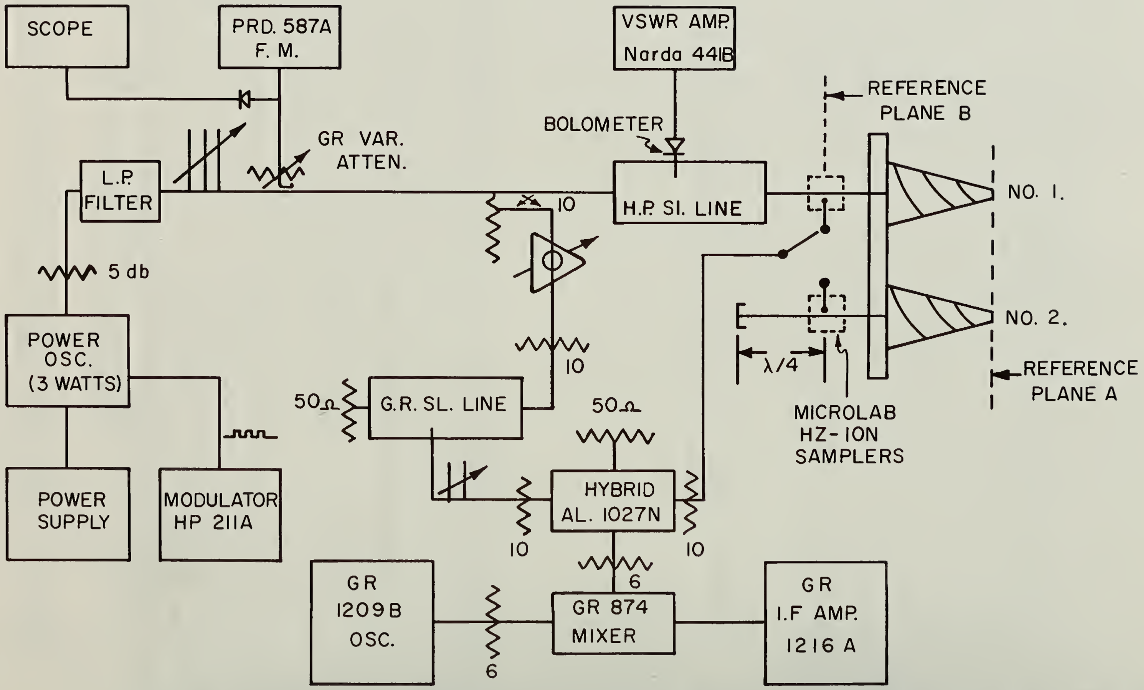

Figure 11. Experimental Set Up for Measuring the Complex Coefficient of Coupling and Mutual Impedance

# 4. MEASUREMENTS

## 4.1 Coefficient of Coupling

### 4.1.1 Parallel Arrays

The magnitude of the coupling coefficient for parallel antennas is plotted in Figure 12. The measured coupling is low, approximately -27 db for $\alpha$ of $60^{o}$, and -41 db for $\alpha$ of $73^{o}$ and $83^{o}$ at $S = \lambda/2$. The antennas having a wider beamwidth($\alpha = 60^{o}$) are more closely coupled than those with a narrower beamwidth. There is some scatter of the measured points for larger separations. This was attributable to back scatter at the site. Although the antennas were outdoors, it was determined that there is approximately a 5 db possible error due to the site for separations on the order of a wavelength or more where the coupling level was -50 db or greater. The coupling for $\alpha = 60$ and $73^{o}$ decreases approximately 6 db each time the spacing is doubled. For $\alpha = 83^{o}$ the measured decrease is somewhat greater possibly due to the increased directivity of these antennas.

The variation in terminal coupling as a function of relative rotation of one of the antennas is plotted in Figure 13. These antennas are more closely coupled when oriented in a like manner, and loosely coupled when rotated $90^{o}$ with respect to each other. The major portion of this variation was traceable to coupling between the truncated tips of the antennas. At the tip truncation, the arms leave the spiral geometry and effectively become a small dipole lying in a plane perpendicular to the axis of the cone. When the antennas were oriented for $\phi = 0$ these "dipoles" were parallel and the total measured coupling is due to this dipole feed and the conical spiral arms. This is shown quite well in Figure 14, where contrawound antennas were pointed directly at each other and one rotated with respect to the other. Maximum coupling occurs when the dipole feeds are parallel and minimum coupling occurs when they are orthogonal.

The truncated tip of these antennas was $.1\lambda$ at the frequency that all measurements were made, and although the variation in coupling with rotation, and the general level of coupling as well, depends upon the size of this tip truncation, it was felt that these data are representative. The conical antenna will rarely be used in arrays at frequencies such that the tip truncation is greater than $.2\lambda$ and in most applications it will probably

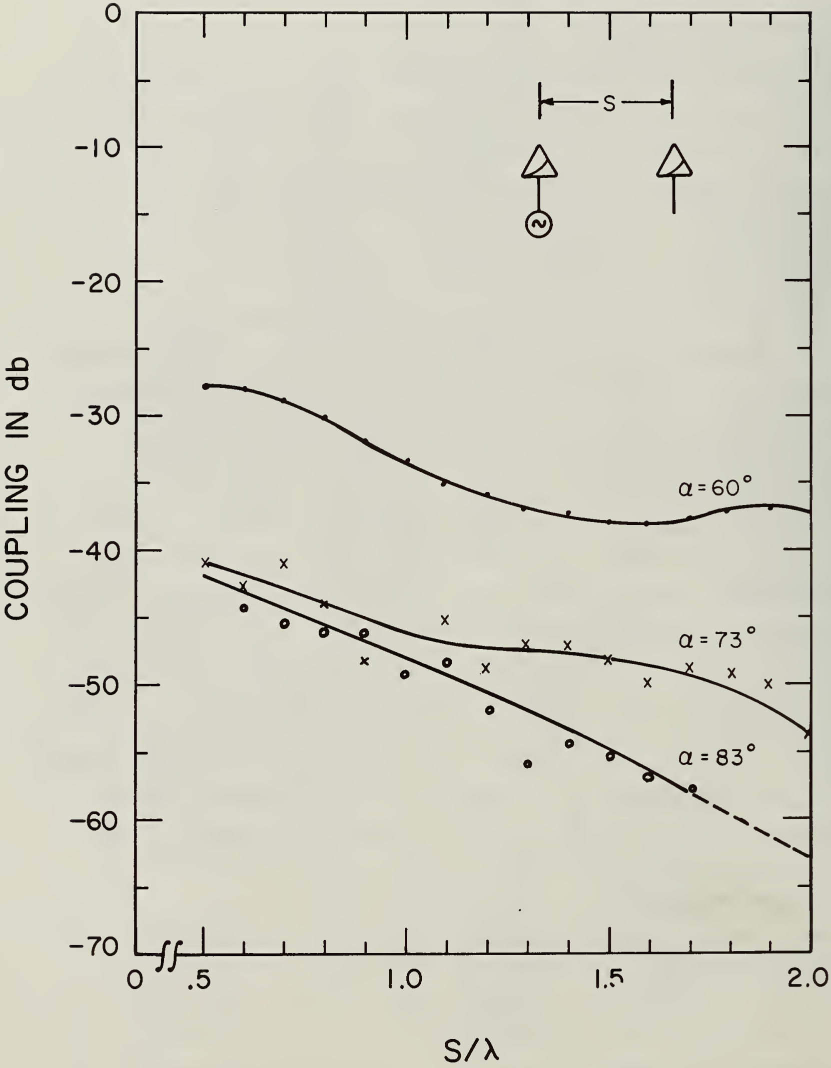

Figure 12. Magnitude of Coupling Coefficient Measured Between Parallel Antennas as a Function of Spacing Between Antennas in a Parallel Array

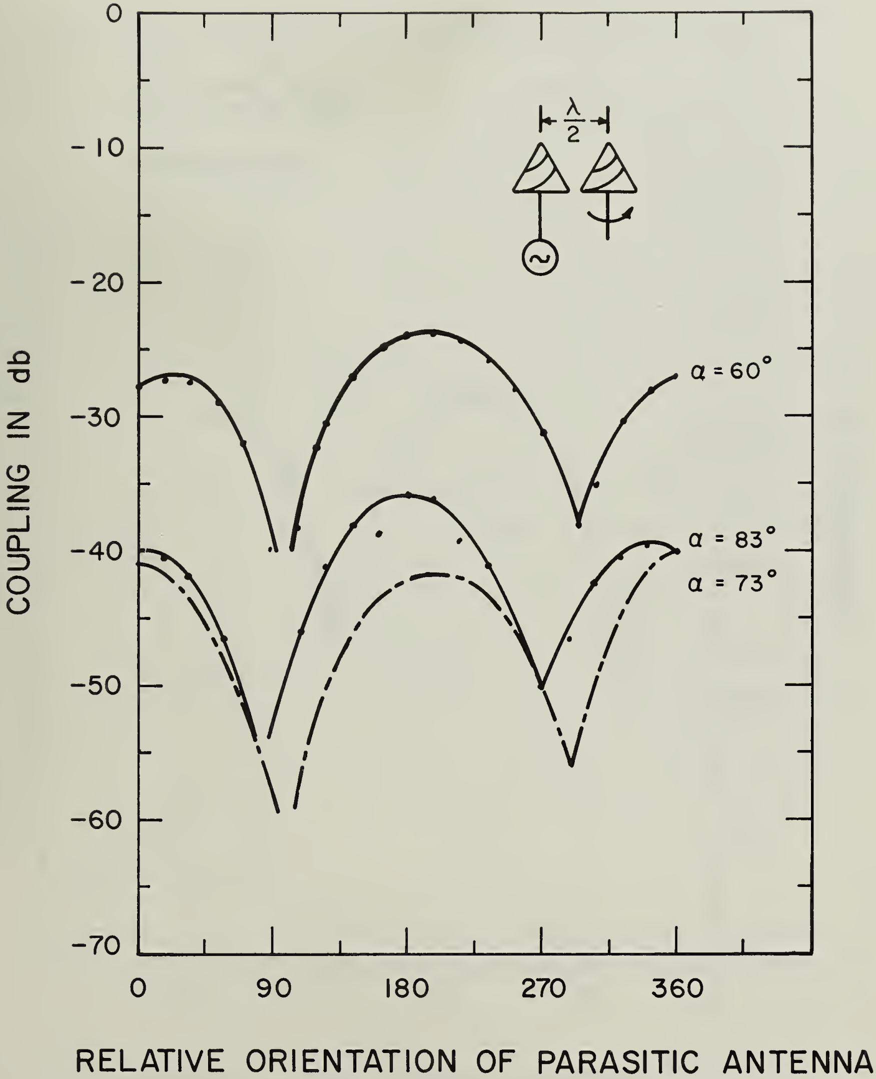

Figure 13. Coupling as a Function of Rotation in a Parallel Array

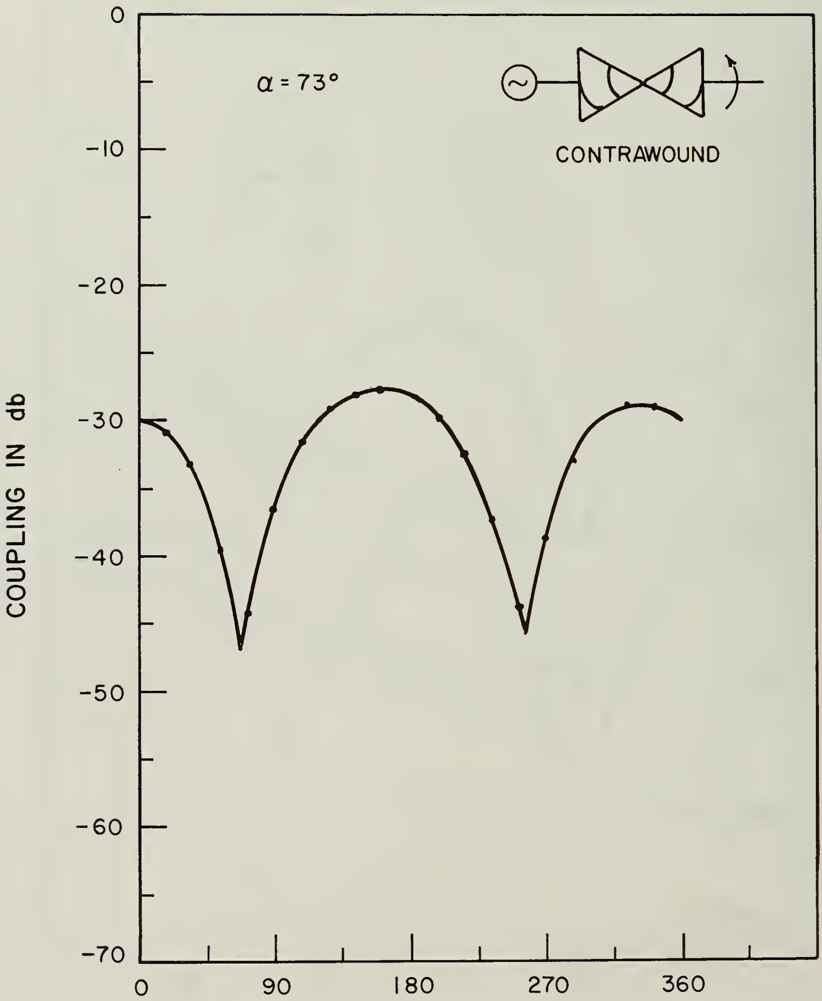

RELATIVE ORIENTATION OF ANTENNAS

Figure 14. Coupling Between Contrawound Antennas Directed at Each Other to Indicate Dipole Coupling Effect

be less than .1λ. Thus the general level of coupling measured should be representative or even conservative. Although a rotation of these antennas to phase an array would cause as much as 10 db variation in the coupling, the general level of coupling is so low that, as indicated later, the change in mutual impedance is small compared to the self impedance of the antennas.

Figure 15 indicates that the coupling from the $n^{th}$ to the $n + 1$ and at least to the $n + 2$ element must be considered. It is interesting to note that there is almost a 90° shift between curves B and C. This shift varied from 90° for 83° antennas to only 20° for $\alpha = 60°$ antennas. The period of curve C shifts slightly along the horizontal axis with rotation of the center antenna, indicating that there must be some coupling through or reradiation from the center antenna as well as direct coupling between the outside antennas. Again the general level and variation with rotation is influenced by the "dipole feed".

Terminal coupling between right and left hand wound antennas shown in Figure 16 is on the same order of magnitude as that between like antennas, with the coupling between the contrawound antennas actually a little higher for close spacing. The term contrawound is used in this paper to mean an antenna with a winding of the opposite sense to that of the antenna to which it is coupled. It is not used to mean one antenna with arms wound in both a right and left hand direction. The character of the curves is undoubtedly a function of the reflections at the site which return with the opposite sense of polarization. The dashed lines may be a more valid estimate of the true coupling. In Figure 17 the data measured as a function of rotation does not exhibit a well-defined character and again the variations are probably due in part to reflected energy.

### 4.1.2 Conical Arrays

The coupling between conical log-spiral antennas in a conical array is considerably greater, as shown in Figure 18. Data was taken for a range of $\psi$, the array angle. For minimum $\psi$, approximately 17°, the struts of these antennas were just touching. In this position the separation angle between the surface of the cones was 2 degrees. Unlike the parallel case, the surfaces of the cones are now closely coupled over the portion of the antenna that supports a strong surface wave. In addition the tip of the parasitic antenna is in strong fields radiated back toward the tip of the driven element.

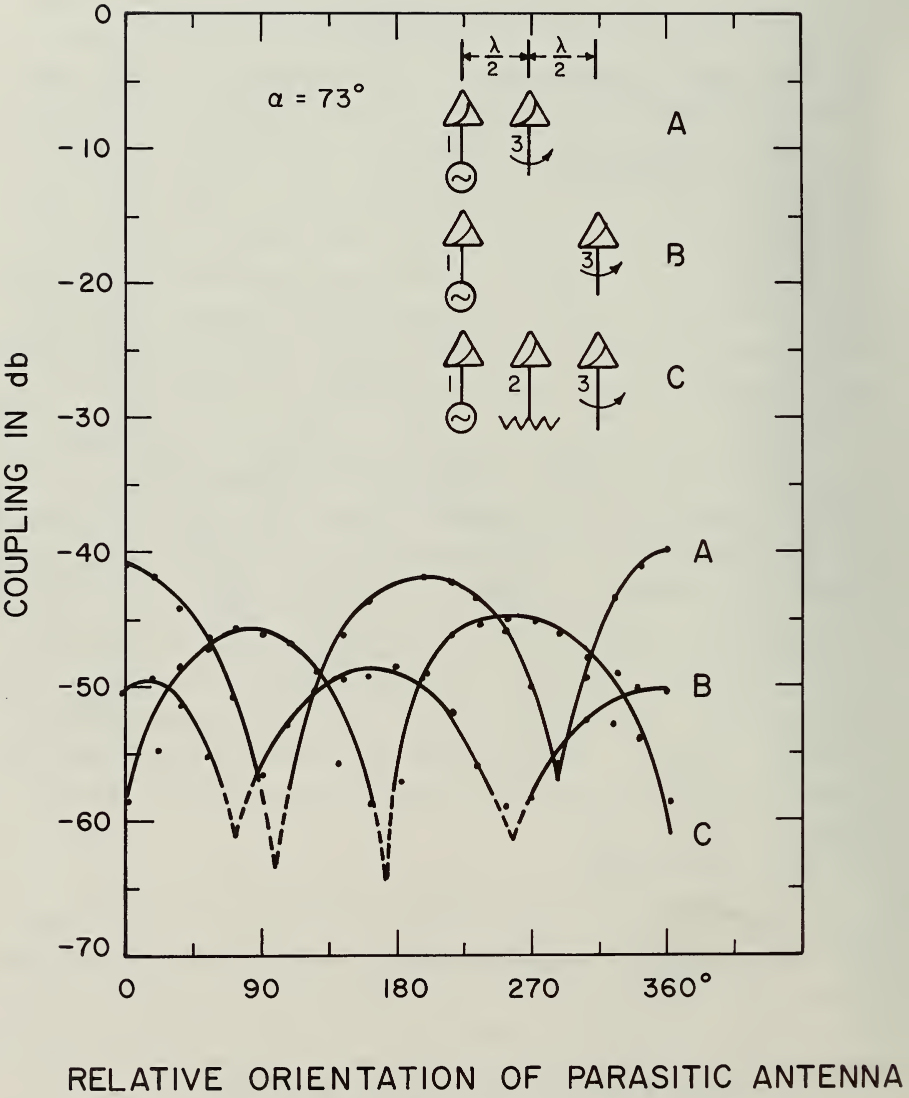

Figure 15. Coupling Between the n<sup>th</sup> and n+2 Element in a Parallel Array

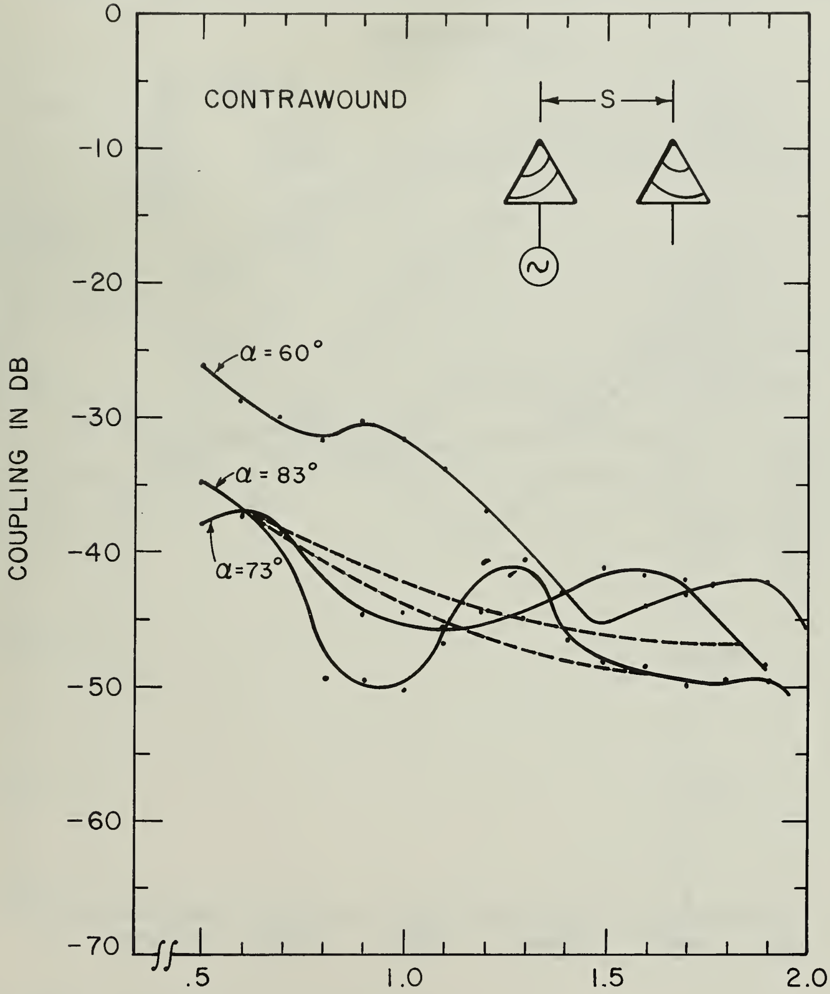

Figure 16. Coupling Between Contrawound Antennas as a Function of Spacing in a Parallel Array

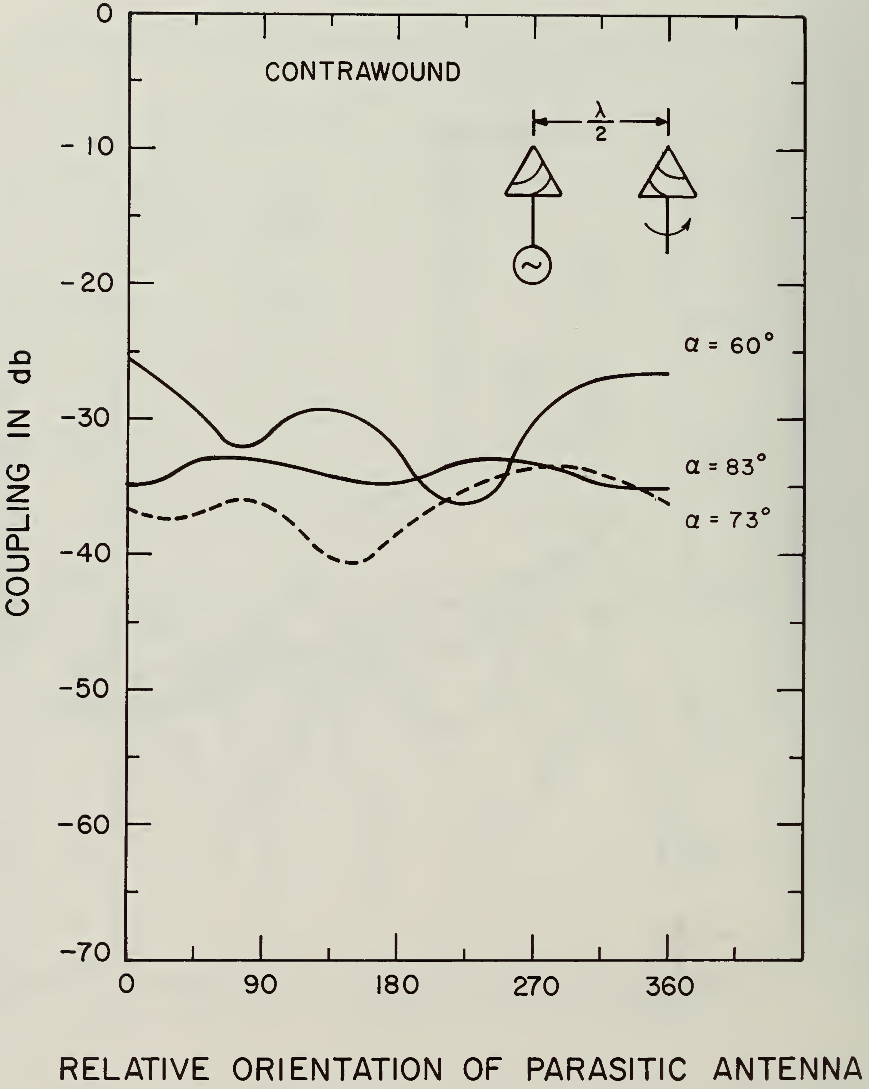

Figure 17. Coupling Between Contrawound Antennas in a Parallel Array as a Function of Relative Rotation

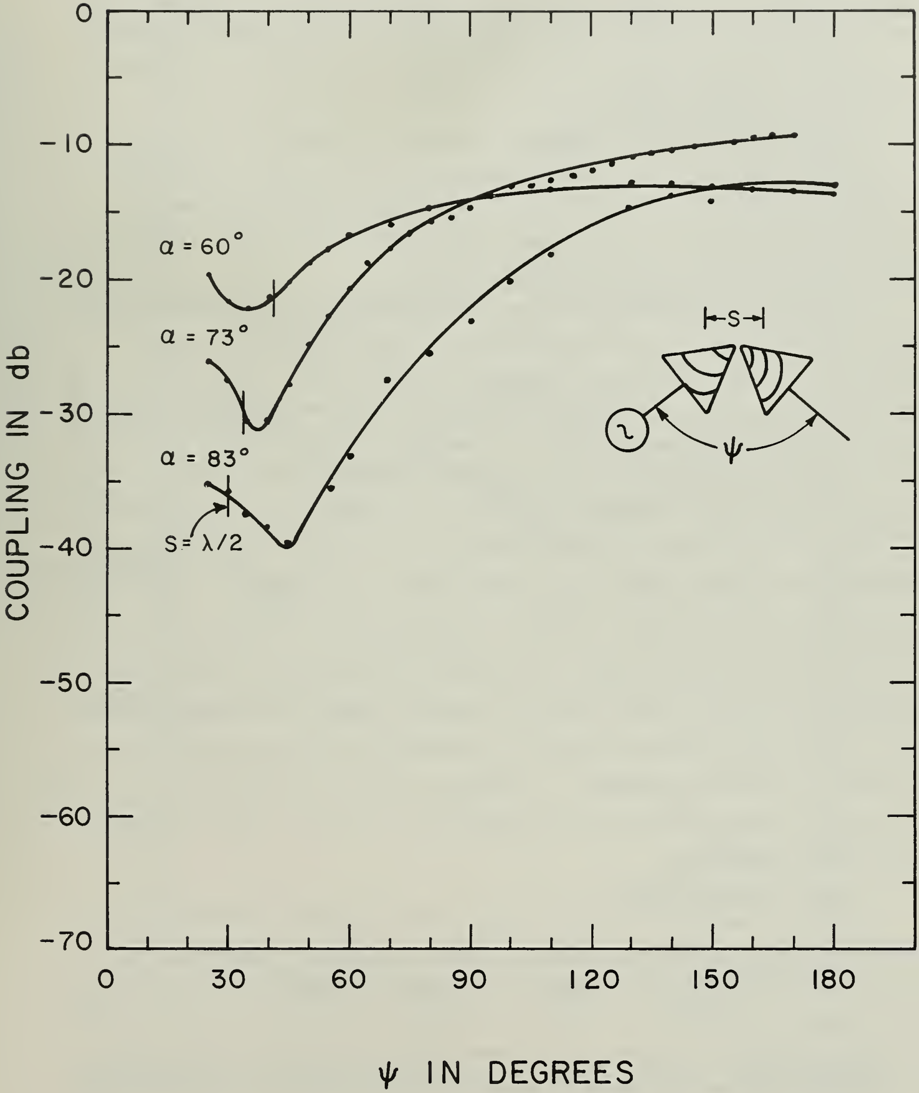

Figure 18. Magnitude of Coupling Coefficient Measured Between Antennas in a Conical Array as a Function of the Array Angle

Measured values of terminal coupling were approximately -18, -26, and -35 db for $\alpha$ of 60°, 73°, and 83°. As the radiation patterns indicate in a later section, in this case more of the coupled energy appears to be reradiated than reflected back to the feed.

As the array angle was increased, coupling decreased to a minimum at an angle of approximately 35 to 50° depending upon the spiral angle $\alpha$. A further increase in $\psi$ increased the coupling due to the fact that the antennas were tending to radiate more energy toward each other. In the limit when $\psi \doteq 180°$ there is maximum coupling.

This curve should be interpreted in conjunction with the radiation patterns which indicate that the array angle, $\psi$, will normally be limited to around 60° or less to maintain reasonably low side lobes. Since S is a function of $\psi$, the dual scales on several later figures (Figures 29, 30, 31) may be used as nomograms to convert to spacing in wavelengths.

Figure 19 indicates less variation with rotation than for the parallel configuration. The increase in variation with increasing $\alpha$ is due in part to the fact that these curves are taken with $\lambda/2$ between phase centers, and hence the array angle (and of more significance, the separation angle between the surfaces of the cones) is smaller for the $\alpha = 83°$ antennas. Figure 20 indicates that in this array as well, the coupling to the second antenna in an array is on the same order of magnitude as the coupling to the nearest neighbor. For small array angles the coupling between contrawound antennas in a conical array shown in Figures 21 and 22 is on the same general level as that for identical antennas. It however does not increase with an increase in the array angle since the two antennas are of opposite sense of polarization.

## 4.2 Mutual Impedance

### 4.2.1 Parallel Arrays

The real and reactive parts of $Z_{11}$ and of the mutual impedance, $Z_{12}$, measured between parallel antennas are shown in Figure 23 through 28. As the coefficient of coupling indicates, the mutual impedance is low. For an $\alpha$ equal to or greater than 73° the real and reactive parts of the mutual impedance between antennas with the same sense of winding are less than 1 ohm. For antennas with opposite sense of winding they are less than 2 ohms.

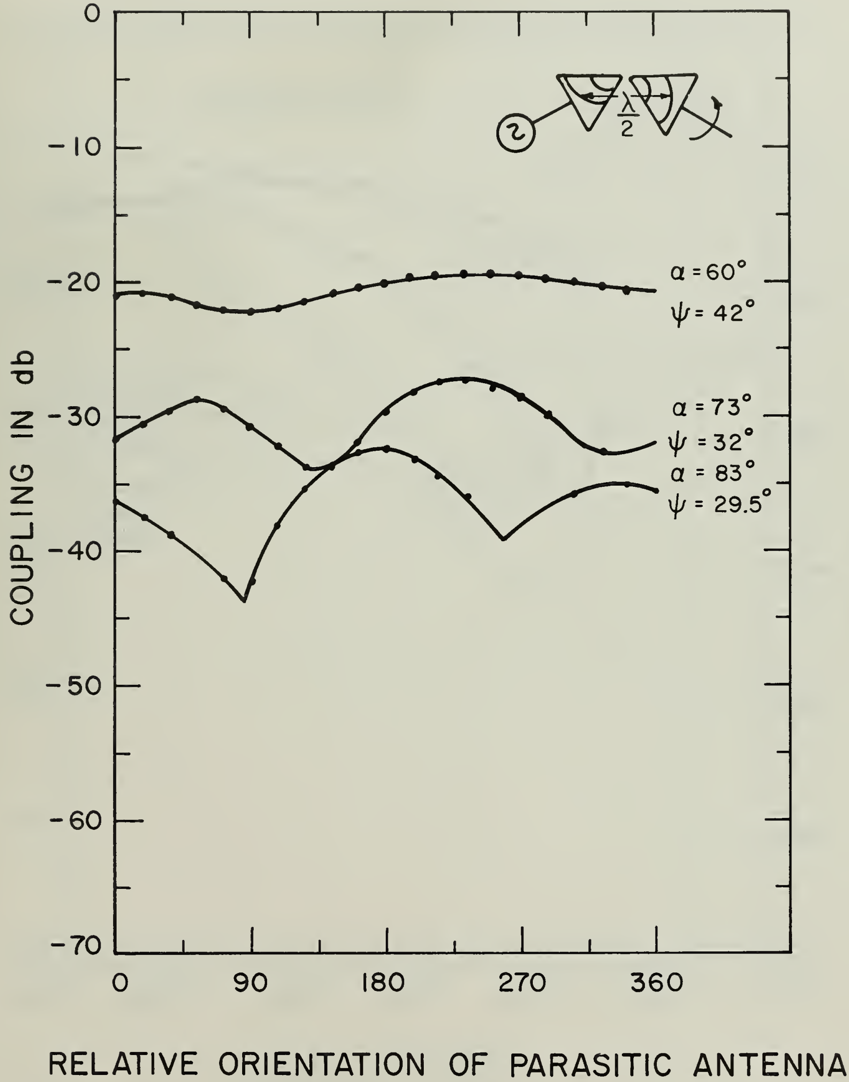

Figure 19. Coupling as a Function of Rotation in a Conical Array

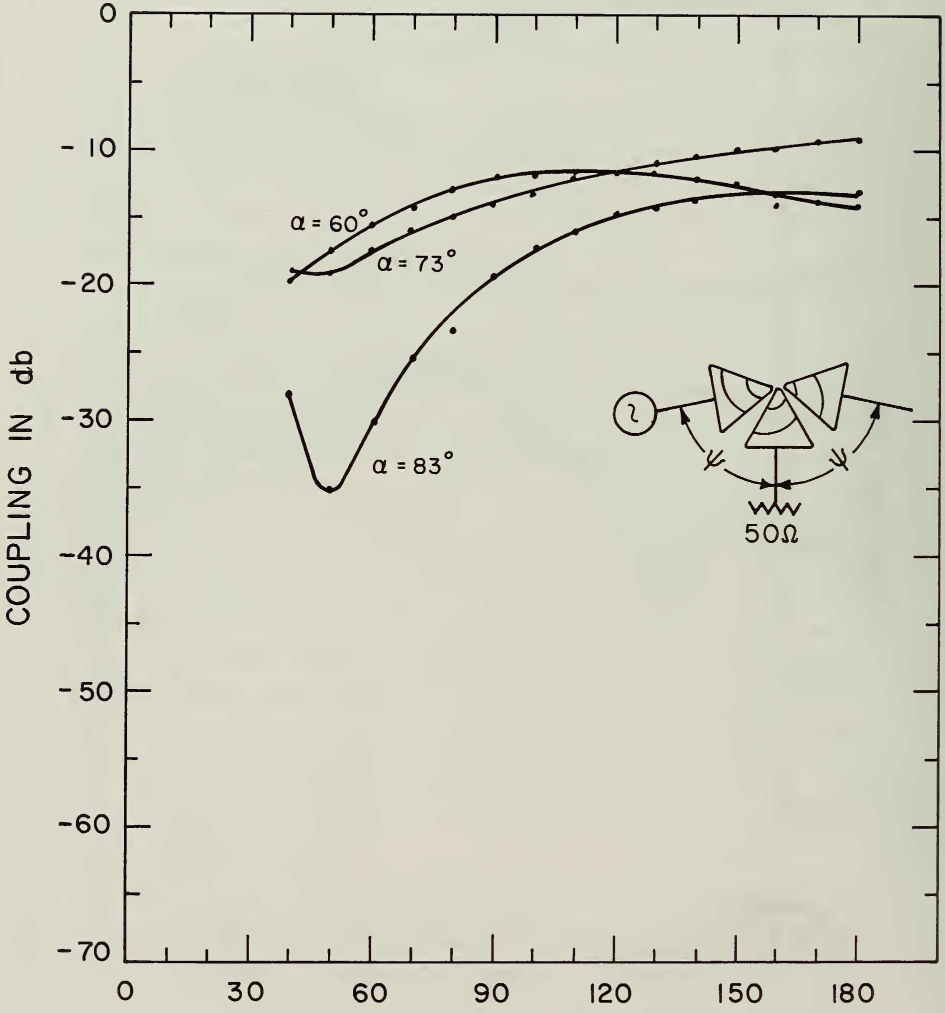

## 2ψ IN DEGREES

Figure 20. Coupling Between the nth and n+2 Element in a Conical Array

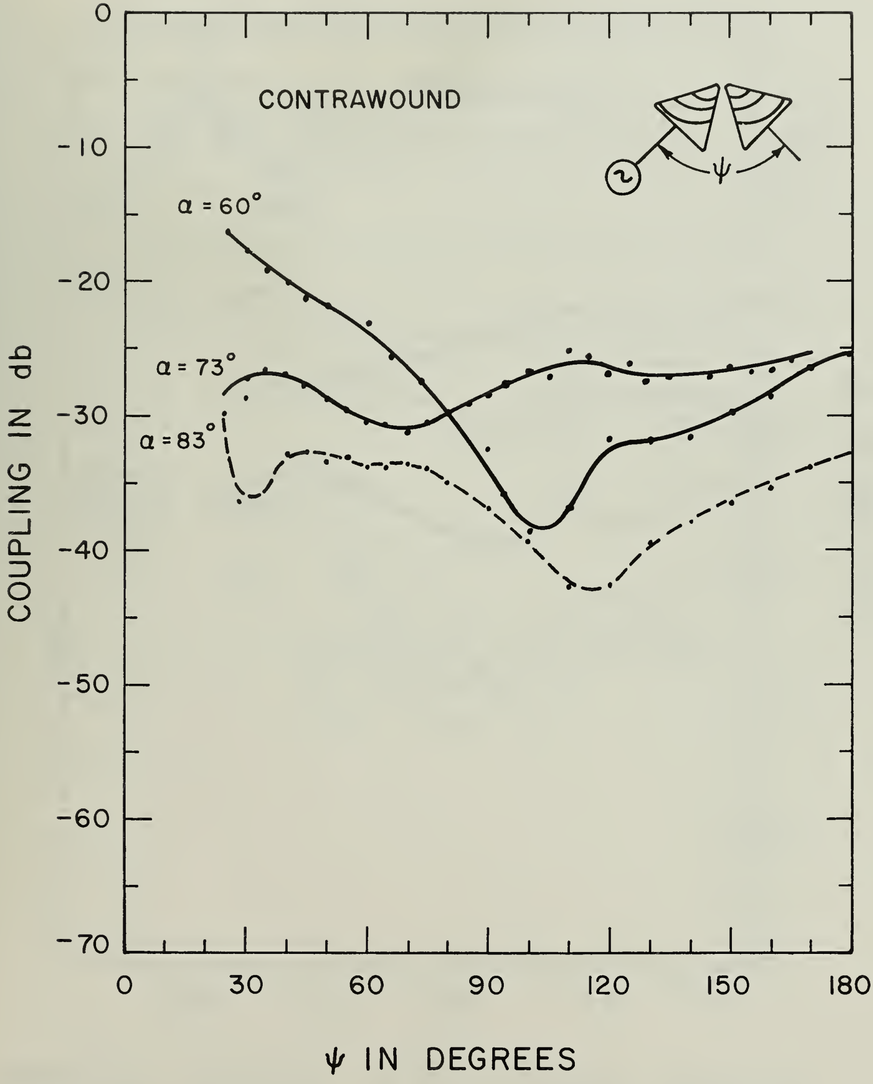

Figure 21. Coupling Between Contrawound Antennas in a Conical Array as a Function of the Array Angle

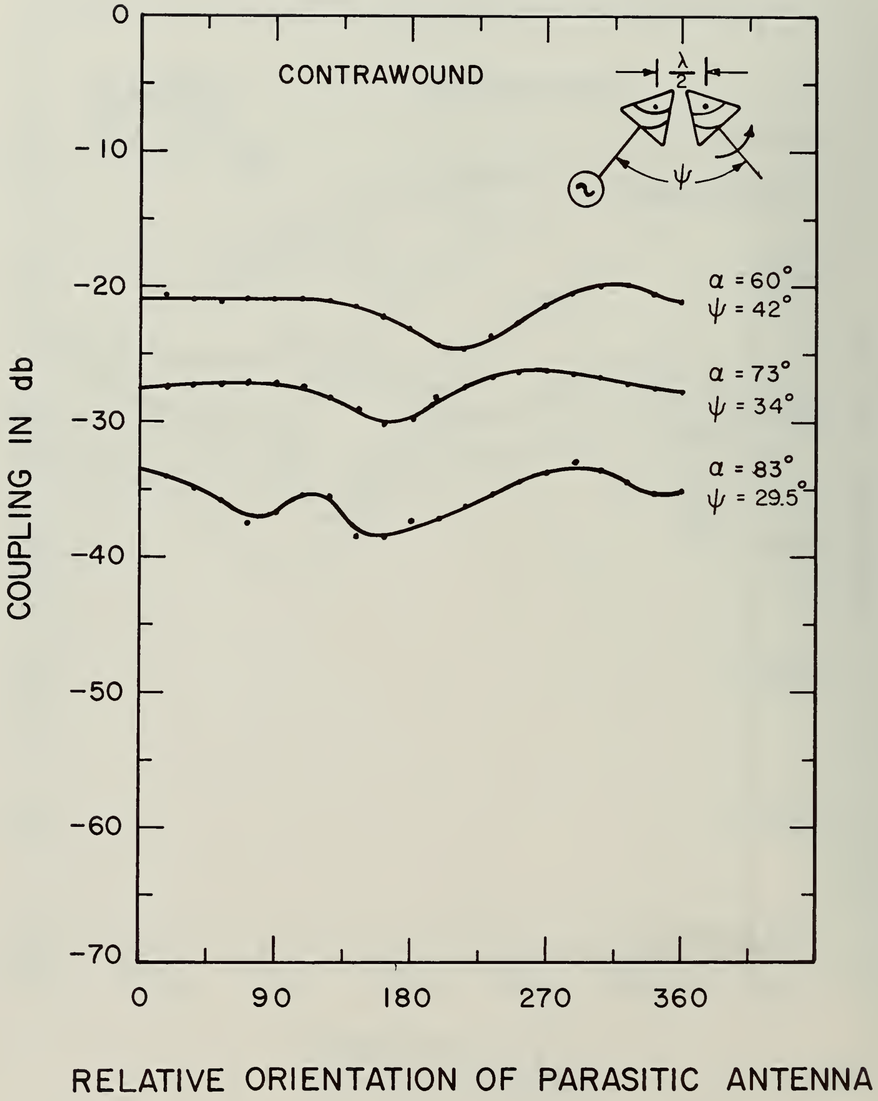

Figure 22. Coupling Between Contrawound Antennas in a Conical Array as a Function of Relative Rotation

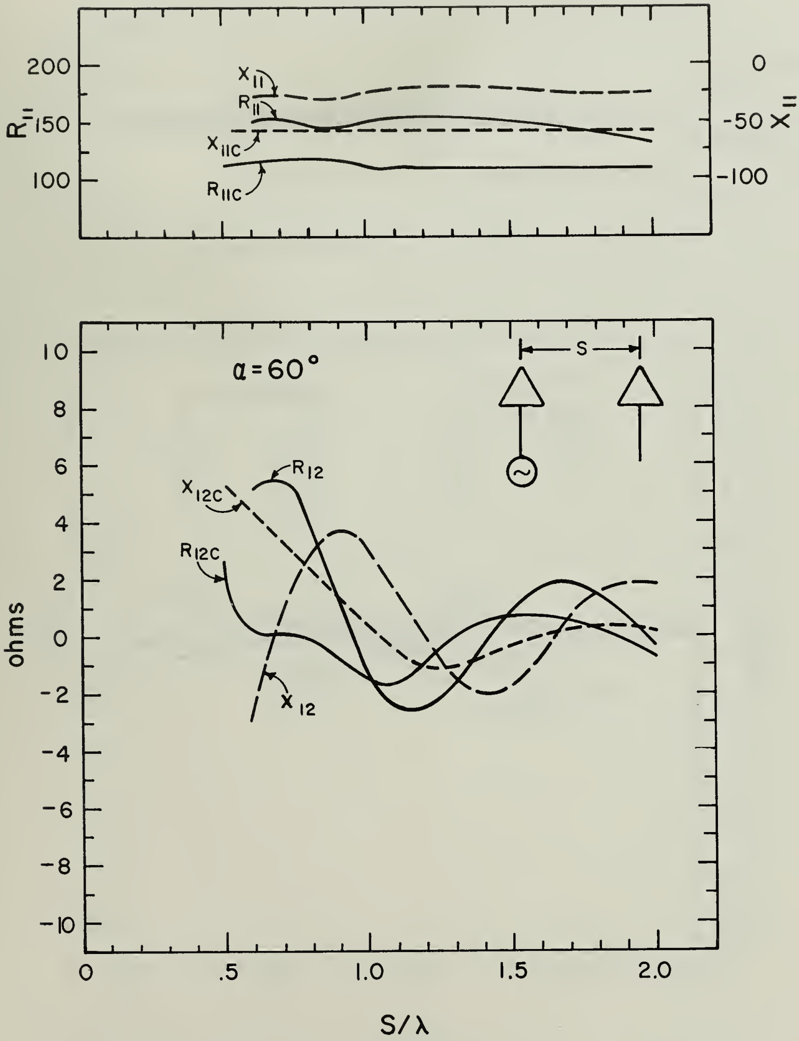

Figure 23. Mutual Impedance as a Function of Spacing in a Parallel Array, $\alpha = 60^{\circ}$ (The subscript C indicates values measured between contrawound antennas)

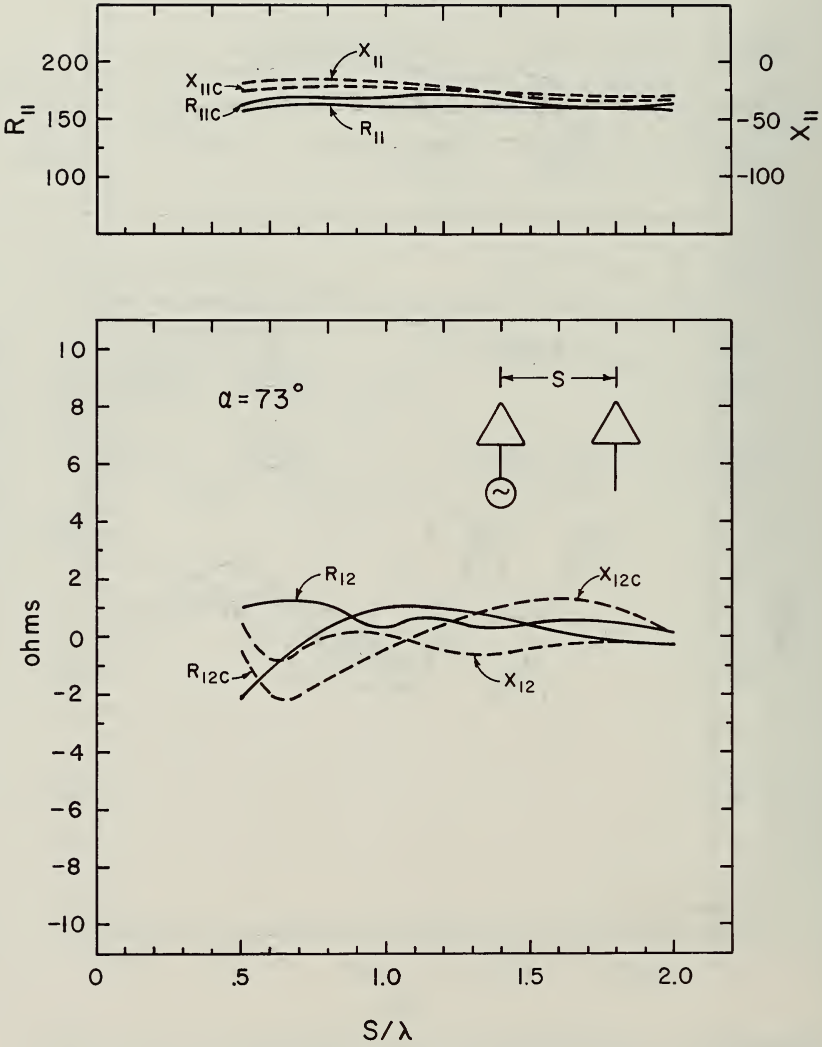

Figure 24. Mutual Impedance as a Function of Spacing in a Parallel Array, $\alpha = 73^{\circ}$

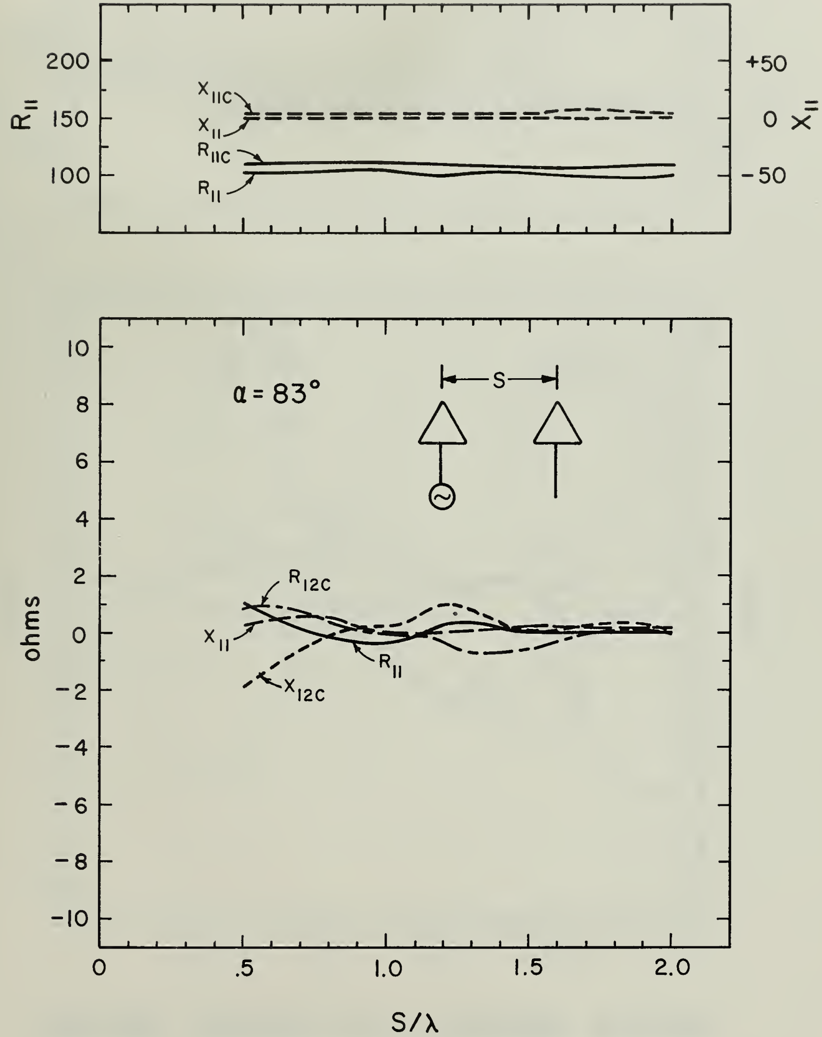

Figure 25. Mutual Impedance as a Function of Spacing in a Parallel Array, $\alpha = 83^{\circ}$

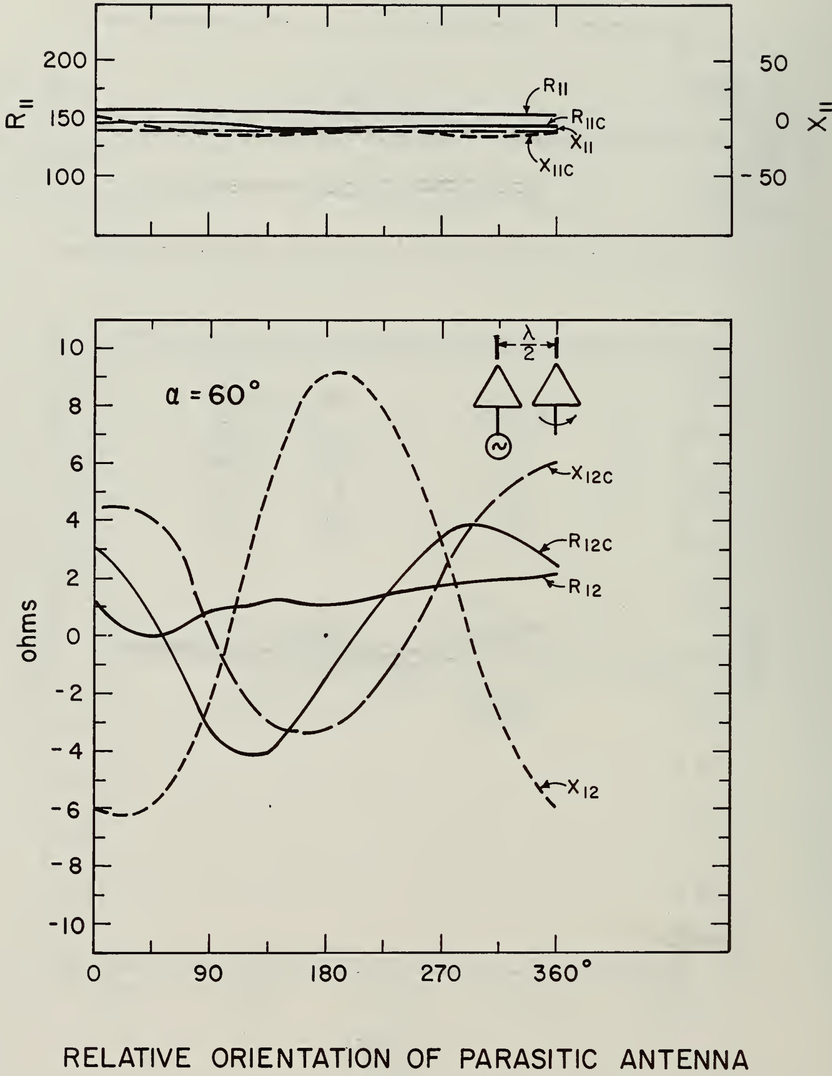

Figure 26. Mutual Impedance as a Function of Rotation in a Parallel Array, α = 60°

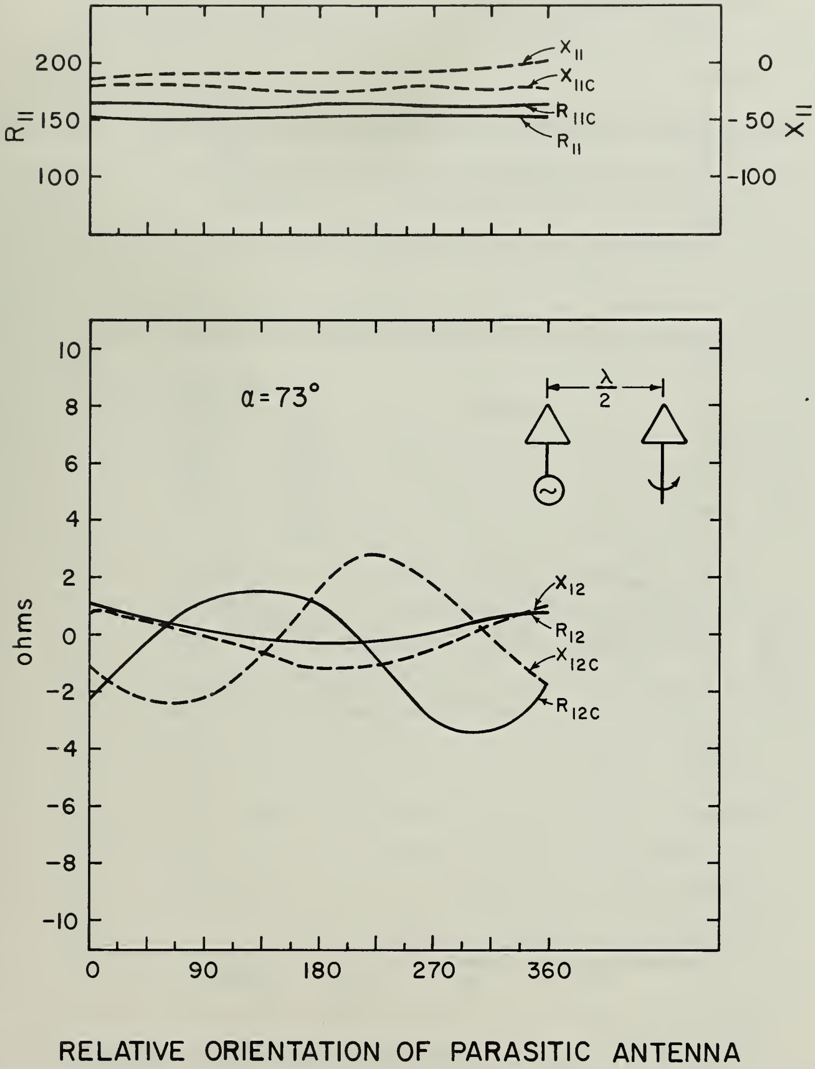

Figure 27. Mutual Impedance as a Function of Rotation in a Parallel Array, $\alpha = 73^{\circ}$

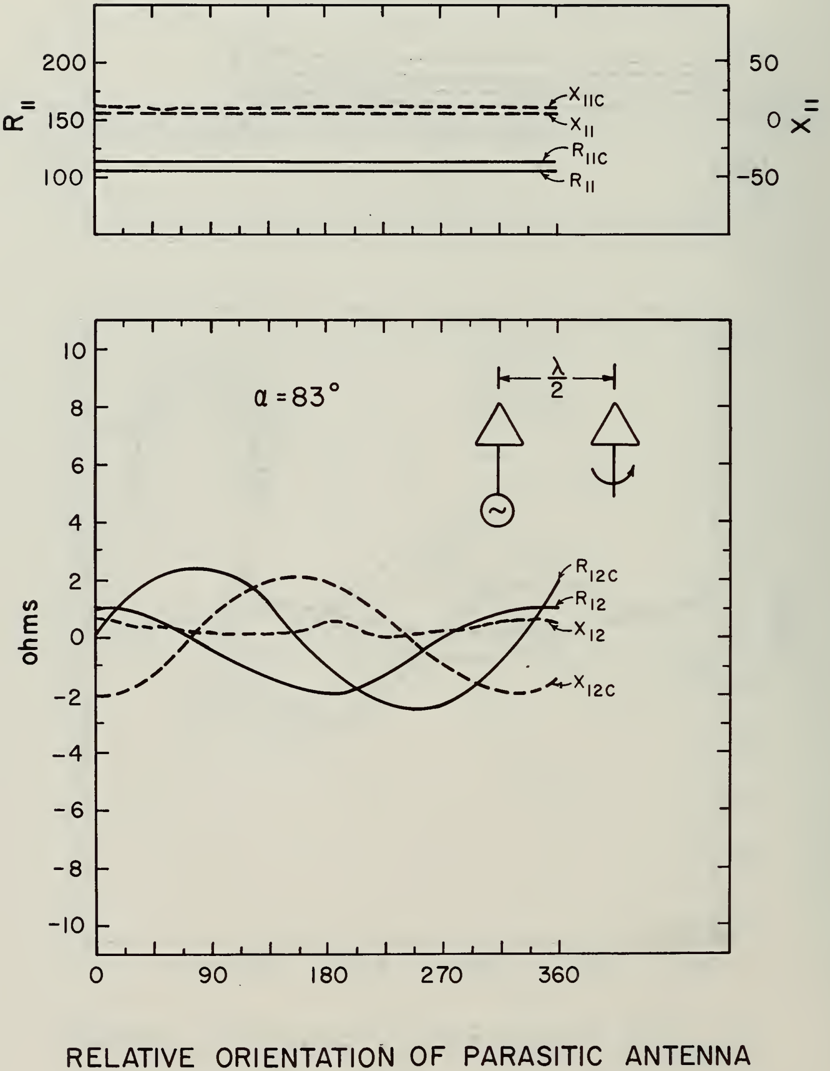

Figure 28. Mutual Impedance as a Function of Rotation in a Parallel Array, α = 83°

The real part of the self impedance of the antennas for these cases lies between 110 and 160 ohms. The subscript "C" on all graphs of measured impedance indicates measured values between contrawound antennas.

### 4.2.2 Conical Arrays

As shown in Figures 29 through 34, the mutual impedance between elements in a conical array is larger than it is in the parallel array. Figures 29 through 31 should be interpreted in the light of pattern considerations which will limit the normal range of the array angle $\psi$ to approximately $60^{o}$ or less. In this range the mutual impedance is quite low for the $73^{o}$ and $83^{o}$ antennas. At spacings up to $S = \lambda/2$ there is little difference in the general level of the mutual impedance between the same or oppositely sensed antennas.

## 4.3 Radiation Patterns

### 4.3.1 Parasitic Arrays

The radiation patterns of the individual antennas are shown in Figures 35-40. Also shown is the distortion in the individual element pattern due to the presence of a parasitic antenna in parallel and conical arrays. For all patterns the feed line to the parasitic element was terminated in its characteristic impedance. There was, however, some mismatch between the line and the antenna. All patterns in this report are electric field patterns and those in Figures 35-40 were taken in the plane of the array. The axial ratio is recorded on the axis of the active element unless stated otherwise. The term parasitic array, used to identify the patterns, is used to mean one driven element with one or more parasitic elements present.

For parallel antennas the principal charge is the introduction of some squint in the $E_{\phi}$ pattern taken in the plane of the array and a broadening of the beamwidths in this plane at a spacing of one half wavelength. As the separation is increased this pattern modification diminishes until at one wavelength the patterns are very similar to the single element pattern. Pattern modification is less when the parasitic antenna is one with an opposite sense of polarization.

As previously pointed out, when the antennas are placed in a conical array the separation between the surface of the elements is reduced and there is consequently considerably stronger coupling. For the smallest array angle used, $\psi = 17^{\circ}$, (i.e., an angular separation between the conical surfaces of $2^{\circ}$) pattern modification is quite severe for antennas with the same sense of polarization. Modification is much less where the parasitic element is of opposite sense although for this close spacing the patterns taken in the plane perpendicular to the array are slightly distorted. In addition the axial ratio on axis may rise sharply as indicated for $\alpha = 83^{\circ}$. Patterns taken in the plane perpendicular to the array were essentially unchanged for the same sense antennas.

As the array angle is increased the pattern distortion rapidly diminshes and for a separation angle of only $10^{\circ}$ the element pattern is modified only slightly by an oppositely sensed parasitic element.

As indicated in Figures 41 and 42, the presence of a second parasitic element restores symmetry to the pattern.

Although the terminal coupling varies considerably with rotation of the parasitic element, the effect of such rotation on the radiation pattern is usually small compared to the effect due to the physical presence of the element. Radiation patterns of a conical parasitic array as a function of rotation of the parasitic antenna are plotted in Figure 43.

Most of the pattern modification in Figures 35-40 can be explained in terms of array theory. For example, a phase delay of less than $\pi/2$ in the excitation of one element of a two element array scans the beam of the array toward this unit. In Figure 39, the separation between the element phase centers is approximately $\lambda/4$, for $\psi = 17^{\circ}$. The radiation patterns taken in the plane of the array in this case are approximately those of a two element array with $S = \lambda/4$ and a phase delay of $\pi/4$ to one element. This would include that a significant portion of the energy is coupled to the parasitic element and reradiated with a phase delay. The excitation of an array with an equivalent phase advance to one element scans the beam in the opposite direction. In the parallel parasitic array in Figure 36 the energy coupled to the parasitic antenna is delayed $180^{\circ}$ by the separation. A further delay in reradiating the energy will appear as a phase advance to that element. The result is a squint away from the parasitic antenna. The fact that a rotation of the parasitic element has only a secondary effect would indicate that the net phase delay, excluding element separation, in the excitation of and reradiation from the parasitic element is approximately the same for any orientation.

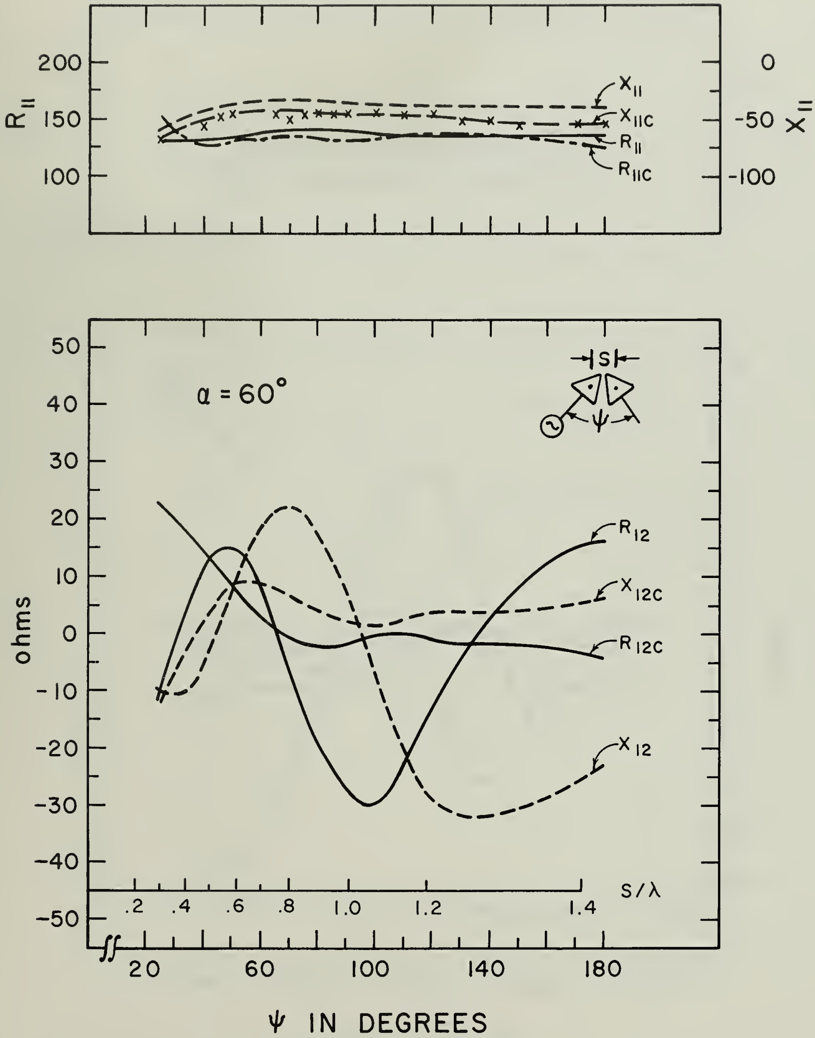

Figure 29. Mutual Impedance Vs Array Angle in a Conical Array, α = 60°

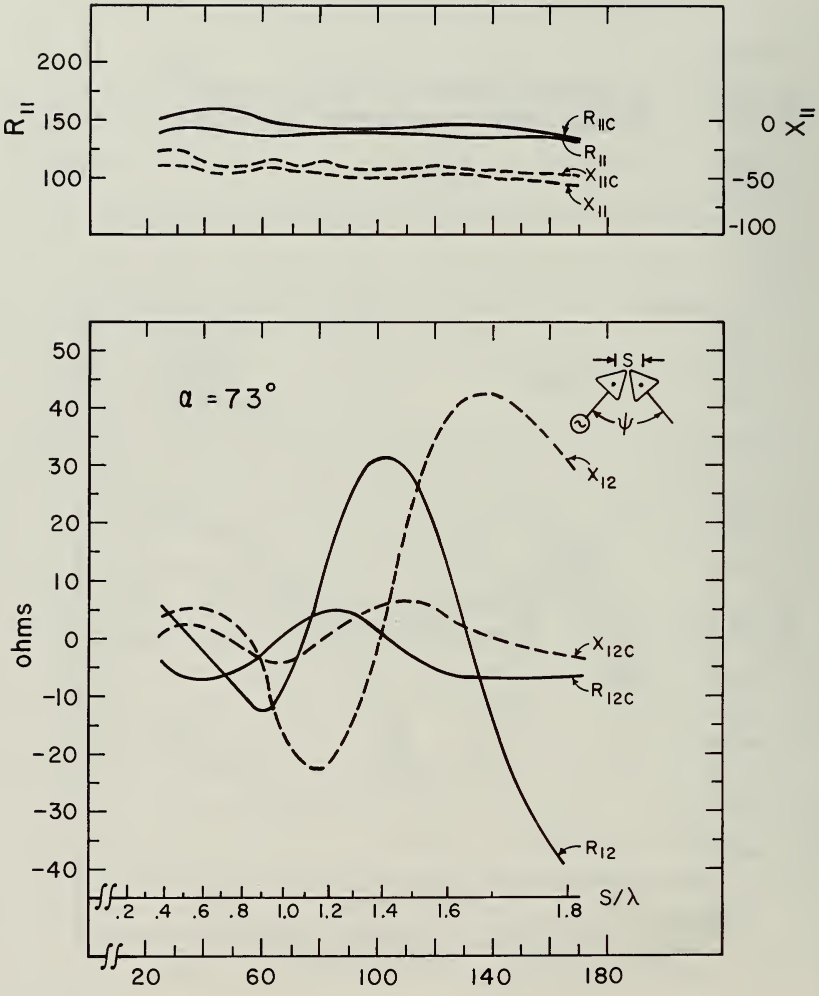

ψ IN DEGREES

Figure 30. Mutual Impedance Vs Array Angle in a Conical Array, $\alpha = 73^{\circ}$

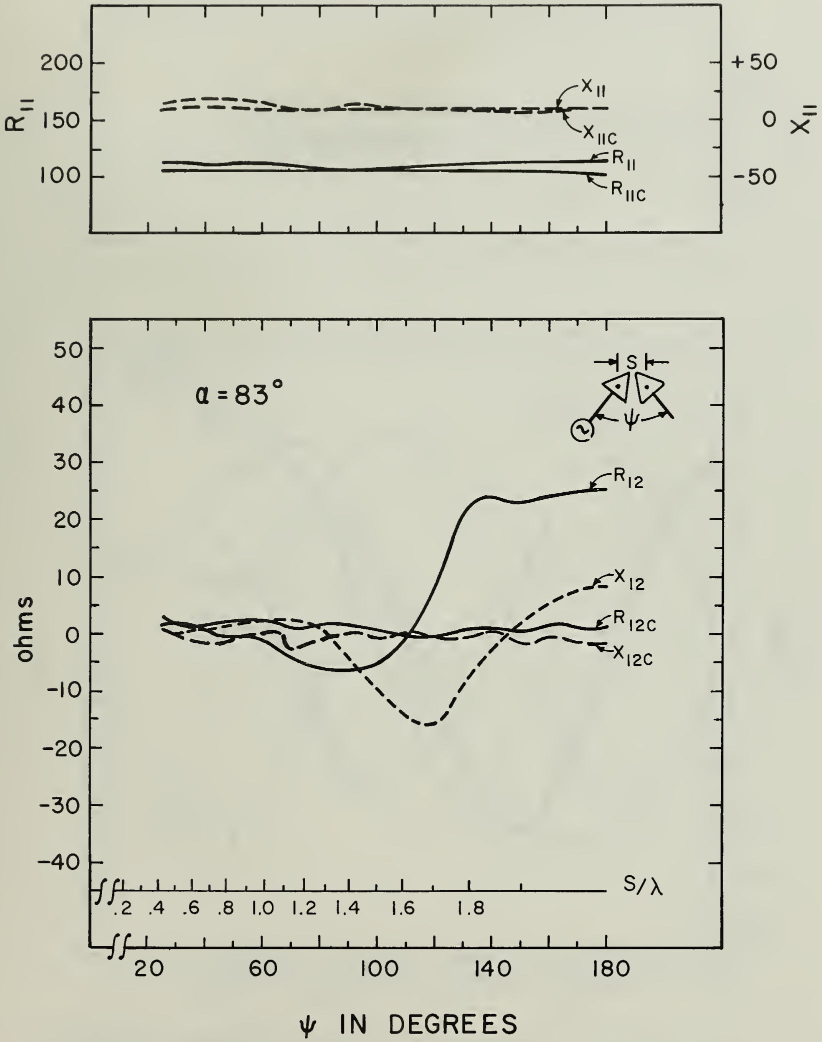

Figure 31. Mutual Impedance Vs Array Angle in a Conical Array, $\alpha = 83^{\circ}$

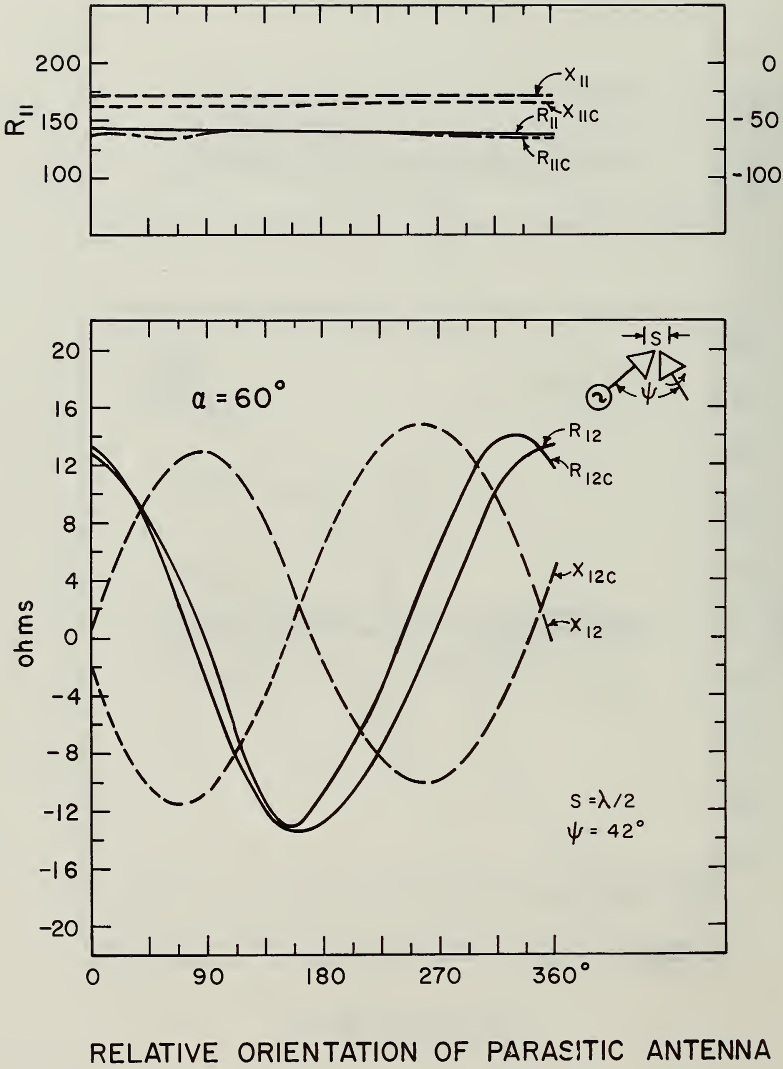

Figure 32. Mutual Impedance Vs Relative Rotation in a Conical Array, α = 60°

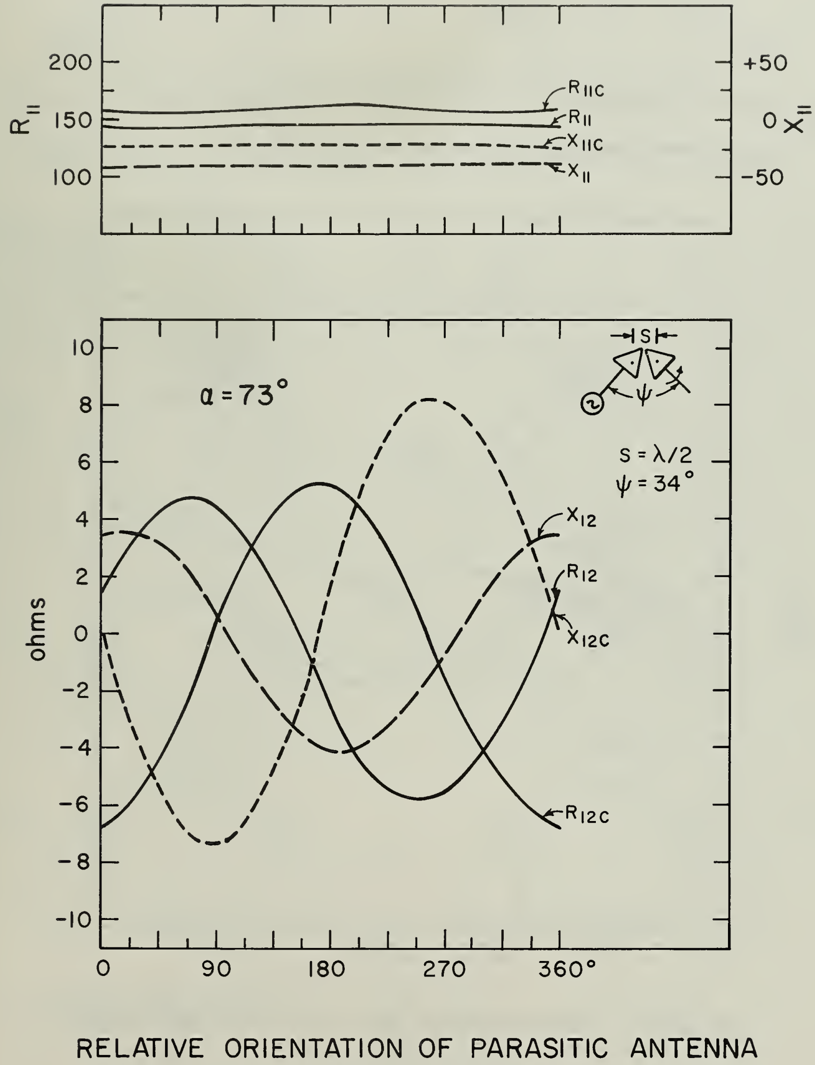

Figure 33. Mutual Impedance Vs Relative Rotation in a Conical Array, $\alpha = 73^{\circ}$

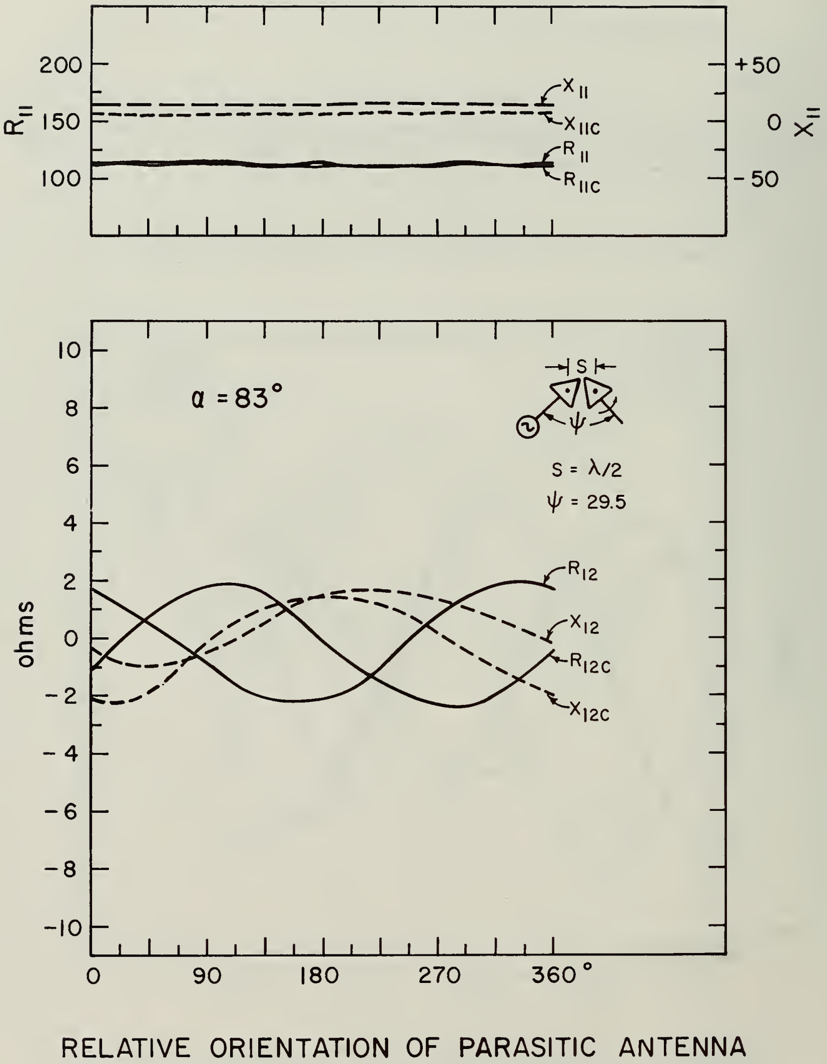

Figure 34. Mutual Impedance Vs Relative Rotation in a Conical Array, $\alpha = 83^{\circ}$

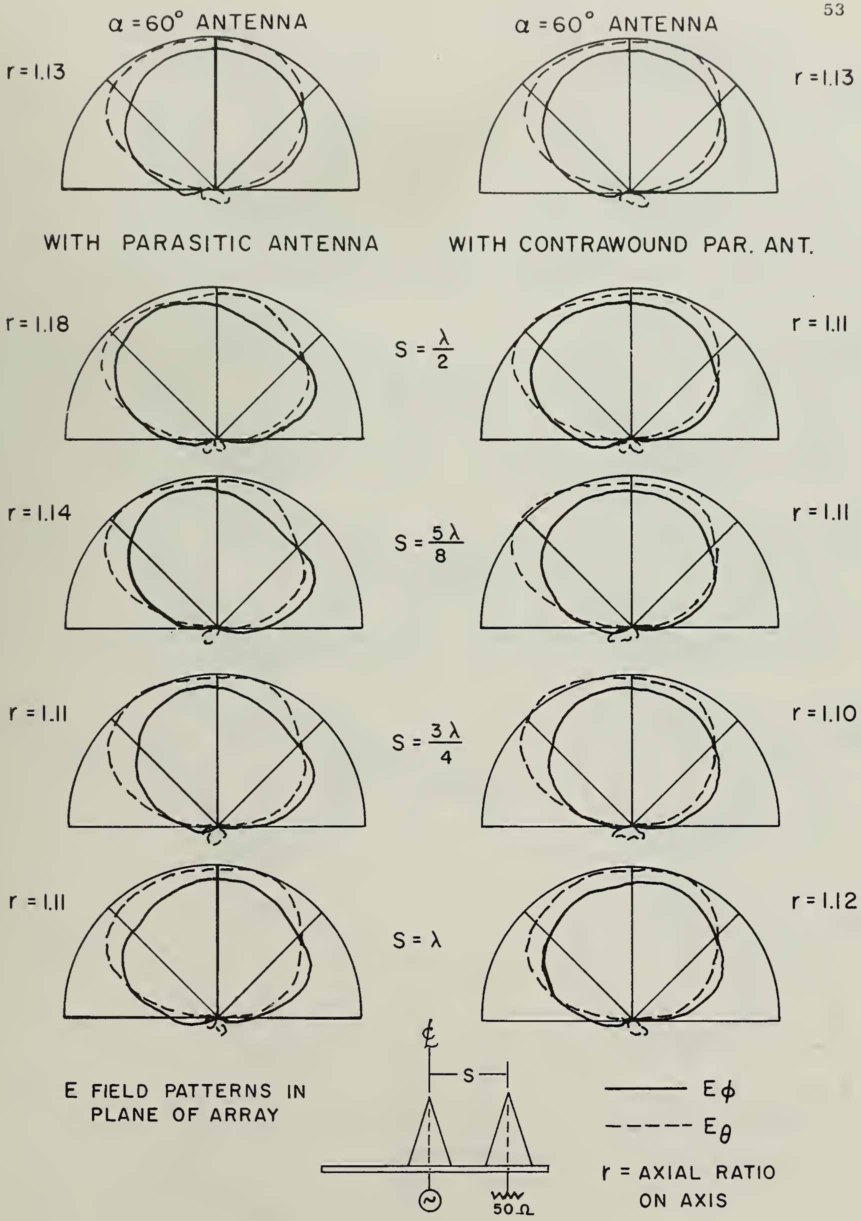

Figure 35. Electric Field Patterns of Conical Log-Spiral Antenna With and Without a Parasitic Antenna Present in a Parallel Array, $\alpha = 60^\circ$

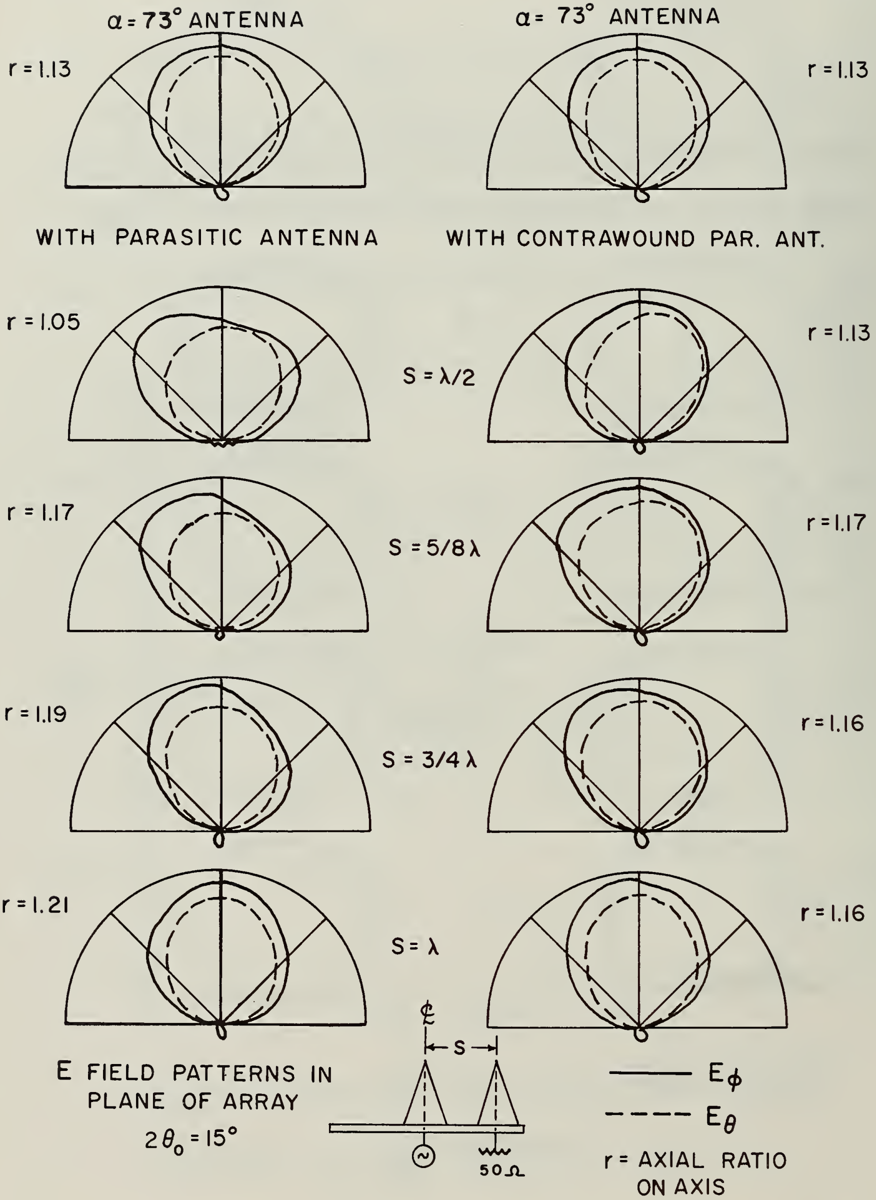

Figure 36. Electric Field Patterns of Conical Log-Spiral Antenna With and Without a Parasitic Antenna Present in a Parallel Array, $\alpha = 73^{\circ}$

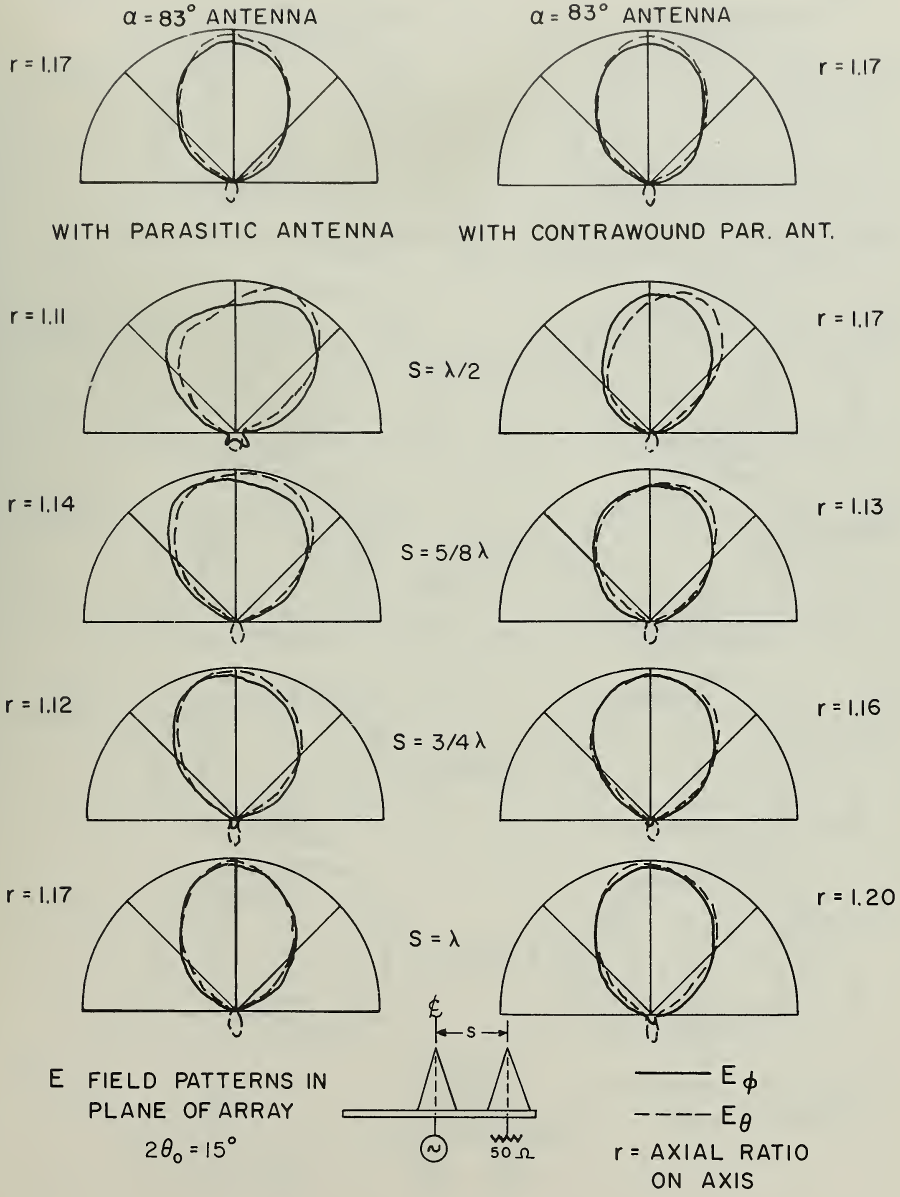

Figure 37. Electric Field Patterns of Conical Antenna With and Without a Parasitic Antenna Present in a Parallel Array, $\alpha = 83^{\circ}$

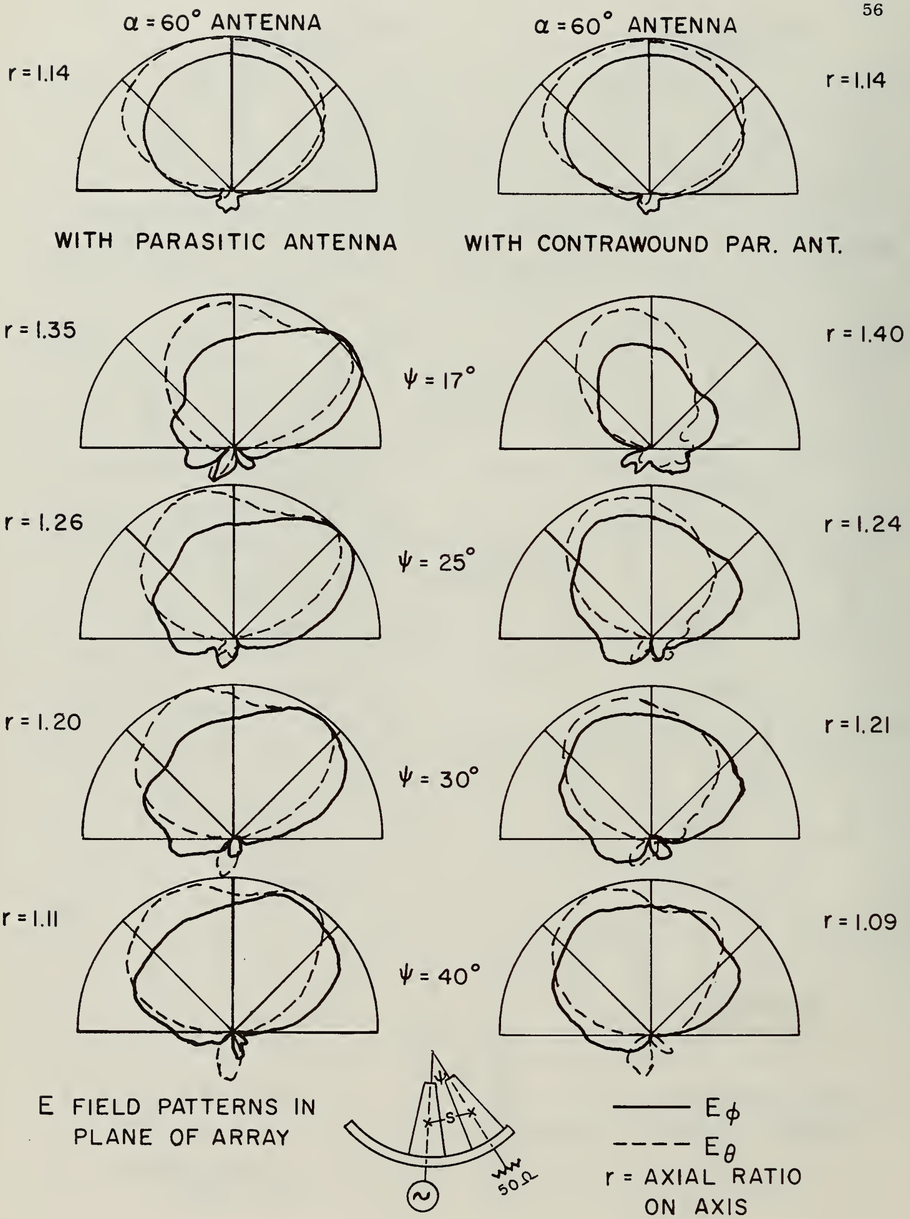

Figure 38. Electric Field Patterns of Conical Antenna With and Without a Parasitic Antenna Present in a Conical Array, $\alpha = 60^{\circ}$

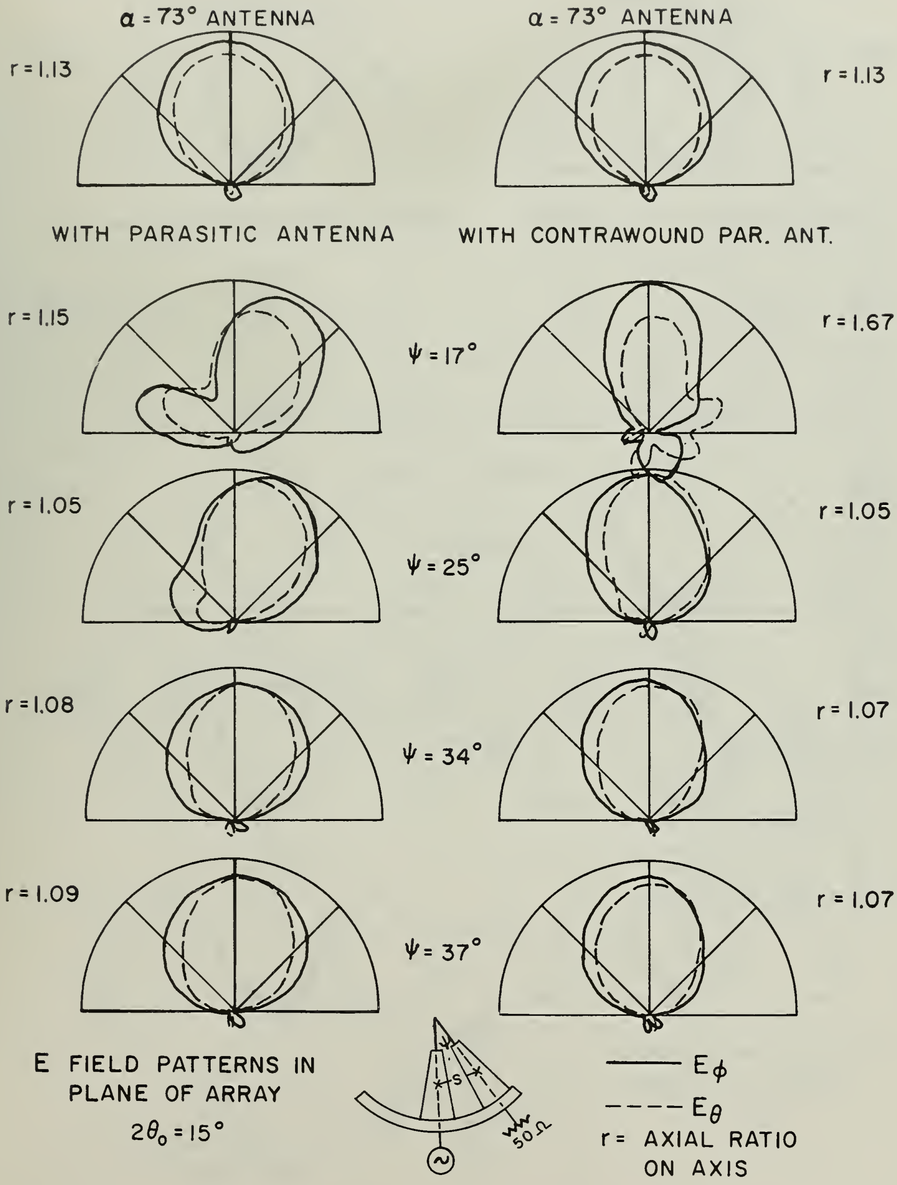

Figure 39. Electric Field Patterns of Conical Antenna With and Without a Parasitic Antenna Present in a Conical Array, $\alpha = 73^{\circ}$

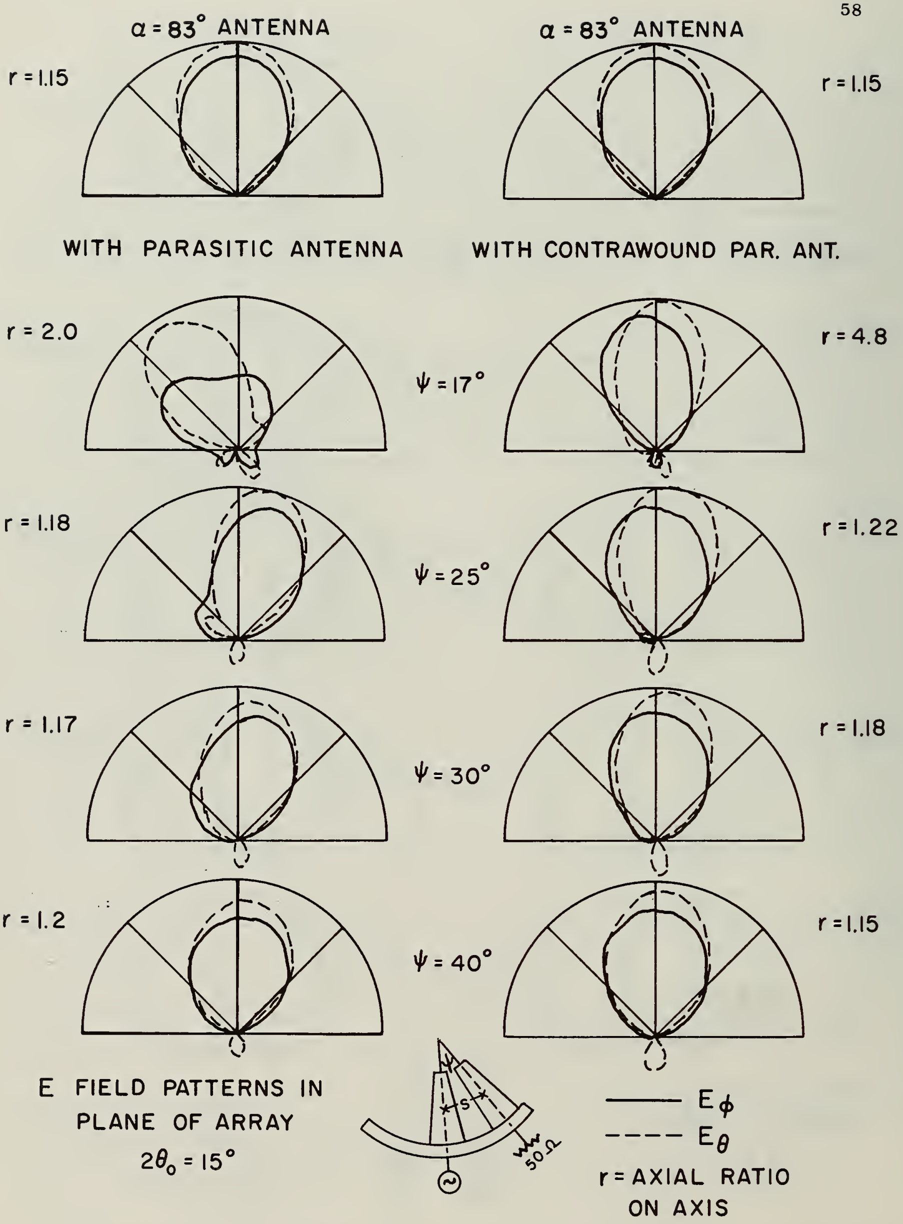

Figure 40. Electric Field Patterns of Conical Antenna With and Without a Parasitic Antenna Present in a Conical Array, α = 83°

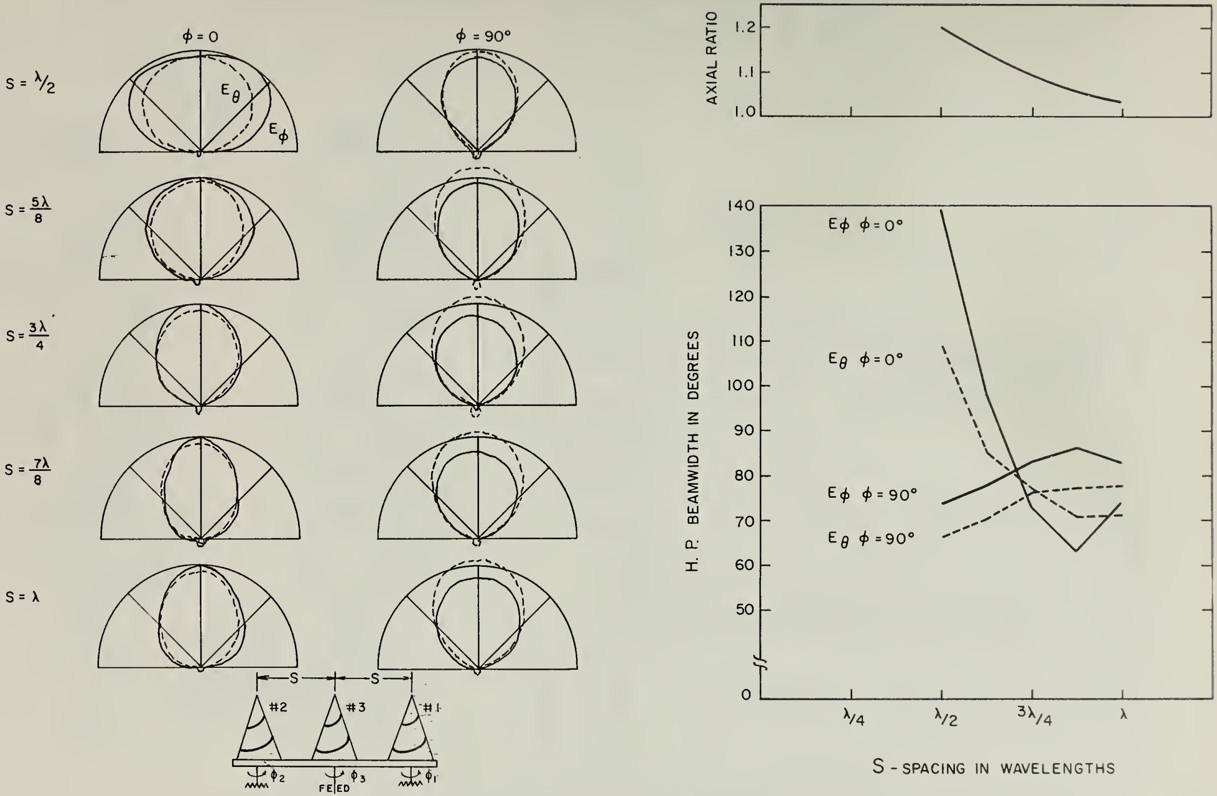

Figure 41. Three Element Parallel Parasitic Array, Variable Spacing. $\phi_2 = \phi_3 = \phi_1$, $\alpha = 73^{\circ}$ (linear array in $\phi = 0$ plane)

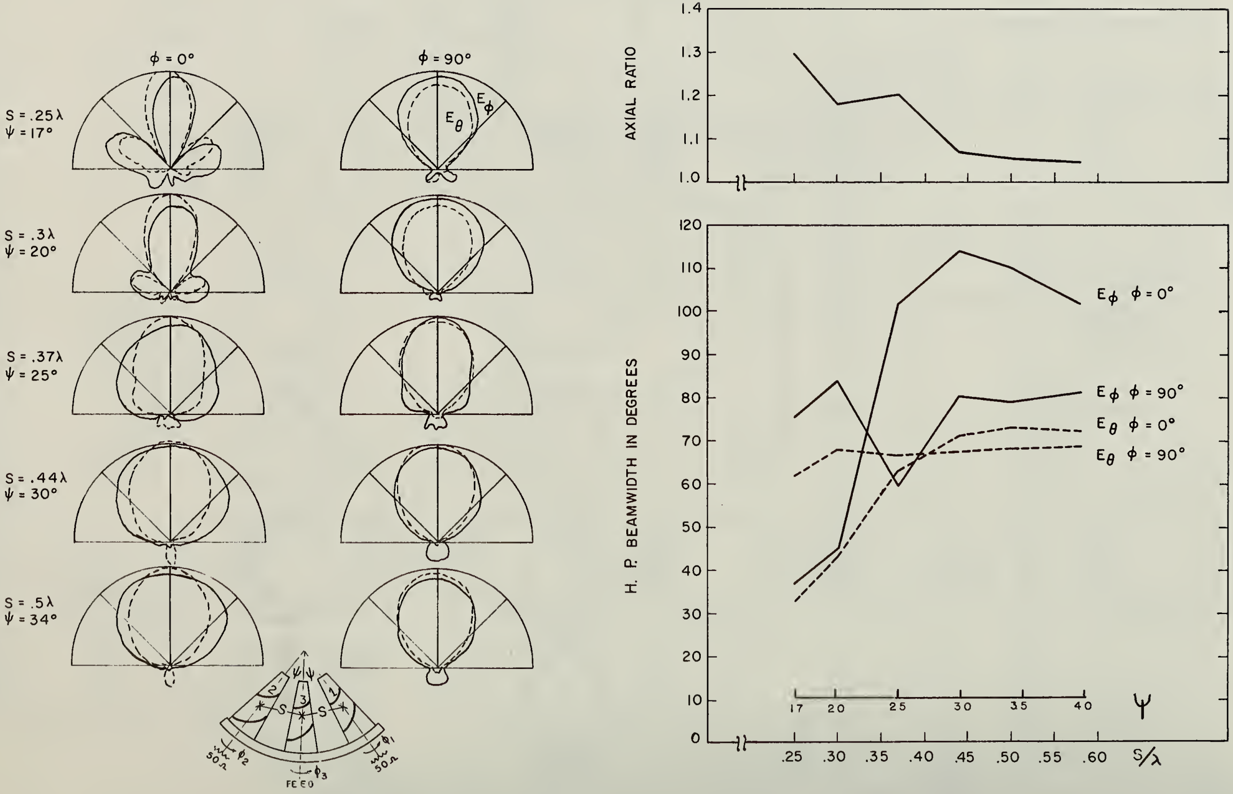

Figure 42. Three Element Conical Parasitic Array, Variable Array Angle. $\phi_1 = \phi_2 = \phi_3$, $\alpha = 73^o$

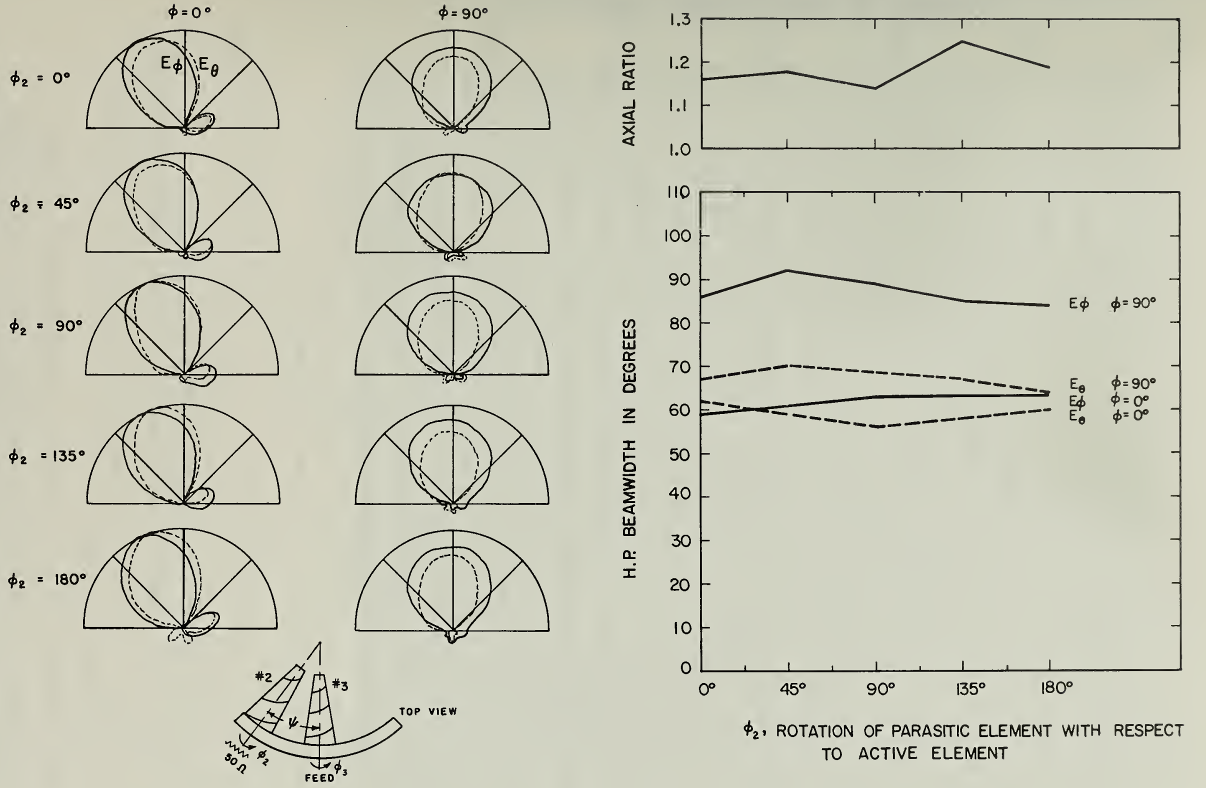

Figure 43. Radiation Patterns of Two Element Conical Parasitic Array as a Function of Rotation of Parasitic Element, $\alpha = 73^{\circ}$, $\psi = 18^{\circ}$.

### 4.3.2 Driven Arrays

The electric field radiation pattern of the isolated antenna may be approximated very well by a function such as $(\cos\theta)^n$. For convenience in estimating the power n, when the element pattern is approximated by the simple function $\cos^n\theta$, values of half-power beamwidth versus n are plotted in Figure 44. The radiation pattern of a parallel two element in-phase array with half-wavelength spacing was calculated using an assumed element function of $\cos^{1.5}$. As shown in Figure 45 this calculated pattern is in good agreement with the measured pattern except that it is approximately one degree narrower at the half-power points. Since Figure 36 indicates that the element pattern is broadened when the element is placed in a linear array a new element function was assumed by fitting a $\cos^n\theta$ curve to these patterns. A calculated array pattern using $\cos^{.8}(\theta \pm 4^\circ) + .04$ for $E_\phi$, and $\cos^{.9}\theta$ for $E_\theta$, was approximately 1 degree wider than the measured patterns.

The measured patterns for a similar parallel array with spacings from $\lambda/2$ to $2\lambda$ are shown in Figure 46. The axial ratio on the maximum of the main beam and the half-power beamwidths of the main beam have also been plotted.

Figure 47 shows the radiation pattern, the axial ratio in the direction of the maximum of the main beam and the half-power beamwidth of the main beam of the two-element array as it is phased by the rotation of one element. A three element in-phase array is shown for various element spacings in Figure 48. These arrays all have predictable patterns and the measured patterns are included only for reference purposes.

The geometry of a conical array is indicated in Figure 49 where the electric field at a distant point is given approximately by

$$E = \cos^n\left(\theta + \frac{\psi}{2}\right) e^{\beta d \sin \psi/2 \sin\theta} + \cos^n\left(\theta - \frac{\psi}{2}\right) e^{-\beta d \sin\psi/2 \sin\theta} \qquad (20)$$

where $\cos^n(\theta + \frac{\psi}{2})$ is the assumed element function, d is the separation between element phase centers, $\psi$ is the array angle, and $\theta$ the angle from the axis of the array in the plane of the array.

The radiation pattern of a two element in-phase conical array was calculated from Equation (20) using $n = 1.5$ and $\psi = 34^\circ$ ($S = .5\lambda$). This pattern is compared to the measured patterns in Figure 50. The half-power

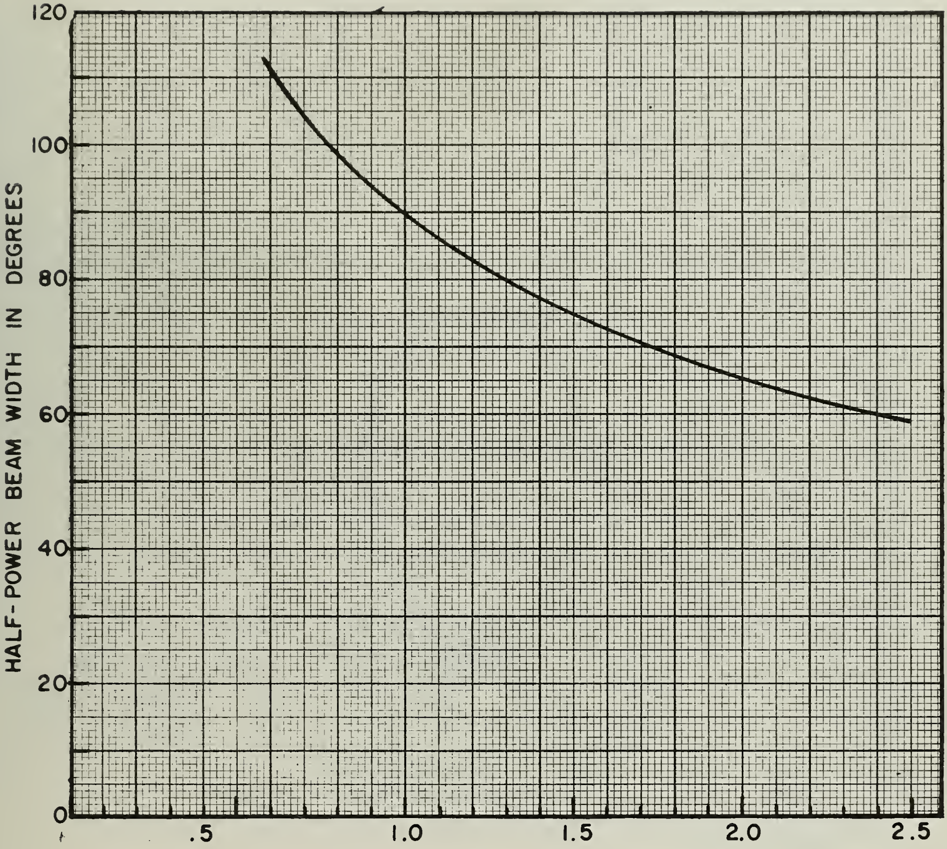

Figure 44. Half Power Beamwidth of the Element Function $\cos^n \theta$

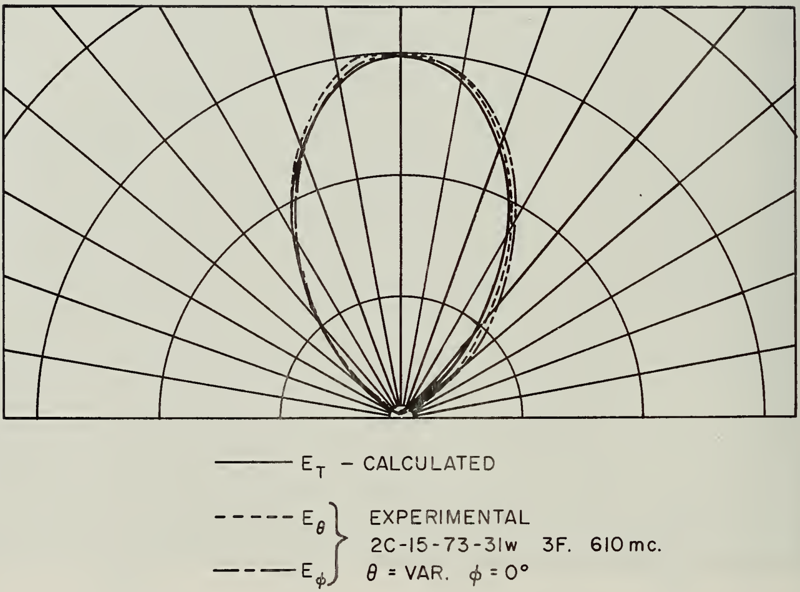

Figure 45. Calculated Array Pattern for Two Element Parallel In-Phase Array, $S = \lambda/2$, $\zeta = 73^{\circ}$

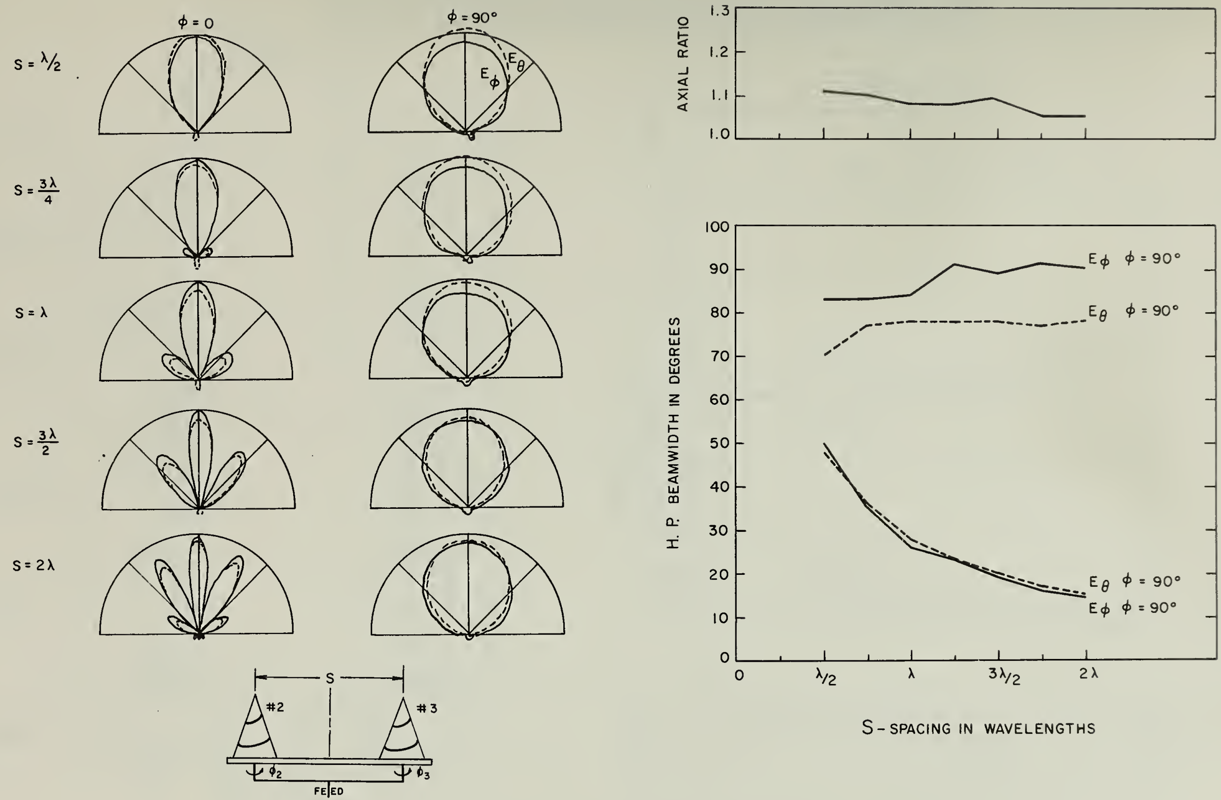

Figure 46. Radiation Patterns of Two Element Parallel Array, Variable Spacing $\phi_2 = \phi_3$, $\alpha = 73^o$ (linear array in $\phi = 0$ plane)

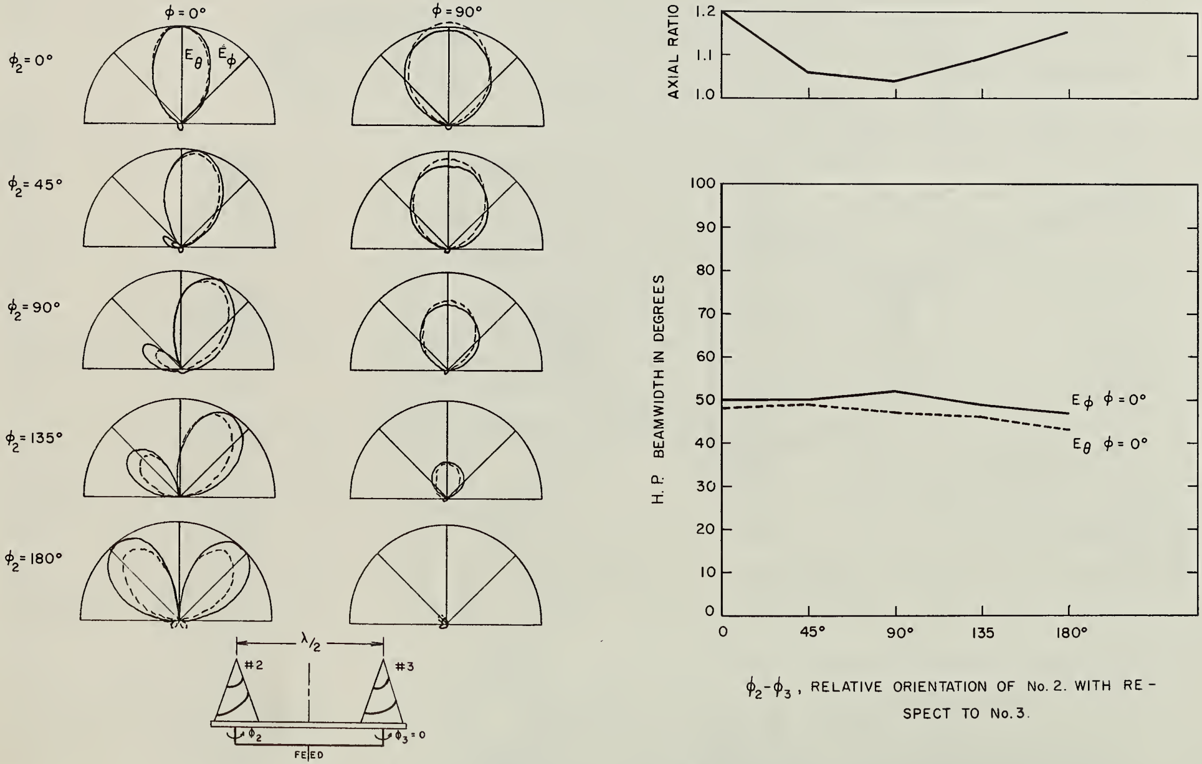

Figure 47. Radiation Patterns of Two Element Parallel Array, Variable Orientation of One Element. $S = \lambda/2$, $\alpha = 73^{\circ}$ (linear array in $\phi = 0$ plane)

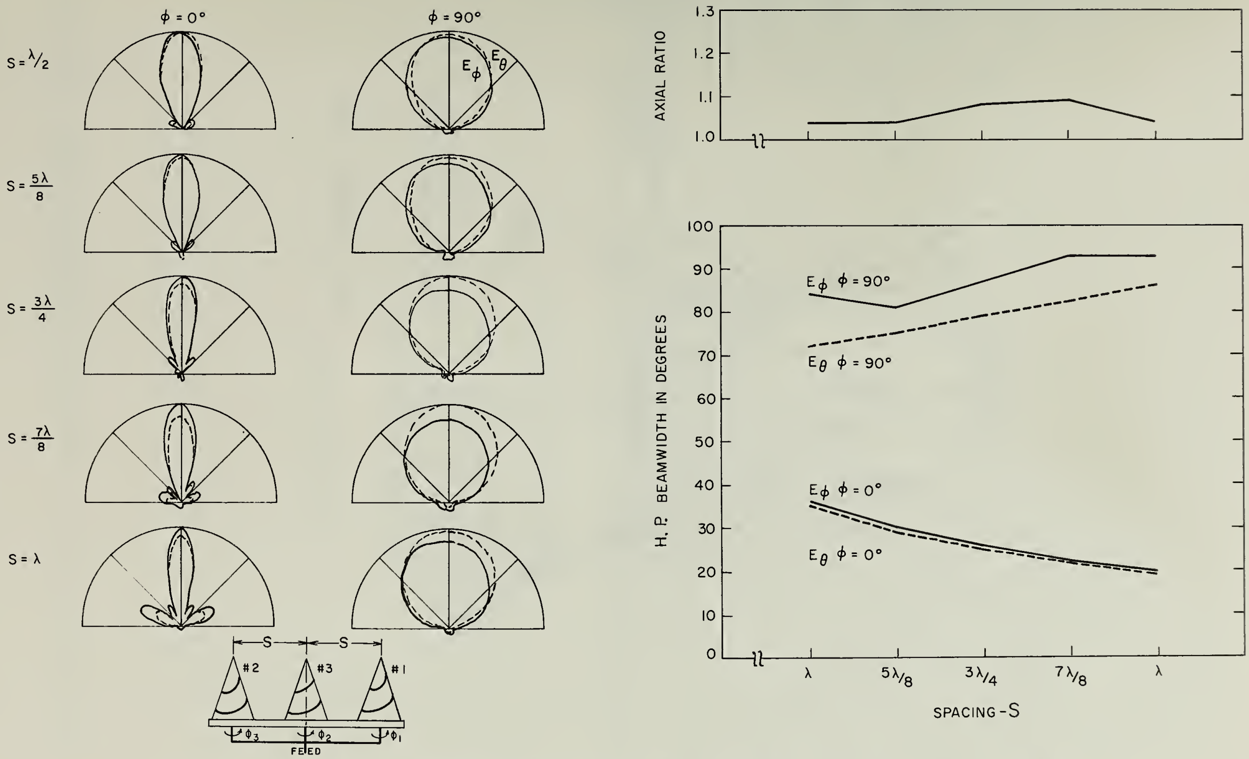

Figure 48. Radiation Patterns of Three Element Parallel Array, Variable Spacing, $\phi_1 = \phi_2 = \phi_3$, $\alpha = 73^{\circ}$ (linear array in $\phi = 0$ plane)

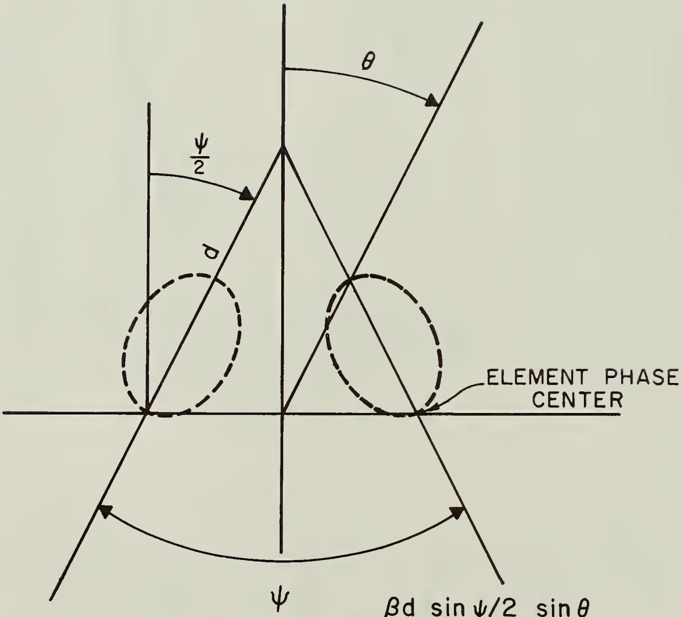

$$E = \cos^n(\theta+\psi/2)\,e^{\beta d \sin\psi/2 \sin\theta} + \cos^n(\theta-\psi/2)\,e^{-\beta d \sin\psi/2 \sin\theta}$$

Figure 49. Geometry of Two Element Conical Array

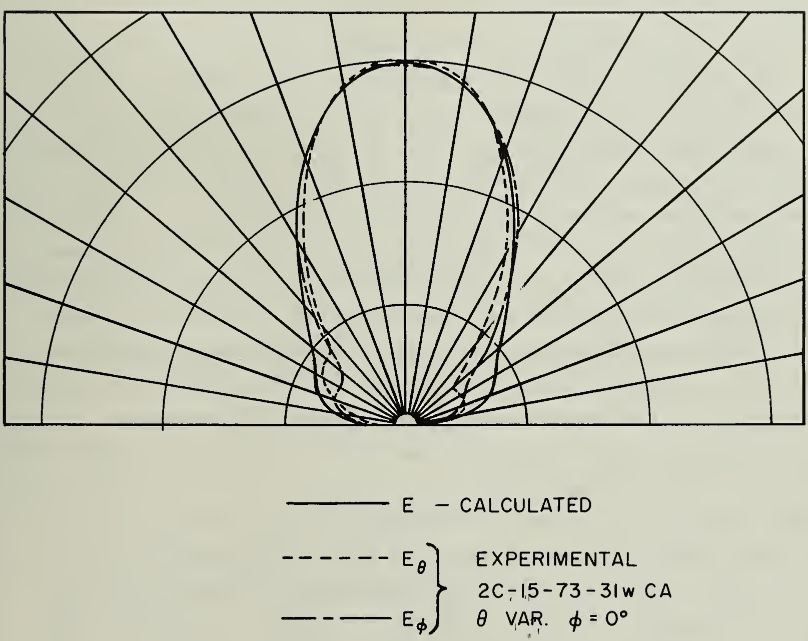

Figure 50. Radiation Pattern for Two Element Conical In-phase Array, $S = \lambda/2$ ($\psi = 34^\circ$), $\alpha = 73^\circ$

beamwidth of the measured $E_\phi$ pattern is within one degree of the calculated pattern and there is reasonable agreement between the patterns for $\theta \pm 40$ degrees. Beyond $\theta = 40^\circ$ the measured patterns are somewhat narrower than calculated. The $E_\theta$ array pattern is somewhat narrower than calculated; better agreement could be secured by using a slightly modified element function.

Measured patterns for an in-phase conical array with variable spacing are shown in Figure 51. Data on a phased array of 2 elements is shown in Figure 52 and on a three element in-phase array in Figure 53.

When interpreting the conical array patterns it should be noted that a change in the array angle $\psi$, which brings about a change in the spacing between the phase centers of the elements is not equivalent to a change in the element spacing in a parallel array. In a parallel array the change in radiation characteristics with frequency can be simulated by maintaining the frequency constant and varying the element spacing, provided the element pattern does not change with frequency. In a conical array this is not true since a change in $\psi$ changes the element pattern with respect to the array geometry. The element pattern can be approximated by a function such as $\cos^n (\theta + \frac{\psi}{2})$. Thus a change in S, and hence $\psi$, effectively changes this function as well as changing the element spacing. The array patterns show a sharp decrease in beamwidth with increasing $\psi$, up to approximately $70^\circ$ the maximum angle investigated, and incidentally increasing S.

That the conical array geometry does preserve the beamwidth of the array with changing frequency of operation is shown in Figure 54. The conical array half-power beamwidth remains essentially constant (within the limits of the pattern range) over a two to one change in frequency. The half-power beamwidth of a linear array of the same elements decreased 40 percent. In addition a four element array, a "conical quad-spiral array" has been constructed to cover a 10 to 1 range of frequencies[22]. This particular array has a nominal directivity of 12 db over a circularly polarized isotropic source.

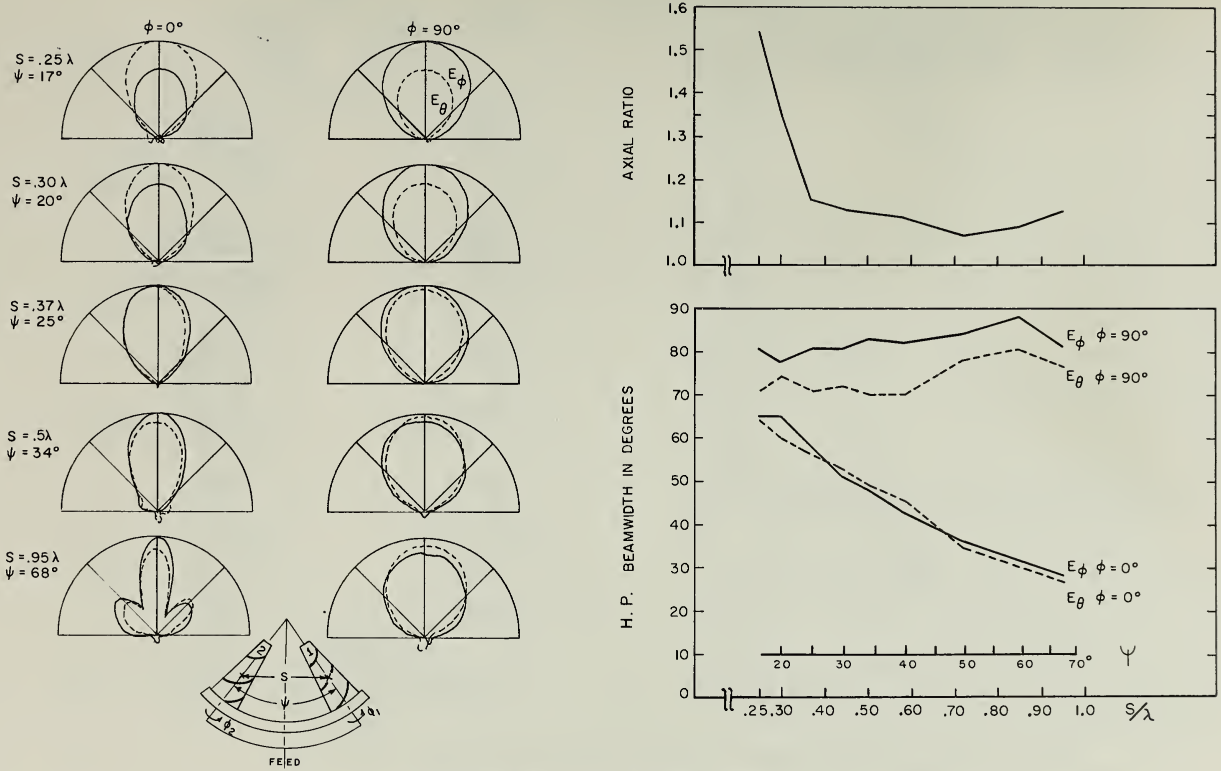

Figure 51. Radiation Patterns for Two Element Conical Array, Variable Array Angle. $\phi_1 = \phi_2$, $\alpha = 73^{\circ}$ (linear array in $\phi = 0$ plane)

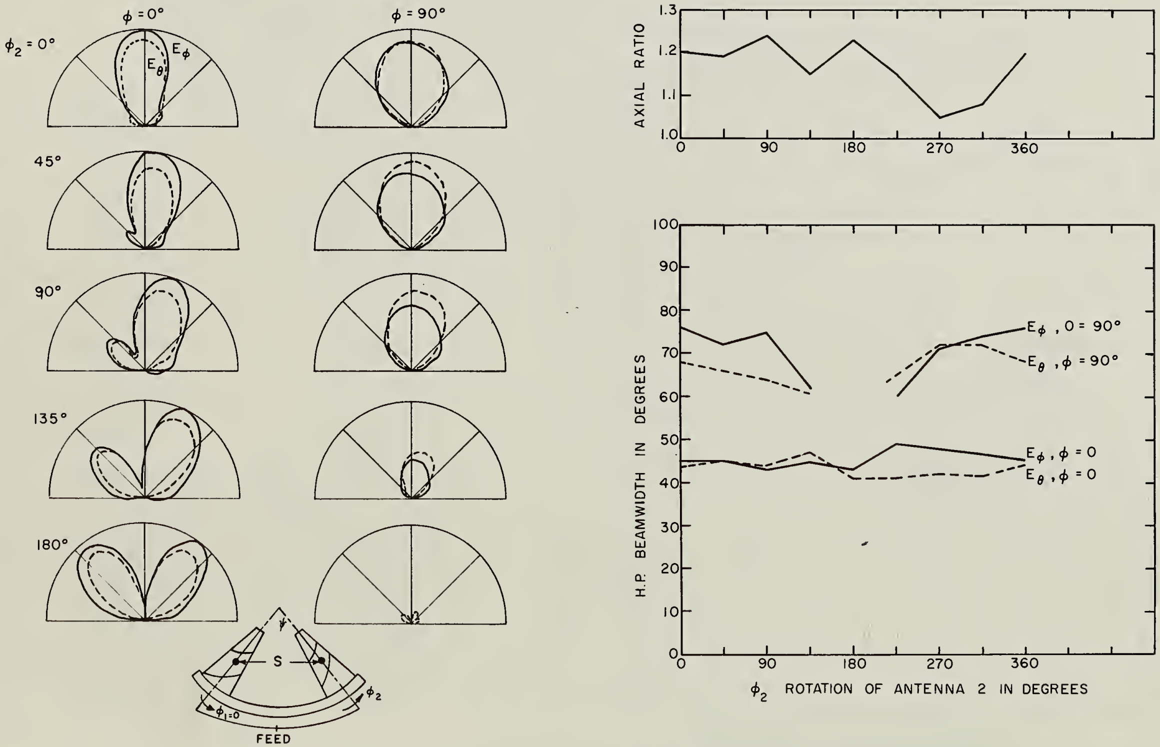

Figure 52. Radiation Patterns for Two Element Conical Array, Variable Orientation of One Element, $S = \lambda/2$, $\alpha = 73^o$ (linear array in $\phi = 0$ plane)

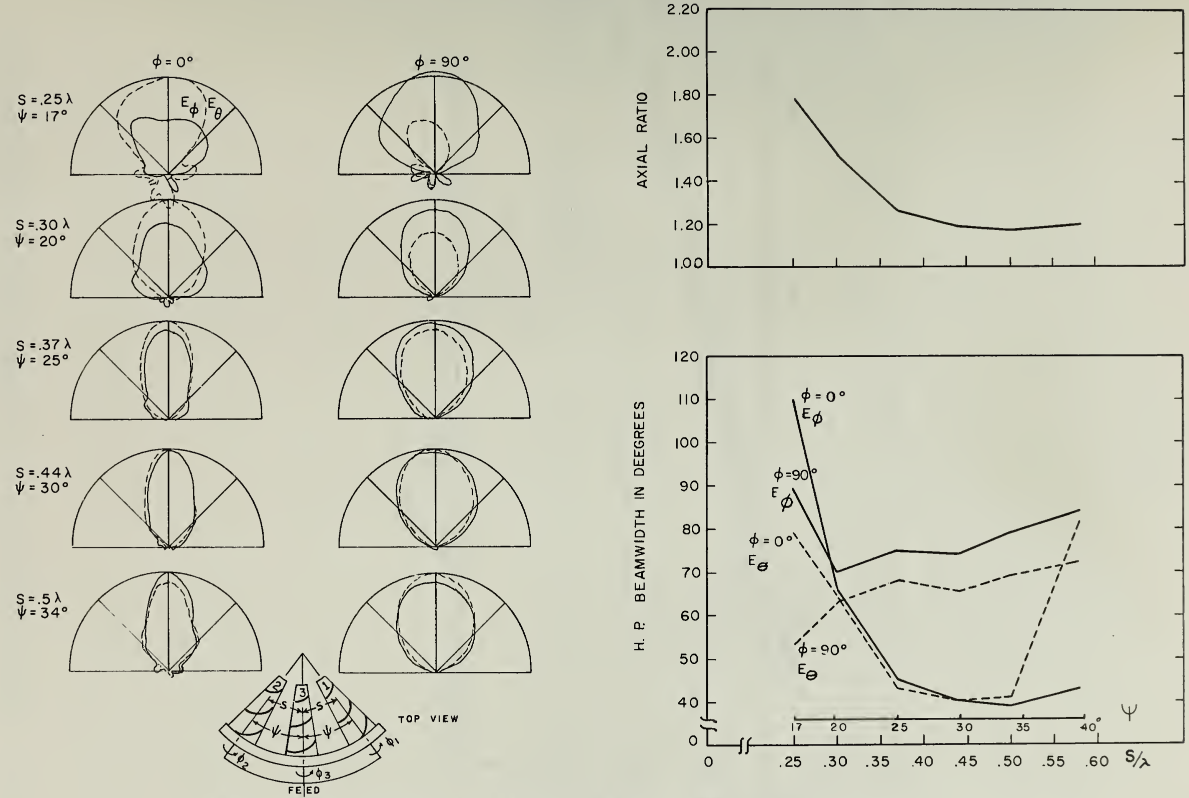

Figure 53. Radiation Patterns for Three Element Conical Array, Variable Array Angle. $\phi_1 = \phi_2 = \phi_3$ $a = 73^o$ (linear array in $\phi = 0$ plane)

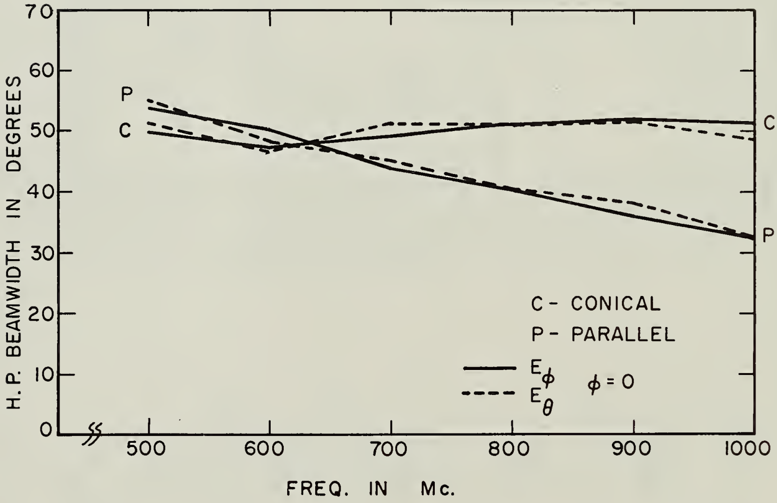

Figure 54. Half-power Beamwidth of Two Element Parallel and Conical Arrays

# 5. CONCLUSIONS

A consideration of the conical log-spiral antenna as a locally periodic slow wave structure has led to somewhat better understanding of its characteristics and operation. Under this concept an approximate expression for the location of the phase center of the antenna has been obtained.

An experimental investigation of the coupling between conical log-spiral antennas indicates (1) that coupling is low; on the order of -30 db or greater for element to element spacing of $\lambda/2$ or more in a parallel array. (2) This coupling varies with rotation, being a minimum for a 90° rotation between elements. (3) Coupling is on the order of 10 db greater in the conical array. Minimum coupling for 15° cones occurs at an array angle of approximately 35 to 50° depending upon the spiral angle $\alpha$. (4) Changes in the basic element pattern caused by the presence of other elements are minor for an element to element spacing of at least one-half wavelength, and consist mainly of a broadening of the element pattern beamwidth in the plane of the array. (5) A good approximation to the array pattern of small arrays may be gained from the use of the isolated element pattern function.

## REFERENCES

1. Dyson, J. D., "A Survey of the Very Wide Band and Frequency Independent Antennas - 1945 to the Present", Journal of Research of the N.B.S. Vol. 66D, No. 1, pp. 1-6, Jan.-Feb. 1962.

2. Dyson, J. D., "The Conical Log-Spiral Antenna in Simple Arrays", Abstracts of the 11th Annual Symposium on the USAF Antenna Res. and Dev. Program, sponsored by Aeronautical Systems Div., Air Force Systems Command, Oct. 16, 1961.

3. DuHamel, R. H. and Berry, D. G., "Logarithmically Periodic Antenna Arrays," IRE WESCON Conv. Record, Part I, 1958, pp. 161-177.

4. Webster, R. and Lyles, J. F., "Application of Frequency Independent Feeds to Automatic Tracking Antennas," Abstracts of the 11th Annual Symposium on the USAF Antenna Res. and Dev. Program, sponsored by Aeronautical Systems Div., Air Force Systems Command, October 16, 1961.

5. Bales, B. W. and Voklenburg, E., "Antenna Feed Has Ten-to-One Bandwidth," Electronics, Vol. 34, No. 48, pp. 56-58, Dec. 1, 1961.

6. Bresler, A. D., Jasik, H. and Kampensky, A., "A Wide Band Conical Scan Antenna Feed System," The Microwave Journal, Vol. 4, pp. 97-101, Dec. 1961.

7. King, R. W. P., "Coupled Antennas and Transmission Lines," Proc. IRE, Vol. 31, November, 1943, pp. 626-640.

8. Blasi, E. A., "The Theory and Application of the Radiation Mutual-Coupling Factor," Proc. IRE, Vol. 42, July, 1954, pp. 1179-1183.

9. King, R. W. P., "Theory of Linear Antennas," Harvard University Press, Cambridge, Mass., 1956, p. 349.

10. Stratoti, A. R. and Wilkinson, E. J., "An Investigation of the Complex Mutual Impedance between Short Helical Array Elements," Trans. IRE, Vol. AP-7, July, 1959, pp. 279-280.

11. Rupp, W. E., "Coupled Energy as a Controlling Factor in the Radiation Patterns of Broadside Arrays," Abstracts of the 11th Annual Symp. on the USAF Antenna Res. and Dev. Program, Sponsored by Aeronautical Systems Div., AFSC, Oct. 1961.

12. Mayes, P. E., Deschamps, G. A., and Patton, W. T., "Backward-Wave Radiation from Periodic Structures and Applications to the Design of Frequency-Independent Antennas," Proc. IRE, Vol. 49, No. 5, pp. 962-963, May 1961.

13. Oliner, A. A., and Hessel, A., "Guided Waves on Sinusoidally-Modulated Reactance Surfaces," IRE Trans., Vol. AP-7, Dec. 1959, pp. 8201-8208.

14. Ishimaru, A., and Tuan, H., "Frequency Scanning Atnennas", 1961 IRE International Conv. Record, Part I, pp. 101-109.

15. Sensiper, S., "Electromagnetic Wave Propagation on Helical Conductors," Tech. Report No. 194, Res. Lab. of Elect., MIT, May 16, 1951.

16. Marston, A. E., and Adcock, M. D., "Radiation from Helices," Report 3634, Naval Research Laboratory, March 8, 1950.

17. Maclean, T. S. M., and Kouyoumjian, R. G., "The Bandwidth of Helical Antennas," IRE Trans., Vol. AP-7, Dec., 1959, pp. S379-S386.

18. Patton, W. T., University of Illinois, unpublished work.

19. Mayes, P. E., "Coupled Mode Analysis of Stop-Band Characteristics of Modulated Reactance Surfaces," Internal TM 62-2, Antenna Lab., University of Illinois, February 1962 (Unpublished).

20. Dyson, J. D. and Mayes, P. E., "New Circularly Polarized Frequency Independent Antennas with Conical Beam or Omnidirectional Patterns," IRE Trans., Vol. AP-9, July 1961, pp. 334-352.

21. McClelland, O. L., "An Investigation of the Near Fields on the Conical Equiangular Spiral Antenna," M.S. Thesis, Dept. of Electrical Engineering, University of Illinois, 1962. Also TR No. 55, Antenna Laboratory, University of Illinois, Urbana, Illinois, May 1962.

22. Dyson, J. D., "An Antenna to Cover the 220 through 2400 Mc Telemetering Bands," Proceedings 1962 National Telemetering Conference, Vol. I, May 1962.

# APPENDIX A

1. To determine $Z_{11}$ and $Z_{12}$ from $Z'_{11}$ and $Z'_{12}$: Given measured quantities

$$Z'_{11} \text{ and } \left|\frac{V'_1}{V'_2}\right| \angle\xi$$

at some reference plane B on the transmission line. We see from Figure 2a that for

$$I'_2 = 0 \tag{A.1}$$

$$Z_{A_2OC} = -j\, Z_o \operatorname{Cot} \beta\ell_2 \tag{A.2}$$

$$Z_{A_1OC} = Z_{11} - \frac{{Z_{12}}^2}{Z_{22} + Z_{A_2OC}} \tag{A.3}$$

$$Z'_{11} = Z_{B_1OC} = Z_o \frac{Z_{A_1OC} + j\, Z_o \tan \beta\ell_1}{Z_o + j\, Z_{A_1OC} \tan \beta\ell_1} \tag{A.4}$$

and

$$Z'_{12} = Z'_{11} \left(\frac{V'_2}{V'_1}\right) \tag{A.5}$$

where $Z_{A_2OC}$, $Z_{A_1OC}$, and $Z_{B_1OC}$ are the impedances to the right at planes $A_2$, $A_1$ and $B_1$ with $I'_2 = 0$. $Z'_{11}$, $V'_2$ and $V'_1$ are measured at reference planes $B_1$ and $B_2$. From (A.4)

$$Z_{A_1OC} = Z_o \frac{Z'_{11} - j\, Z_o \tan \beta\ell_1}{Z_o - j\, Z'_{11} \tan \beta\ell_1} \tag{A.6}$$

From (A.3)

$$Z_{11}\,Z_{22} + Z_{11}\,Z_{A_2OC} - Z_{22}\,Z_{A_1OC} - Z_{A_1OC}\,Z_{A_2OC} - Z_{12}^{\,2} = 0 \qquad (A.7)$$

Now consider the equivalent circuit of Figure 2b which includes $\ell_1$ and $\ell_2$. For $V_2' = 0$.

$$\frac{V_1'}{I_1'} = Z_{B_1SC} = Z_{11}' - \frac{{Z_{12}'}^{2}}{Z_{22}'} \qquad (A.8)$$

and

$$Z_{A_2SC} = j\,Z_o \tan \beta\ell_2 \qquad (A.9)$$

$$Z_{A_1SC} = (Z_{11} - Z_{12}) + \frac{Z_{12}\,(Z_{22} - Z_{12} + Z_{A_2SC})}{Z_{22} + Z_{A_2SC}} \qquad (A.10)$$

$$Z_{B_1SC} = (Z_{11}' - Z_{12}') + \frac{Z_{12}'\,(Z_{22}' - Z_{12}')}{Z_{22}'} \qquad (A.11)$$

also

$$Z_{A_1SC} = \frac{Z_{B_1SC} - j\,Z_o \tan \beta\ell_1}{Z_o - j\,Z_{B_1SC} \tan \beta\ell_1}\;Z_o \qquad (A.12)$$

From (A.10)

$$Z_{11}\,Z_{22} + Z_{11}\,Z_{A_2SC} - Z_{22}\,Z_{A_1SC} - Z_{A_1SC}\,Z_{A_2SC} - Z_{12}^{\,2} = 0 \qquad (A.13)$$

Equating (A.7) and (A.13)

$$Z_{11} = \frac{Z_{A_1SC} Z_{A_2SC} - Z_{A_1OC} Z_{A_2OC}}{(Z_{A_2SC} - Z_{A_2OC}) + (Z_{A_1OC} - Z_{A_1SC})} \qquad (A.14)$$

Substitution of Equation (A.2), (A.6), (A.9), (A.8), and (A.12) leads to Equation (7).

From (A.7)

$$Z_{12}^{2} = Z_{11}^{2} + Z_{11} Z_{A_2OC} - Z_{11} Z_{A_1OC} - Z_{A_1OC} Z_{A_2OC} \qquad (A.15)$$

Substitution of Equation (A.2) and (A.6) leads to Equation (8).

2. To determine $Z'_{12}$, $Z'_{22}$, and $Z'_{12}$ from the terminal quantities and feed line lengths:

From Figure 2

$$\begin{aligned} V_1 &= Z_{11} I_1 + Z_{12} I_2 \\ V_2 &= Z_{21} I_1 + Z_{22} I_2 \end{aligned} \qquad (A.16)$$

and

$$\begin{aligned} V'_1 &= Z'_{11} I'_1 + Z'_{12} I'_2 \\ V'_2 &= Z'_{21} I'_1 + Z'_{22} I'_2 \end{aligned} \qquad (A.17)$$

For $Z_{12} = Z_{21}$ and $I'_2 = 0$

$$Z_{A_2OC} = -j Z_o \operatorname{Cot} \beta \ell_2 \qquad (A.18)$$

$$Z_{A_1OC} = Z_{11} - \frac{Z_{12}^{\ 2}}{Z_{22} + Z_{A_2OC}} \qquad \text{(A.19)}$$

$$Z'_{11} = Z_{B_1OC} = Z_o \frac{Z_{A_1OC} + j\,Z_o \tan \beta\ell_1}{Z_o + j\,Z_{A_1OC} \tan \beta\ell_1} \qquad \text{(A.20)}$$

Now with $V'_2 = 0$

$$\frac{V'_1}{I'_1} = Z_{B_1SC} = Z'_{11} - \frac{Z'^{\ 2}_{12}}{Z'_{22}} \qquad \text{(A.21)}$$

$$Z_{A_2SC} = j\,Z_o \tan \beta\ell_2 \qquad \text{(A.22)}$$

$$Z_{A_1SC} = Z_{11} - \frac{Z_{12}^{\ 2}}{Z_{22} + Z_{A_2SC}}$$

(A.23)

$$Z_{B_1SC} = Z_o \frac{Z_{A_1SC} + j\,Z_o \tan \beta\ell_1}{Z_o + j\,Z_{A_1SC} \tan \beta\ell_1}$$

With $I'_1 = 0$

$$Z_{A_1OCL} = -j\,Z_o \text{ Cot } \beta\ell_1 \qquad \text{(A.24)}$$

Note: the subscript L indicates the impedance looking to the left. All previous impedances have been to the right.

$$Z_{A_2OCL} = Z_{22} - \frac{Z_{12}^{\ 2}}{Z_{11} + Z_{A_1OCL}} \qquad \text{(A.25)}$$

$$Z_{B_2OCL} = Z_o \frac{Z_{A_2OCL} + j\, Z_o \tan \beta\ell_2}{Z_o + j\, Z_{A_2OCL} \tan \beta\ell_2} \tag{A.26}$$

$$= Z'_{22}$$

From Equations (A.18), (A.19), and (A.20)

$$Z'_{11} = \frac{Z_o \left[\left(Z_{11} - \dfrac{Z_{12}^{\,2}}{Z_{22} - j\, Z_o \operatorname{Cot} \beta\ell_2}\right) + j\, Z_o \tan \beta\ell_1\right]}{\left[Z_o + j\left(Z_{11} - \dfrac{Z_{12}^{\,2}}{Z_{22} - j\, Z_o \operatorname{Cot} \beta\ell_2}\right) \tan \beta\ell_2\right]} \tag{A.27}$$

From Equations (A.24), (A.25), and (A.26)

$$Z'_{22} = \frac{Z_o \left[\left(Z_{22} - \dfrac{Z_{12}^{\,2}}{Z_{11} - j\, Z_o \operatorname{Cot} \beta\ell_1}\right) + j\, Z_o \tan \beta\ell_2\right]}{\left[Z_o + j\left(Z_{22} - \dfrac{Z_{12}^{\,2}}{Z_{11} - j\, Z_o \operatorname{Cot} \beta\ell_1}\right) \tan \beta\ell_2\right]} \tag{A.28}$$

and from (A.21), (A.22), (A.23), and (A.24)

$$Z'_{12} = (Z'_{11}\, Z'_{22} - Z_{B_1SC}\, Z'_{22})^{1/2} \tag{A.29}$$

or

$$Z'_{12} = \left[ Z'_{11}\, Z'_{22} - Z'_{22} \left\{ Z_o \frac{\left(Z_{11} - \dfrac{Z_{12}^{\,2}}{Z_{22} + j\, Z_o \tan \beta\ell_2}\right) + j\, Z_o \tan \beta\ell_1}{Z_o + j\left(Z_{11} - \dfrac{Z_{12}^{\,2}}{Z_{22} + j\, Z_o \tan \beta\ell_2}\right) \tan \beta\ell_1} \right\} \right]^{1/2} \tag{A.30}$$

## ANTENNA LABORATORY
## TECHNICAL REPORTS AND MEMORANDA ISSUED

Contract AF33(616)-310

"Synthesis of Aperture Antennas," Technical Report No. 1, C.T.A. Johnk, October, 1954.*

"A Synthesis Method for Broad-band Antenna Impedance Matching Networks," Technical Report No. 2, Nicholas Yaru, 1 February 1955.* AD 61049.

"The Assymmetrically Excited Spherical Antenna," Technical Report No. 3, Robert C. Hansen, 30 April 1955.*

"Analysis of an Airborne Homing System," Technical Report No. 4, Paul E. Mayes, 1 June 1955 (CONFIDENTIAL).

"Coupling of Antenna Elements to a Circular Surface Waveguide," Technical Report No. 5, H. E. King and R. H. DuHamel, 30 June 1955.*

"Axially Excited Surface Wave Antennas," Technical Report No. 7, D. E. Royal, 10 October 1955.*

"Homing Antennas for the F-86F Aircraft (450-2500 mc)," Technical Report No. 8, P. E. Mayes, R. F. Hyneman, and R. C. Becker, 20 February 1957, (CONFIDENTIAL).

"Ground Screen Pattern Range," Technical Memorandum No. 1, Roger R. Trapp, 10 July 1955.*

Contract AF33(616)-3220

"Effective Permeability of Spheroidal Shells," Technical Report No. 9, E. J. Scott and R. H. DuHamel, 16 April 1956.

"An Analytical Study of Spaced Loop ADF Antenna Systems," Technical Report No. 10, D. G. Berry and J. B. Kreer, 10 May 1956. AD 98615

"A Technique for Controlling the Radiation from Dielectric Rod Waveguides," Technical Report No. 11, J. W. Duncan and R. H. DuHamel, 15 July 1956.*

"Directional Characteristics of a U-Shaped Slot Antenna," Technical Report No. 12, Richard C. Becker, 30 September 1956.**

"Impedance of Ferrite Loop Antennas," Technical Report No. 13, V. H. Rumsey and W. L. Weeks, 15 October 1956. AD 119780

"Closely Spaced Transverse Slots in Rectangular Waveguide," Technical Report No. 14, Richard F. Hyneman, 20 December 1956.

"Distributed Coupling to Surface Wave Antennas," Technical Report No. 15, Ralph Richard Hodges, Jr., 5 January 1957.

"The Characteristic Impedance of the Fin Antenna of Infinite Length," Technical Report No. 16, Robert L. Carrel, 15 January 1957.*

"On the Estimation of Ferrite Loop Antenna Impedance," Technical Report No. 17, Walter L. Weeks, 10 April 1957.* AD 143989

"A Note Concerning a Mechanical Scanning System for a Flush Mounted Line Source Antenna," Technical Report No. 18, Walter L. Weeks, 20 April 1957.

"Broadband Logarithmically Periodic Antenna Structures," Technical Report No. 19, R. H. DuHamel and D. E. Isbell, 1 May 1957. AD 140734

"Frequency Independent Antennas," Technical Report No. 20, V. H. Rumsey, 25 October 1957.

"The Equiangular Spiral Antenna," Technical Report No. 21, J. D. Dyson, 15 September 1957. AD 145019

"Experimental Investigation of the Conical Spiral Antenna," Technical Report No. 22, R. L. Carrel, 25 May 1957.** AD 144021

"Coupling between a Parallel Plate Waveguide and a Surface Waveguide," Technical Report No. 23, E. J. Scott, 10 August 1957.

"Launching Efficiency of Wires and Slots for a Dielectric Rod Waveguide," Technical Report No. 24, J. W. Duncan and R. H. DuHamel, August 1957.

"The Characteristic Impedance of an Infinite Biconical Antenna of Arbitrary Cross Section," Technical Report No. 25, Robert L. Carrel, August 1957.

"Cavity-Backed Slot Antennas," Technical Report No. 26, R. J. Tector, 30 October 1957.

"Coupled Waveguide Excitation of Traveling Wave Slot Antennas," Technical Report No. 27, W. L. Weeks, 1 December 1957.

"Phase Velocities in Rectangular Waveguide Partially Filled with Dielectric," Technical Report No. 28, W. L. Weeks, 20 December 1957.

"Measuring the Capacitance per Unit Length of Biconical Structures of Arbitrary Cross Section," Technical Report No. 29, J. D. Dyson, 10 January 1958.

"Non-Planar Logarithmically Periodic Antenna Structure," Technical Report No. 30, D. E. Isbell, 20 February 1958. AD 156203

"Electromagnetic Fields in Rectangular Slots," Technical Report No. 31, N. J. Kuhn and P. E. Mast, 10 March 1958.

"The Efficiency of Excitation of a Surface Wave on a Dielectric Cylinder," Technical Report No. 32, J. W. Duncan, 25 May 1958

"A Unidirectional Equiangular Spiral Antenna," Technical Report No. 33, J. D. Dyson, 10 July 1958. AD 201138

"Dielectric Coated Spheriodal Radiators," Technical Report No. 34, W. L. Weeks, 12 September 1958 AD 204547

"A Theoretical Study of the Equiangular Spiral Antenna," Technical Report No. 35, P. E. Mast, 12 September 1958. AD 204548

## Contract AF33(616)-6079

"Use of Coupled Waveguides in a Traveling Wave Scanning Antenna," Technical Report No. 36, R. H. MacPhie, 30 April 1959. AD 215558

"On the Solution of a Class of Wiener-Hopf Integral Equations in Finite and Infinite Ranges," Technical Report No. 37, Raj Mittra, 15 May 1959.

"Prolate Spheroidal Wave Functions for Electromagnetic Theory," Technical Report No. 38, W. L. Weeks, 5 June 1959.

"Log Periodic Dipole Arrays," Technical Report No. 39, D. E. Isbell, 1 June 1959. AD 220651

"A Study of the Coma-Corrected Zoned Mirror by Diffraction Theory," Technical Report No. 40, S. Dasgupta and Y. T. Lo, 17 July 1959.

"The Radiation Pattern of a Dipole on a Finite Dielectric Sheet," Technical Report No. 41, K. G. Balmain, 1 August 1959.

"The Finite Range Wiener-Hopf Integral Equation and a Boundary Value Problem in a Waveguide," Technical Report No. 42, Raj Mittra, 1 October 1959.

"Impedance Properties of Complementary Multiterminal Planar Structures," Technical Report No. 43, G. A. Deschamps, 11 November 1959.

"On the Synthesis of Strip Sources," Technical Report No. 44, Raj Mittra, 4 December 1959.

"Numerical Analysis of the Eigenvalue Problem of Waves in Cylindrical Waveguides," Technical Report No. 45, C. H. Tang and Y. T. Lo, 11 March 1960.

"New Circularly Polarized Frequency Independent Antennas with Conical Beam or Omnidirectional Patterns," Technical Report No. 46, J. D. Dyson and P. E. Mayes, 20 June 1960 AD 241321

"Logarithmically Periodic Resonant-V Arrays," Technical Report No. 47, P. E. Mayes, and R. L. Carrel, 15 July 1960. AD 246302

"A Study of Chromatic Aberration of a Coma-Corrected Zoned Mirror," Technical Report No. 48, Y. T. Lo, June 1960

"Evaluation of Cross-Correlation Methods in the Utilization of Antenna Systems," Technical Report No. 49, R. H. MacPhie, 25 January 1961

"Synthesis of Antenna Product Patterns Obtained from a Single Array," Technical Report No. 50, R. H. MacPhie, 25 January 1961.

"On the Solution of a Class of Dual Integral Equations," Technical Report No. 51, R. Mittra, 1 October 1961. AD 264557

"Analysis and Design of the Log-Periodic Dipole Antenna," Technical Report No. 52, Robert L. Carrel, 1 October 1961.* AD 264558

"A Study of the Non-Uniform Convergence of the Inverse of a Doubly-Infinite Matrix Associated with a Boundary Value Problem in a Waveguide," Technical Report No. 53, R. Mittra, 1 October 1961. AD 264556

---

* Copies available for a three-week loan period.

** Copies no longer available.

AF33(657)-8460

## DISTRIBUTION LIST

One copy each unless otherwise indicated

Armed Services Technical Information Agency
Attn: TIP-DR
Arlington Hall Station
Arlington 12, Virginia (10 copies)

Aeronuatical Systems Division
Attn: (ASRNRE-4)
Wright-Patterson Air Force Base
Ohio (3 copies)

Aeronautical Systems Division
Attn: ASDSED, Mr. Mulligan
Wright-Patterson Air Force Base
Ohio

Aeronautical Systems Division
Attn: AFCIN-4B1A
Wright-Patterson Air Force Base
Ohio

Air Force Cambridge Research Laboratory
Attn: CRRD
Laurence G. Hanscom Field
Bedford, Massachusetts

Commander
Air Force Missile Test Center
Patrick Air Force Base
Florida

Commander
Air Force Missile Development Center
Attn: Technical Library
Holloman Air Force Base
New Mexico

Air Force Ballistic Missile Division
Attn: Technical Library, Air Force Unit Post Office
Los Angeles, California

Director
Ballistics Research Laboratory
Attn: Ballistics Measurement Lab.
Aberdeen Proving Ground, Maryland

National Aeronautics & Space Adm.
Attn: Librarian
Langley Field, Virginia

Rome Air Development Center
Attn: RCLTM
Griffiss Air Force Base
New York

Research & Development Command
Hq. USAF (ARDRD-RE)
Washington 25, D. C.

Office of Chief Signal Officer
Engineering & Technical Division
Attn: SIGNET-5
Washington 25, D. C.

Commander
U. S. Army White Sands Signal Agency
Attn: SIGWS-FC-02
White Sands, New Mexico

Director
Surveillance Department
Evans Area
Attn: Technical Document Center
Belman, New Jersey

Commander
U. S. Naval Air Test Center
Attn: WST-54, Antenna Section
Patuxent River, Maryland

Material Laboratory, Code 932
New York Naval Shipyard
Brooklyn 1, New York

Commanding Officer
Diamond Ordnance Fuse Laboratories
Attn: 240
Washington 25, D. C.

Director
U. S. Navy Electronics Laboratory
Attn: Library
San Diego 52, California

Adams-Russell Company
200 Sixth Street
Attn: Library (Antenna Section)
Cambridge, Massachusetts

Aero Geo Astro
Attn: Security Officer
1200 Duke Street
Alexandria, Virginia

NASA Goddard Space Flight Center
Attn: Antenna Section, Code 523
Creenbelt, Maryland

Airborne Instruments Labs., Inc.
Attn: Librarian (Antenna Section)
Walt Whitman Road
Melville, L. I., New York

American Electronic Labs
Box 552 (Antenna Section)
Lansdale, Pennsylvania

Andrew Alfred Consulting Engineers
Attn: Librarian (Antenna Section)
299 Atlantic Ave.
Boston 10, Massachusetts

Ampheol-Borg Electronic Corporation
Attn: Librarian (Antenna Section)
2801 S. 25th Avenue
Broadview, Illinois

Bell Aircraft Corporation
Attn: Technical Library
(Antenna Section)
Buffalo 5, New York

Bendix Radio Division of
Bendix Aviation Corporation
Attn: Technical Library
(For Dept. 462-4)
Baltimore 4, Maryland

Boeing Airplane Company
Aero Space Division
Attn: Technical Library
M/F Antenna & Radomes Unit
Seattle, Washington

Boeing Airplane Company
Attn: Technical Library
M/F Antenna Systems Staff Unit
Wichita, Kansas

Chance Vought Aircraft Inc.
THRU: BU AER Representative
Attn: Technical Library
M/F Antenna Section
P. O. Box 5907
Ballas 22, Texas

Collins Radio Company
Attn: Technical Library (Antenna Section)
Dallas, Texas

Convair
Ft. Worth Division
Attn: Technical Library (Antenna Section)
Grants Lane
Fort Worth, Texas

Convair
Attn: Technical Library (Antenna Section)
P. O. Box 1050
San Diego 12, California

Dalmo Victor Company
Attn: Technical Library (Antenna Section)
1515 Industrial Way
Belmont, California

Dorne & Margolin, Inc.
Attn: Technical Library (Antenna Section)
30 Sylvester Street
Westbury, L. I., New York

Dynatronics Inc.
Attn: Technical Library (Antenna Section)
Orlando, Florida

Electronic Communications, Inc.
Research Division
Attn: Technical Library
1830 York Road
Timonium, Maryland

Fairchild Engine & Airplane Corporation
Fairchild Aircraft & Missiles Division
Attn: Technical Library (Antenna
Section)
Hagerstown 10, Maryland

Georgia Institute of Technology
Engineering Experiment Station
Attn: Technical Library
M/F Electronics Division
Atlanta 13, Georgia

General Electric Company
Electronics Laboratory
Attn: Technical Library
Electronics Park
Syracuse, New York

General Electronic Labs., Inc.
Attn: Technical Library (Antenna
Section)
18 Ames Street
Cambridge 42, Massachusetts

General Precision Lab., Division of
General Precision Inc.
Attn: Technical Library (Antenna
Section)
63 Bedford Road
Pleasantville, New York

Goodyear Aircraft Corporation
Attn: Technical Library
M/F Dept. 474
1210 Massilon Road
Akron 15, Ohio

Granger Associates
Attn: Technical Library (Antenna
Section)
974 Commercial Street
Palo Alto, California

Grumman Aircraft Engineering Corp.
Attn: Technical Library
M/F Avionics Engineering
Bethpage, New York

The Hallicrafters Company
Attn: Technical Library (Antenna
Section)
4401 W. Fifth Avenue
Chicago 24, Illinois

Hoffman Laboratories Inc.
Attn: Technical Library (Antenna
Section)
Los Angeles 7, California

John Hopkins University
Applied Physics Laboratory
8621 Georgia Avenue
Silver Springs, Maryland

Hughes Aircraft Corporation
Attn: Technical Library (Antenna
Section)
Florence & Teal Street
Culver City, California

ITT Laboratories
Attn: Technical Library (Antenna
Section)
500 Washington Avenue
Nutley 10, New Jersey

U. S. Naval Ordnance Lab.
Attn: Technical Library
Corona, California

Lincoln Laboratories
Massachusetts Institute of Technology
Attn: Document Room
P. O. Box 73
Lexington 73, Massachusetts

Litton Industries
Attn: Technical Library (Antenna
Section)
4900 Calvert Road
College Park, Maryland

Lockheed Missile & Space Division
Attn: Technical Library (M/F Dept-58-40, Plant 1, Bldg. 130)
Sunnyvale, California

The Martin Company
Attn: Technical Library (Antenna Section)
P. O. Box 179
Denver 1, Colorado

The Martin Company
Attn: Technical Library (Antenna Section)
Baltimore 3, Maryland

The Martin Company
Attn: Technical Library (M/F Microwave Laboratory)
Box 5837
Orlando, Florida

W. L. Maxson Corporation
Attn: Technical Library (Antenna Section)
460 West 34th Street
New York 1, New York

McDonnell Aircraft Corporation
Attn: Technical Library (Antenna Section)
Box 516
St. Louis 66, Missouri

Melpar, Inc.
Attn: Technical Library (Antenna Section)
3000 Arlington Blvd.
Falls Church, Virginia

University of Michigan
Radiation Laboratory
Willow Run
201 Catherine Street
Ann Arbor, Michigan

Mitre Corporation
Attn: Technical Library (M/F Electronic Warfare Dept. D-21)
Middlesex Turnpike
Bedford, Massachusetts

North American Aviation Inc.
Attn: Technical Library (M/F Engineering Dept.)
4300 E. Fifth Avenue
Columbus 16, Ohio

North American Aviation Inc.
Attn: Technical Library (M/F Dept. 56)
International Airport
Los Angeles, California

Northrop Corporation
NORAIR Division
1001 East Broadway
Attn: Technical Information (3924-3)
Hawthorne, California

Ohio State University Research Foundation
Attn: Technical Library (M/F Antenna Laboratory)
1314 Kinnear Road
Columbus 12, Ohio

Philco Corporation
Government & Industrial Division
Attn: Technical Library (M/F Antenna Section)
4700 Wissachickon Avenue
Philadelphia 44, Pennsylvania

Westinghouse Electric Corporation
Air Arms Division
Attn: Librarian (Antenna Lab)
P. O. Box 746
Baltimore 3, Maryland

Wheeler Laboratories
Attn: Librarian (Antenna Lab)
Box 561
Smithtown, New York

Electrical Engineering Research Laboratory
University of Texas
Box 8026, Univ. Station
Austin, Texas

University of Michigan Research Institute
Electronic Defense Group
Attn: Dr. J. A. M. Lyons
Ann Arbor, Michigan

Radio Corporation of America
RCA Laboratories Division
Attn: Technical Library
(M/F Antenna Section)
Princeton, New Jersey

Radiation, Inc.
Attn: Technical Library (M/F)
Antenna Section
Drawer 37
Melbourne, Florida

Radioplane Company
Attn: Librarian (M/F Aerospace Lab)
8000 Woodly Avenue
Van Nuys, California

Ramo-Wooldridge Corporation
Attn: Librarian (Antenna Lab)
Conoga Park, California

Rand Corporation
Attn: Librarian (Antenna Lab)
1700 Main Street
Santa Monica, California

Rantec Corporation
Attn: Librarian (Antenna Lab)
23999 Ventura Blvd.
Calabasas, California

Raytheon Electronics Corporation
Attn: Librarian (Antenna Lab)
1089 Washington Street
Newton, Massachusetts

Republic Aviation Corporation
Applied Research & Development
Division
Attn: Librarian (Antenna Lab)
Farmingdale, New York

Sanders Associates
Attn: Librarian (Antenna Lab)
95 Canal Street
Nashua, New Hampshire

Southwest Research Institute
Attn: Librarian (Antenna Lab)
8500 Culebra Road
San Antonio, Texas

H. R. B. Singer Corporation
Attn: Librarian (Antenna Lab)
State College, Pennsylvania

Sperry Microwave Electronics Company
Attn: Librarian (Antenna Lab)
P. O. Box 1828
Clearwater, Florida

Sperry Gyroscope Company
Attn: Librarian (Antenna Lab)
Great Neck, L. I., New York

Stanford Electronic Laboratory
Attn: Librarian (Antenna Lab)
Stanford, California

Stanford Research Institute
Attn: Librarian (Antenna Lab)
Menlo Park, California

Sylvania Electronic System
Attn: Librarian (M/F Antenna &
Microwave Lab)
100 First Street
Waltham 54, Massachusetts

Sylvania Electronic System
Attn: Librarian (Antenna Lab)
P. O. Box 188
Mountain View, California

Technical Research Group
Attn: Librarian (Antenna Section)
2 Aerial Way
Syosset, New York

Ling Temco Aircraft Corporation
Temco Aircraft Division
Attn: Librarian (Antenna Lab)
Garland, Texas

Texas Instruments, Inc.
Attn: Librarian (Antenna Lab)
6000 Lemmon Ave.
Dallas 9, Texas

A. S. Thomas, Inc.
Attn: Librarian (Antenna Lab)
355 Providence Highway
Westwood, Massachusetts

New Mexico State University
Head Antenna Department
Physical Science Laboratory
University Park, New Mexico

Bell Telephone Laboratories, Inc.
Whippany Laboratory
Whippany, New Jersey
Attn: Technical Reports Librarian
Room 2A-165

Robert C. Hansen
Aerospace Corporation
Box 95085
Los Angeles 45, California

Dr. Richard C. Becker
10829 Berkshire
Westchester, Illinois

Dr. Harry Letaw, Jr.
Raytheon Company
Surface Radar and Navigation
Operations
State Road West
Wayland, Massachusetts

Dr. Frank Fu Fang
IBM Research Laboratory
Poughkeepsie, New York

Mr. Dwight Isbell
1422 11th West
Seattle 99, Washington

Dr. Robert L. Carrel
Collins Radio Corporation
Antenna Section
Dallas, Texas

Dr. A. K. Chatterjee
Vice Principal & Head of the Department
of Research
Birla Institute of Technology
P. O. Mesra
District-Ranchi (Bihar) India

Aeronautical Systems Division
Attn: ASAD - Library
Wright-Patterson Air Force Base
Ohio

National Bureau of Standards
Department of Commerce
Attn: Dr. A. G. McNish
Washington 25, D. C.